

**TIME STUDY OF PHOTOGRAFTING POLY (N-  
ISOPROPYLACRYLAMIDE-CO-ACRYLAMIDE) ONTO  
POLYSTYRENE SURFACE FOR TISSUE CULTURE  
ENGINEERING**

**BY**

**AYE YU YU SWE**

**A THESIS SUBMITTED IN PARTIAL FULFILLMENT OF  
THE REQUIREMENTS FOR THE DEGREE OF MASTER OF  
ENGINEERING (ENGINEERING TECHNOLOGY)  
SIRINDHORN INTERNATIONAL INSTITUTE OF TECHNOLOGY  
THAMMASAT UNIVERSITY  
ACADEMIC YEAR 2015**

**TIME STUDY OF PHOTOGRAFTING POLY (N-  
ISOPROPYLACRYLAMIDE-CO-ACRYLAMIDE) ONTO  
POLYSTYRENE SURFACE FOR TISSUE CULTURE  
ENGINEERING**

**BY**

**AYE YU YU SWE**

**A THESIS SUBMITTED IN PARTIAL FULFILLMENT OF  
THE REQUIREMENTS FOR THE DEGREE OF MASTER OF  
ENGINEERING (ENGINEERING TECHNOLOGY)  
SIRINDHORN INTERNATIONAL INSTITUTE OF TECHNOLOGY  
THAMMASAT UNIVERSITY  
ACADEMIC YEAR 2015**



TIME STUDY OF PHOTOGRAFTING POLY (N-ISOPROPYLACRYLAMIDE-  
CO-ACRYLAMIDE) ONTO POLYSTYRENE SURFACE FOR TISSUE CULTURE  
ENGINEERING

A Thesis Presented

By

AYE YU YU SWE

Submitted to

Sirindhorn International Institute of Technology

Thammasat University

In partial fulfillment of the requirements for the degree of  
MASTER OF ENGINEERING (ENGINEERING TECHNOLOGY)

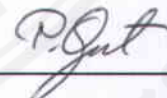
Approved as to style and content by

Advisor and Chairperson of Thesis Committee



(Asst. Prof. Dr. Wanwipa Siriwatwechakul, Ph.D.)

Committee Member and  
Chairperson of Examination Committee



(Assoc. Prof. Dr. Pakorn Opaprakasit, Ph.D.)

Committee Member



(Asst. Prof. Dr. Siwarutt Boonyarattanakalin, Ph.D.)

Committee Member



(Asst. Prof. Dr. Kwanchanok Viravaidya-Pasuwat, Ph.D.)

NOVEMBER 2015

## Abstract

### TIME STUDY OF PHOTOGRAFTING POLY (N-ISOPROPYLACRYLAMIDE- CO-ACRYLAMIDE) ONTO POLYSTYRENE SURFACE FOR TISSUE CULTURE ENGINEERING

by

AYE YU YU SWE

Bachelor of Engineering, Sirindhorn International Institute of Technology (SIIT),  
Thammasat University, 2013

Poly (*N-isopropyl acrylamide-co-acrylamide*) (PNIAM-co-AM) is a temperature-responsive polymer that has been widely utilized for modification of tissue culture surfaces in cell sheet engineering. Its phase transition from hydrophobic to hydrophilic characteristics occurs at the lower critical solution temperature (LCST) of 32°C which can support cell adhesion and detachment under human physiological conditions. This study investigates the ultraviolet (UV) irradiation method to graft PNIAM-co-AM onto tissue culture polystyrene surface (TCPS) and the effect of UV polymerization time on the grafted amount of PNIAM-co-AM onto TCPS surfaces. The purpose is to determine the effective UV exposure time which provides the optimum grafting density of 1.4–2  $\mu\text{g}/\text{cm}^2$  that is suitable for proper cell adhesion and detachment. This quantitative analysis on the amount of grafted copolymer with different UV exposure times was characterized by Attenuated Total Reflection Fourier Transform Infrared Spectroscopy (ATR-FTIR). The relationship between the peak area ratio ( $A_{1654}/A_{1600}$ ) and grafting density ( $\mu\text{g}/\text{cm}^2$ ) was determined. From the results of ATR-FTIR measurement, the grafted PNIAM-co-AM amount increases with increasing UV polymerization time from 30 minutes to 2.50 hours. From 1 to 2 hours of UV exposure time, the amount of grafted copolymer was obtained between 1.68 and 2.03  $\mu\text{g}/\text{cm}^2$ . From the estimation of PNIAM content in the copolymer

grafted layer by FTIR and NMR analysis, the grafted amount of PNIAM in 1–2-hour UV exposure surfaces was obtained between 1.3 and 1.7  $\mu\text{g}/\text{cm}^2$  which is close to the optimum range of grafting density. The hydrophobic-hydrophilic transition behaviour of the grafted PNIAM-co-AM surfaces was also examined by contact angle measurement. The grafted surface with the UV exposure time of between 1 and 2 hours showed an obvious transition in contact angles when the temperature was lowered from 40 to 10°C. The results of cell study analysis show that a successful detachment of a Human Dermal Fibroblast (HDFa) monolayer cell sheet is observed in PNIAM-co-AM grafted surfaces with 1- and 2-hour UV exposure time.

Along with this research, synthesis of PNIAM-co-AM was also carried out in order to reach the quantitative analysis of ATR-FTIR. The synthesized PNIAM-co-AM was first confirmed as a linear copolymer by using KBr technique of Fourier Transform Infrared Spectroscopy (FTIR). The estimated composition of PNIAM in the synthesized copolymer was obtained as 76.3% and 80.6% from FTIR and NMR analysis. The resulting linear copolymer was applied in the preparation of the known grafted amount of PNIAM-co-AM grafted surfaces. It was very useful in constructing the calibration curve of the peak area ratio ( $A_{1654}/A_{1600}$ ) and grafting density ( $\mu\text{g}/\text{cm}^2$ ). As a related study, the natures of synthesized PNIAM-co-AM in aqueous solution at 10, 20 and 37°C were also studied by intrinsic viscosity determination. From the results, the drop in viscosity from 10°C to 37°C refers to the change in conformation of PNIAM from extended chain at below LCST to coiled-globule at above LCST. A significant drop of intrinsic viscosity is observed at 20°C which can be affected by the temperature-dependent factors such as the interaction between water and PNIAM, molecular weight, and radial of gyration of the synthesized copolymer.

**Keywords:** Poly (N-isopropylacrylamide-co-acrylamide), Temperature-responsive surface, UV grafting, Cell adhesion and detachment, Cell sheet engineering

## Acknowledgements

I would like to first express the deepest appreciation to my advisor, Assistant Professor Dr. Wanwipa Siriwatwechakul, for her continuous encouragement and guidance throughout this research. It would be impossible to complete this study without her valuable advice and support. Secondly, I am very grateful to members of thesis committee, Assoc. Prof. Dr. Pakorn Opaprakasit, Asst. Prof. Dr. Siwarutt Boonyarattanakalin and Asst. Prof. Dr. Kwanchanok Viravaidya-Pasuwat, for their useful suggestions and comments throughout my study. I also wish to express my gratitude to Asst. Prof. Dr. Paiboon Sreearunothai for providing the equipment for contact angle measurement. I would like to give a sincere thank to Mr. Phongphot Sakulaue, a graduate student at Sirindhorn International Institute of Technology (SIIT), Thammasat University, for providing a spin-coating machine to apply in this research. Besides, my special thank is offered to Ms. Narisara Jaikaew, a graduate student at SIIT, Thammasat University, for her kind help in  $^1\text{H}$  NMR spectroscopy measurement. I would also like to express my appreciation to Ms. Kanokaon Benchapathanphorn, a graduate student at Biological Engineering Program, King Mongkut's University of Technology Thonburi (KMUTT), for supporting in the cell study analysis data for this research. I also would like to offer my grateful acknowledgements to my lab colleagues for sharing their lab techniques and their helps. In addition, I wish to acknowledge for Construction and Maintenance Technology Research Center – CONTEC at SIIT, for providing Center of Excellence (CoE) Scholarship. Finally, I wish to express a sense of gratitude and love to my beloved parents and sisters for their supports, cares and everything.

## Table of Contents

Chapter	Title	Page
	Signature Page	i
	Abstract	ii
	Acknowledgements	iv
	Table of Contents	v
	List of Tables	viii
	List of Figures	x
1	Introduction	1
	1.1 Background of study	1
	1.2 Motivations and Goals of Thesis	3
	1.3 Thesis Organizations	5
2	Literature Review	7
	2.1 Temperature-responsive behavior of PNIAM at LCST	7
	2.2 Comparison of grafting methods of PNIAM	8
	2.3 Principle of photo-induced polymerization by UV irradiation	10
	2.4 Effect of irradiation intensity and exposure time on photo-polymerization	10
	2.5 Effect of grafting density of PNIAM on cell adhesion/ detachment properties	13
	2.6 Characterization methods	15
	2.6.1 Attenuated Total Reflection Fourier Transform Infrared Spectroscopy (ATR-FTIR) measurement	15
	2.6.2 KBr- Fourier Transform Infrared Spectroscopy (KBr-FTIR) measurement	17

2.6.3	Contact Angle Measurement	18
2.6.4	Intrinsic Viscosity Measurement	20
3	Methodology	23
3.1	Materials required for UV-induced grafting of PNIAM-co-AM on PS surface	23
3.2	Overview of UV-induced grafting mechanism	23
3.3	Procedures for grafting PNIAM-co-AM on TCPS surface	25
3.3.1	Preparation of PNIAM-co-AM grafted TCPS surface using the protocol in Wong-in et al.	25
3.3.2	Preparation of PNIAM-co-AM grafted TCPS surface with varying UV exposure time	26
3.4	Synthesis of linear poly(N-isopropylacrylamide-co-acrylamide)	27
3.4.1	Materials required for synthesis	28
3.4.2	Procedure of synthesizing PNIAM-co-AM	28
3.5	Characterization methods	29
3.5.1	KBr-FTIR measurement for synthesized PNIAM-co-AM	29
3.5.2	Intrinsic Viscosity Determination	29
3.5.3	Quantitative analysis by ATR-FTIR measurement	30
3.5.3.1	Preparation of known concentration for calibration curve construction	31
3.5.3.2	Procedure for calibration curve construction	32
3.5.4	Contact angle Measurement	32
3.6	Protocol for cell study analysis	33
4	Result and Discussion	34
4.1	Characterization results of synthesized PNIAM-co-AM	34
4.1.1	Peak analysis in KBr-FTIR spectra of PNIAM-co-AM	34
4.1.2	Results of intrinsic viscosity measurement at different temperatures	39



4.2	Result comparison of the influence of UV intensity and exposure time on polymerization process	43
4.3	Quantitative analysis results of PNIAM-co-AM grafted TCPS surfaces	45
4.3.1	Calibration curve construction by using peak area ratio	45
4.3.2	Graft density results of PNIAM-co-AM grafted TCPS surfaces with different UV exposure times	48
4.4	Contact angle results of PNIAM-co-AM grafted TCPS surfaces with different UV exposure times	51
4.5	Estimation of PNIAM content in the grafted copolymer	52
4.5.1	Analysis by FTIR	53
4.5.2	Analysis by NMR	54
4.5.3	Determination of grafted PNIAM on TCPS surfaces	56
4.6	Results from cell study analysis	58
5	Conclusions and Recommendations	60
5.1	Summary of findings	60
5.1.1	Summary of synthesized PNIAM-co-AM	60
5.1.2	Summary of UV exposure time study for PNIAM-co-AM grafted surfaces	61
5.2	Recommendation for further study	62
	References	63
	Appendices	68
	Appendix A	69
	Appendix B	76
	Appendix C	78

## List of Tables

Tables	Page
1.1 Physicochemical properties of PNIAM-grafted surfaces with different graft densities and thicknesses	3
2.1 Comparison of grafting methods of PNIAM	8
2.2 Surface wettability and cell adhesion/ detachment properties of PNIAM with different graft densities	13
3.1 Chemicals required for UV grafting process	23
3.2 Comparison of UV energy at the exposure distance of 0 cm and 10 cm	25
3.3 Synthesis of PNIAM-co-AM (1:1 ratio)	28
3.4 Synthesis of PNIAM-co-AM (2:1 ratio)	28
3.5 Pre-determined concentrations of PNIAM-co-AM based on the expected range of grafting density ( $\mu\text{g}/\text{cm}^2$ )	31
4.1 Characteristic absorption peaks in FTIR spectrum of synthesized linear PNIAM-co-AM [30, 35, 36]	35
4.2 Average flow time and reduced viscosity of 1:1 ratio PNIAM-co-AM at 10°C and 37°C	39
4.3 Average flow time and reduced viscosity of 2:1 ratio PNIAM-co-AM at 10°C and 37°C	41
4.4 Average flow time and reduced viscosity of 1:1 ratio and 2:1 ratio of PNIAM-co-AM at 20°C	42
4.5 Average peak area ratios from eight different positions of known grafted amount of PNIAM-co-AM surfaces	45
4.6 Peak area ratio at eight different positions of commercial Upcell™ surface	47
4.7 Results of peak area ratios and grafting densities of PNIAM-co-AM grafted samples with varying UV exposure time	49
4.8 Contact angle measurement of un-grafted polystyrene surface and PNIAM-co-AM grafted TCPS surfaces at 40°C and 10°C	51
4.9 Peak results of synthesized PNIAM-co-AM (1:1 ratio)	53
4.10 Composition of PNIAM and AM in 1:1 ratio of PNIAM-co-AM	54

<b>Tables</b>	<b>Page</b>
4.11 Estimated grafted amount of PNIAM in copolymer grafted surfaces	56
4.12 Summary of grafted PNIAM amount on the surfaces with 1 – 2.5-hour UV exposure time	58



## List of Figures

Figures	Page
1.1 (A) Tissue culture; (B) Degradation of both ECM and cell-to-cell junction proteins due to trypsinization; (C) Cell sheet released from temperature responsive culture surfaces <sup>[2, 4]</sup>	1
1.2 Structure of scope of work	5
2.1 Chemical structure of PNIAM	7
2.2 Cell culture on PNIAM grafted surface <sup>[16]</sup>	8
2.3 Relationship between the grafting yield and the irradiation intensity <sup>[10]</sup>	11
2.4 Relationship between the grafting yield and the irradiation time at different ratios of initiator to monomer (BP/DEAAm) <sup>[10]</sup>	11
2.5 Effects of irradiation time on the graft polymerization of PAAc onto the PET film surface <sup>[26]</sup>	13
2.6 Influence of PNIAM-grafted densities on chain mobility and cell-adhesive characteristics <sup>[12]</sup>	14
2.7 A multiple reflection in ATR system <sup>[28]</sup>	16
2.8 FTIR spectra of (A) ungrafted TCPS, (B) PNIAM-co-AM grafted TCP surface and (C) linear PNIAM, for wavenumbers ranging from 1800 to 1400 cm <sup>-1</sup>	16
2.9 IR spectra of linear PNIAM-co-AM and cross-linked microspheres <sup>[30]</sup>	18
2.10 Temperature-dependent wettability changes for PNIAM grafted surfaces at 10°C and 37°C <sup>[12]</sup>	18
2.11 Contact angles of the PNIAM-co-AM grafted surface and ungrafted surface at various temperatures <sup>[6, 9]</sup>	19
2.12 Graphical determination of the intrinsic viscosity	21
2.13 Reduced viscosity Vs. concentration of PNIAM-co-AM (NIAM/AM=85) in deionized water at 30°C and 40°C <sup>[34]</sup>	21
3.1 Basic steps in UV-induced grafting procedure	23
3.2 Relationship between UV intensity and distance	25
3.3 The schematic of UV induced grafting polymerization of PNIAM-co-AM on TCPS surface	27

<b>Figures</b>	<b>Page</b>
3.4 Copolymer synthesis of PNIAM-co-AM	28
3.5 A temperature-controlled water bath and a viscometer chamber	30
3.6 FTIR with a diamond ATR crystal (Single bounce technique)	31
3.7 Positions on a PNIAM grafted surface selected for ATR measurement	32
3.8 Sample placed on a heat-exchanger aluminium plate in the set up for contact angle measurement	33
4.1 Structures of linear PNIAM-co-AM and its monomers	34
4.2 KBr-FTIR spectrum of linear PNIAM-co-AM (1:1 ratio)	36
4.3 KBr-FTIR spectrum of recrystallized NIAM and AM monomers	37
4.4 Comparison of KBr-FTIR spectra of (a) crosslinked PNIAM-co-AM (2:1 ratio) and (b) linear PNIAM-co-AM (2:1 ratio) after reprecipitation	38
4.5 Intrinsic viscosity of 1:1 ratio of PNIAM-co-AM at 10 and 37°C	40
4.6 Intrinsic viscosity of 2:1 ratio of PNIAM-co-AM at 10 and 37°C	41
4.7 Intrinsic viscosity of 1:1 and 2:1 ratio of PNIAM-co-AM at 20°C	42
4.8 ATR-FTIR spectra of PNIAM-co-AM grafted surfaces with different conditions of UV exposure and un-grafted TCPS surface	44
4.9 ATR-FTIR spectra of known grafted amounts of PNIAM-co-AM on TCPS surfaces	46
4.10 Relationship between the peak area ratio and the grafted amount of PNIAM-co-AM	46
4.11 ATR-FTIR spectra of (a) commercial Upcell™ PNIAM grafted TCPS surface; (b) Un-grafted TCPS surface	47
4.12 ATR-FTIR spectra of un-grafted TCPS surface and PNIAM-co-AM grafted TCPS surfaces with different UV exposure times	49
4.13 Amount of grafted PNIAM-co-AM on TCPS surfaces at different UV exposure times	50
4.14 Contact angles of PNIAM-co-AM grafted surfaces with varying UV exposure time	52
4.15 <sup>1</sup> H NMR spectrum of 1:1 ratio of synthesized PNIAM-co-AM	55
4.16 Relationship between peak area ratio and amount of grafted PNIAM	56

<b>Figures</b>	<b>Page</b>
4.17 Estimated grafted amount of PNIAM on TCPS surfaces at different UV exposure times	57
4.18 Detachment of human dermal fibroblast monolayer cell sheet from PNIAM-co-AM grafted surfaces	59



# Chapter 1

## Introduction

### 1.1 Background of study

In recent years, cell sheet technology has been developed for the regeneration of damaged tissues. This technology involves in using of temperature-responsive surfaces which are capable of controlling cell adhesion and detachment from the tissue culture surfaces [1]. This is an alternative approach to overcome a major drawback in conventional enzymatic treatment of tissue culture. In the conventional treatment, trypsinization process uses protease enzymes such as trypsin or dispase, or chelating agents such as ethylenediaminetetraacetic acid (EDTA) in harvesting cells. Those reagents damage the protein in cell-to-cell junction and destroy extracellular matrix (ECM) so that resulting cells cannot be detached as a cell sheet from the culture surface as shown in Figure 1.1(B). These issues can be solved by using temperature-responsive surfaces due to the presence of their unique property that can control the cell adhesion and detachment by changing temperature [1-4].

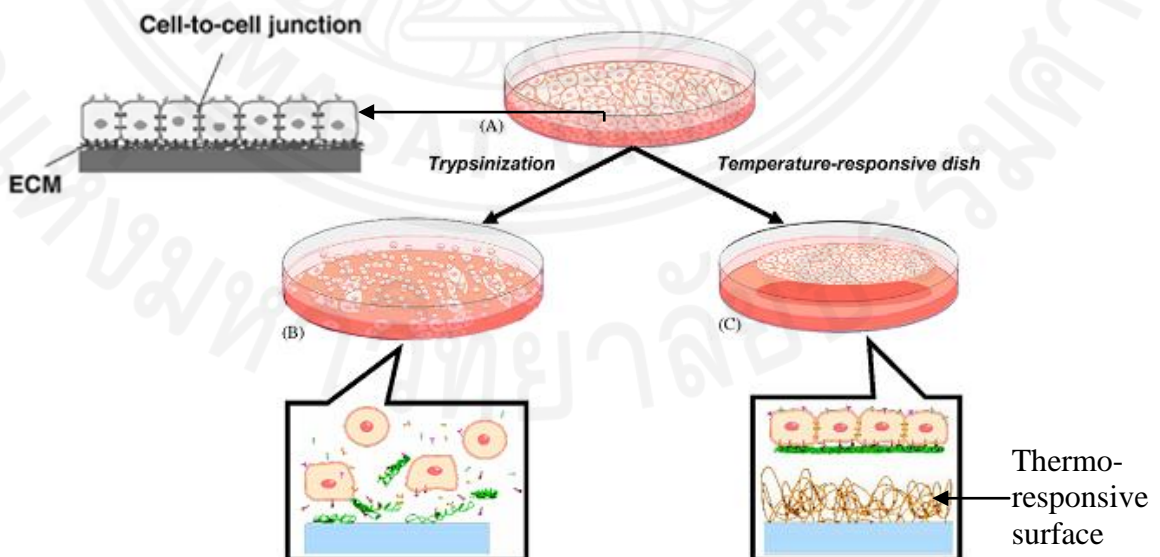


Figure 1.1 (A) Tissue culture; (B) Degradation of both ECM and cell-to-cell junction proteins due to trypsinization; (C) Cell sheet released from temperature responsive culture surfaces [2, 4]

Therefore, modification of tissue culture surface is required to graft temperature-responsive polymers onto tissue culture polystyrene surface (TCPS). One of the distinct properties of temperature-responsive polymers is the presence of a critical solution temperature at which the transition of hydrophobic to hydrophilic characteristics take place [5]. Among different types of polymers, poly(N-isopropylacrylamide) (PNIAM) and its copolymers have been researched for a lot of biomedical applications because their phase transition occurs at the lower critical solution temperature (LCST) of 32°C, which is close to human physiological temperature. Above 32°C, the polymer stays as a compact structure and is hydrophobic. This hydrophobic surface supports cell adhesion and proliferation. Below 32°C, the polymer is fully-hydrated, and changes to extended chain conformation. The surface is hydrophilic and then, allows the adherent cells to be lifted up as a cell sheet without damaging the cell membrane and extracellular matrix (ECM) as shown in Figure 1.1(C) [2, 4, 5].

Three main radiation-induced techniques have been developed to graft PNIAM onto the tissue culture polystyrene (TCPS) dish, which are electron beam (EB) irradiation, plasma polymerization and UV irradiation. Okano and his coworkers have successfully used the electron beam method to graft PNIAM on TCPS dishes and the resulting modified surfaces provide nearly a hundred percent cell detachment [5-8]. Those tissue culture dishes have been commercially produced as “Upcell™” (CellSeed, Tokyo, Japan). However, there are still some issues such as shape restriction and surface area limitation for construction of larger cell sheets. Also, the cost of Upcell™ is about five times higher than that of tissue culture polystyrene (TCPS) dishes [9]. As for plasma polymerization, it is a one-step vapor-phase method with more complicated procedure, using costly devices [10, 11], and therefore, this method is not applicable for mass production.

The last technique, UV induced polymerization, is a promising method for application in tissue culture engineering from the economical point of view because large-scale production can be done without involving any expensive equipment. However, UV polymerization requires additional chemicals such as photo-initiators and cross-linkers due to its lower irradiation intensity compared to EB irradiation. Wong-in et al. (2011) has proposed that applying UV irradiation can successfully



graft the copolymer, poly (N-isopropylacrylamide-co-acrylamide) PNIAM-co-AM, onto the TCPS dish by using the monomer concentration of N-isopropylacrylamide (NIAM) (1 mol/L) and acrylamide (AM) (1.04 mol/L) with the help of a periodate photo-initiator [9, 12]. However, the results of cell study have not achieved a hundred percent cell detachment without any further improvement.

## 1.2 Motivations and Goals of Thesis

This study focuses on UV polymerization method for grafting the copolymer, PNIAM-co-AM, onto the TCPS dish and aims to achieve the higher percentage of cell detachment. Based on the research work by Wong-in et al., grafting of PNIAM-co-AM in the mole ratio of 1:1 onto the TCPS dish has been proposed by applying UV irradiation for 1 hour. However, the amount of the grafted copolymer layer has not been determined as well as the controlling factors for UV polymerization process.

In radiation induced polymerization, the main controlling factors for the properties of polymer grafted layer are photo-polymerization time, intensity and concentration of reactants. From the studies, all these factors have an effect on the amount of grafted polymer on the substrate [1, 13-15]. The grafted amount can be expressed in terms of a thickness of grafted layer (nm) or grafting density ( $\mu\text{g}/\text{cm}^2$ ) leading to the changes in the wettability of surface in the case of PNIAM grafted surface. The amount of grafted PNIAM is an important factor for controlling cell adhesion and detachment in response to temperature. Table 1.1 shows the properties of PNIAM-grafted surfaces with different graft densities and thicknesses [1, 14, 15].

Table 1.1 Physicochemical properties of PNIAM-grafted surfaces with different graft densities and thicknesses

Density of grafted PIPAAm ( $\mu\text{g cm}^{-2}$ ) [a]		1.4 $\pm$ 0.1	2.9 $\pm$ 0.1	1,080
Thickness of the grafted PIPAAm (nm) [b]		15.5 $\pm$ 7.2	29.3 $\pm$ 8.4	5,000
Contact angle (degrees) [c]	(37 $^{\circ}$ C)	77.9 $\pm$ 0.6	69.5 $\pm$ 1.2	49.6 (40 $^{\circ}$ C)
	(20 $^{\circ}$ C)	65.2 $\pm$ 1.2	60.0 $\pm$ 0.1	11.5 (10 $^{\circ}$ C)
Cell adhesion	(37 $^{\circ}$ C)	Yes	No adhesion	No adhesion
	(20 $^{\circ}$ C)	Yes	- [d]	- [d]

[a]  $n = 4$ , mean $\pm$ SD. [b]  $n = 4$ , mean $\pm$ SD. [c]  $n = 3$ , mean $\pm$ SD. [d] Not determined

Okano and his coworkers reported that the optimal grafted amount of PNIAM for cell adhesion, proliferation and detachment falls within the range of 1.4 – 2.0  $\mu\text{g}/\text{cm}^2$ . Their results indicate that cell can adhere and proliferate on the surface with the density of grafted PNIAM less than 1.4  $\mu\text{g}/\text{cm}^2$ , but cell detachment cannot occur on that surface when lowering the temperature. Similarly, cell adhesion cannot occur on the surfaces with more than 2.0  $\mu\text{g}/\text{cm}^2$  grafting yield. Their contact angle results also show that higher grafted amount of PNIAM causes lower contact angles at both temperatures which means that the property of hydrophobic–hydrophilic transition at LCST is greatly reduced [1, 14, 15]. Thus, the grafted amount of PNIAM is very important in controlling the behavior of PNIAM for cell adhesion and detachment process.

Therefore, this study first investigated the main controlling factor for UV polymerization process by comparing the effect of UV exposure time and UV intensity based on the proposed procedure by Wong-in et al. [9, 12] After confirming the fact that UV exposure time is the main factor which can influence on the grafted copolymer layer on the TCPS surface, the effect of UV polymerization time has been studied by varying the UV exposure time from 30 minutes to 3 hours. The aim of this study is to determine the effective UV exposure time which can provide the optimum grafted copolymer density of 1.4 – 2.0  $\mu\text{g}/\text{cm}^2$  that is suitable for proper cell adhesion and detachment.

The grafting density of PNIAM-co-AM on TCPS surface can be determined by the quantitative analysis of Attenuated Total Reflection Fourier Transform Infrared Spectroscopy (ATR-FTIR). The contact angle measurement is also used to observe the change in surface wettability of the different grafted amount of PNIAM-co-AM grafted surfaces with respect to temperature. In addition, synthesis of linear PNIAM-co-AM is studied in order to use in constructing a calibration curve of the known concentration of PNIAM-co-AM for quantitative ATR-FTIR analysis. As a supplementary study, intrinsic viscosity measurement is also carried out for the copolymer obtained from synthesis in order to study the behavior of PNIAM-co-AM in response to temperature.

The objectives of this study are:

1. To study the effect of UV exposure time on the grafting density of PNIAM-co-AM on TCPS surface.
2. To determine the grafted amount of PNIAM-co-AM on TCPS surface by the quantitative ATR-FTIR analysis.
3. To observe the improvement in the percentage of cell detachment after the optimum amount of grafted PNIAM-co-AM on TCPS surface is obtained.

The following flow chart shows a brief description on the scope of work.

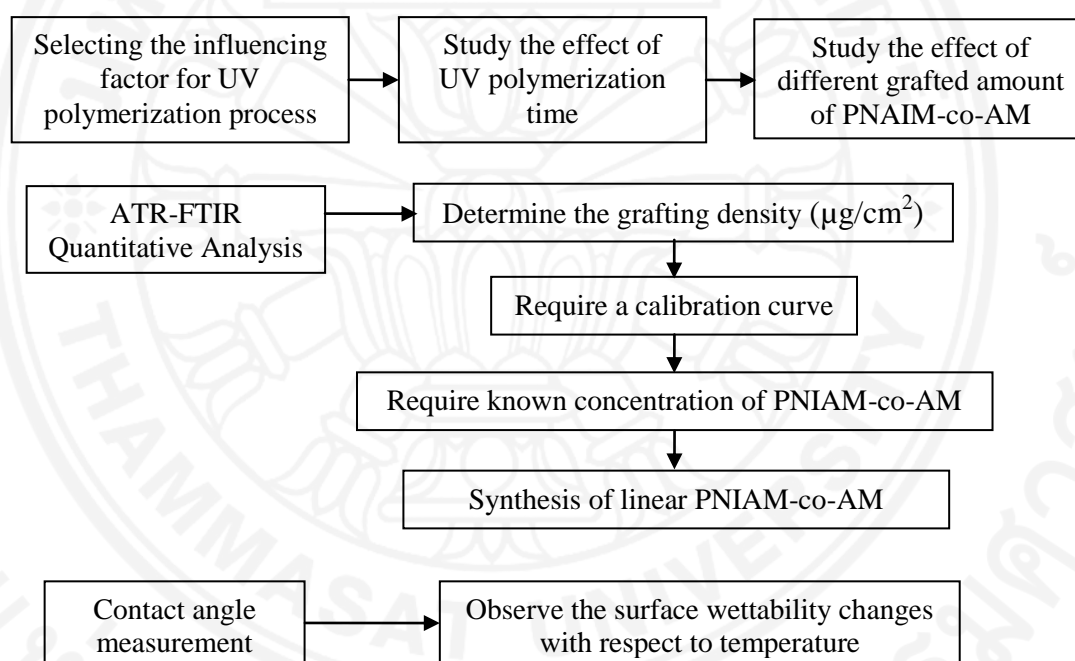


Figure 1.2: Structure of scope of work

### 1.3 Thesis Organizations

The following outline describes the organization of study in each chapter.

Chapter 1: This chapter includes background, goals of study and scope of work.

Chapter 2: This chapter provides literature reviews on the understanding of temperature-responsive behavior of PNAIM at LCST, comparison of grafting methods of PNIAM on TCPS surface, principle of photo-induced polymerization, the effect of irradiation intensity and exposure time on UV-induced polymerization, the

effect of PNIAM grafted density on surface wettability and cell adhesion/ detachment process and characterization methods.

Chapter 3: This chapter describes materials and methodology used in UV-induced grafting of PNIAM-co-AM on TCPS surface, synthesis of linear PNIAM-co-AM, cell study, and characterization methods.

Chapter 4: This chapter discusses the comparison of characterization results between high UV intensity and longer UV exposure time, the results of FTIR measurement and intrinsic viscosity measurement of synthesized PNIAM-co-AM, quantitative analysis results of PNIAM-co-AM grafted surfaces with different UV exposure times, contact angle results with the explanation of surface wettability and grafting density, estimation of PNIAM content in the grafted copolymer layer, and cell study analysis results.

Chapter 5: This chapter describes the summary of findings and recommendation and suggestion for the further study.

## Chapter 2

### Literature Review

#### 2.1 Temperature-responsive behavior of PNIAM at LCST

Hydrophilic-hydrophobic phase transition behavior of PNIAM at its LCST (32°C) is essential for controlling cell adhesion and cell detachment in different types of tissue culture [16]. Both hydrophilic amide group and hydrophobic isopropyl group are present in the structure of PNIAM as shown in Figure 2.1. Intra-molecular forces of both groups hold together to form the structure of PNIAM. Among these two groups, the hydrophilic amide group can interact with water molecules with respect to temperature when PNIAM is in aqueous solution. It leads to two types of interactions which are intermolecular (between polymer and water) and intra-molecular (between constituent groups in polymer) interactions. Due to these interactions at the LCST, PNIAM is able to change its conformation with respect to temperature, and supportive for cell adhesion and detachment process [17].

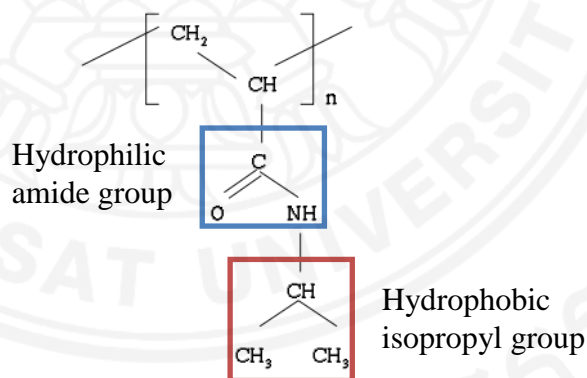


Figure 2.1: Chemical structure of PNIAM

Figure 2.2 shows a brief process of how the conformational changes of PNIAM at its LCST is applicable in cell culture. Above LCST of 37°C, the intra-molecular force of amide groups in PNIAM chain is steady, and this hydrophilic group has less interaction with water molecules. Thus, PNIAM chains collapse and the hydrophobic isopropyl groups expose more on the surface. These chains are compact together so that structure of PNIAM in hydrophobic state is represented to be coil-globule structure. This hydrophobic surface supports cell adhesion and

proliferation. Below LCST, hydrophilic interaction of PNIAM becomes stronger which is formed by hydrogen bonding between hydrophilic amide groups in PNIAM and water molecules. Therefore, the structure of PNIAM changes to flexible and extended chain conformation [17, 18]. Thus, by lowering the temperature up to 10°C, extended PNIAM chain can release the detached cells as a cell sheet without damaging the cell membrane and extracellular matrix (ECM).

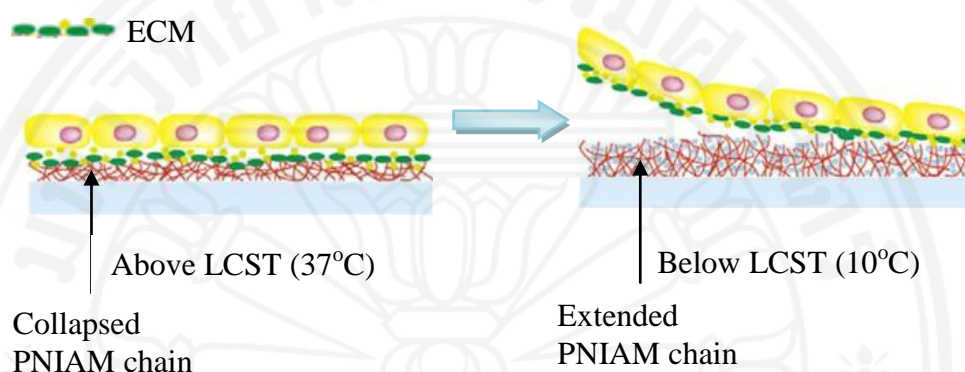


Figure 2.2: Cell culture on PNIAM grafted surface <sup>[19]</sup>

## 2.2 Comparison of grafting methods of PNIAM

From the studies, there are three main methods of grafting PNIAM on given substrates, which are electron beam (EB) irradiation, plasma polymerization and UV irradiation. The comparison of each method is shown in the following Table 2.1.

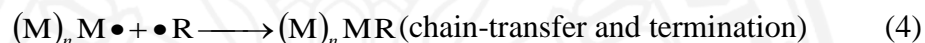
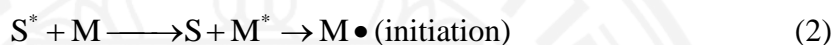
Table 2.1 Comparison of grafting methods of PNIAM

EB irradiation	
Components and process ( by Okano et al.) [5-8]	(1) Use an Area Beam Electron Processing System to produce 0.25–0.3 MGy EB irradiation at ~200 kV (2) EB ionizes 30-100 $\mu$ L of NIAM isopropyl solution to undergo polymerization and graft uniformly on 6-well TCPS plate surfaces
Advantages	(1) Less use of other chemicals and capable of homopolymerizing grafted PNIAM (2) Uniformly grafted surface provides a hundred percent cell detachment

Disadvantages	<ul style="list-style-type: none"> <li>(1) Use of expensive equipment</li> <li>(2) Require well-trained persons for operating system</li> </ul>
<b>Plasma</b>	
Components and process ( by Ratner et al.) [10, 11, 20]	<ul style="list-style-type: none"> <li>(1) Use a radio frequency plasma polymerization reactor</li> <li>(2) Require liquid nitrogen to condense 5 wt% of NIAM monomer solution and energize the monomer vapor in the reactor chamber where the substrate is loaded</li> <li>(3) Maintain plasma at 120 W for promoting adhesion layer between substrate and plasma polymer film</li> </ul>
Advantages	<ul style="list-style-type: none"> <li>(1) Less use of other chemicals and capable of homopolymerizing grafted PNIAM</li> <li>(2) Uniformly well-coated thin polymer film is obtained due to the use of vapor phase method</li> </ul>
Disadvantages	<ul style="list-style-type: none"> <li>(1) Complicated system using high power source</li> <li>(2) Require well-controlled atmosphere</li> <li>(3) Require large amount of monomer solution</li> <li>(4) Expensive operating cost and only lab scale available</li> </ul>
<b>UV irradiation</b>	
Components and process ( by Curti et al. and Wong-in et al.) [9, 12, 21, 22]	<ul style="list-style-type: none"> <li>(1) Use a UV source (254 nm) for activation of substrate surface and polymerization process</li> <li>(2) Add the solution containing 1:1 mole ratio of NIAM and AM monomers with crosslinkers and periodate initiator on the activated substrate, and undergo copolymerization process by UV irradiation</li> </ul>
Advantages	<ul style="list-style-type: none"> <li>(1) Simple method and cost effective approach</li> <li>(2) Large-scale production is possible</li> </ul>
Disadvantages	<ul style="list-style-type: none"> <li>(1) Require supporting chemicals for polymerization</li> <li>(2) Need to control the grafted surface to be uniform</li> </ul>

### 2.3 Principle of photo-induced polymerization by UV irradiation

In photo-induced polymerization process, unstable excited species are produced by absorption of UV irradiation in photosensitizers. Those excited species attack upon monomers and undergo polymerization process by free-radical polymerization, which includes initiation, propagation, chain-transfer and termination as shown in the following [23].



where S = photosensitizer; M = monomer; R = free radical or polymer fragment.

During the initiation step, the excited photosensitizer ( $S^*$ ) induces a monomer to produce a free-radical initiation site ( $M^*$ ), and form a monomer radical ( $M\bullet$ ). This free radical undergoes a series of cross-linking reaction in propagation step. Finally, termination occurs by chain transfer when two radicals at the chain terminals of polymer fragments join to form a single bond. As the mechanism of free-radical production is initiated by UV irradiation, the influencing factors include irradiation source, wavelength and distance between source and the sample surface (i.e. intensity). The other influencing factors involved are concentration of photosensitizer, temperature, solvent and presence of oxygen [23, 24]. Therefore, provided that all the influencing factors are well selected to occur the whole process of photo-induced polymerization, there is still a fact to figure out how long it takes for the whole mechanism to take place.

### 2.4 Effect of irradiation intensity and exposure time on photo-polymerization

According to G. Wu et al. (2006), the effect of UV irradiation intensity, irradiation time and initiator concentration on the grafting yield has been researched on poly (N,N-diethylacrylamide) (PDEAAM) grafted onto the microfiltration nylon membranes. PDEAAM possesses both hydrophobic and hydrophilic groups in its



main structure with the LCST around 33°C. The grafting yield of PDEAAm on the membrane was analyzed by varying the intensity of UV irradiation (330 W high pressure mercury lamp and 254 nm) from 2.0 to 13.5 mW/cm<sup>2</sup> while keeping the initiator to monomer ratio (BP/DEAAm) at 0.05:1, fixed temperature at 50°C, and fixed irradiation time at 4 minutes. They have reported that grafting yield of PDEAAm increases with the increasing irradiation intensity from 2 mW/cm<sup>2</sup> to 13.5 mW/cm<sup>2</sup> as shown in Figure 2.3 [13].

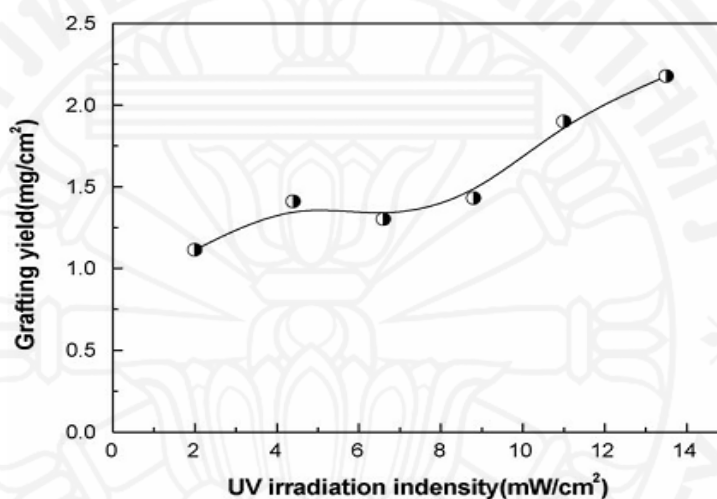


Figure 2.3: Relationship between the grafting yield and the irradiation intensity [13]

Then, they have also studied the effect of irradiation time and the ratio of initiator to monomer on grafting yield by using the intensity of 8 mW/cm<sup>2</sup>. From Figure 2.4, the grafting yield increases with the longer irradiation time, and becomes steady after 4–5 minutes for all ratios of initiator to monomer. The obtained grafting yield range of 1.03–2.88 mg/cm<sup>2</sup> has been studied on the ability to control the water flow rate through the membrane. From their results, the high grafting yield of 2.88 mg/cm<sup>2</sup> can efficiently control the water flow rate through the membrane at the working temperatures of 25–40°C [13]. Therefore, their research indicates that the optimum irradiation intensity, time, and concentration of initiators must be selected depending on the range of grafting yield suitable for application.

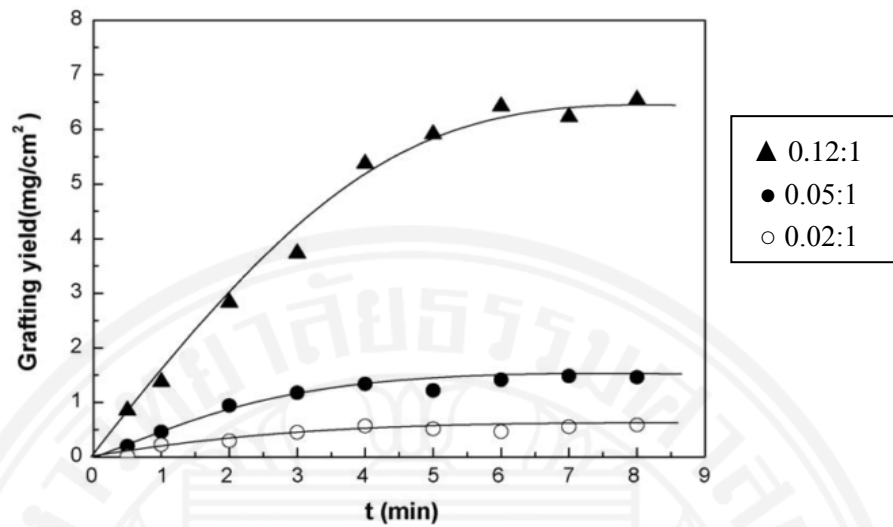


Figure 2.4 : Relationship between the grafting yield and the irradiation time at different ratios of initiator to monomer (BP/DEAAm) <sup>[13]</sup>

On the other hand, Uchida et al. have studied the effect of UV irradiation time on grafting poly (acrylic acid) (PAAc) onto the PET film by using sodium periodate as a photoinitiator in order to increase the surface wettability and adhesion property of PET film which is widely used in fiber and plastic industry. They found the advantage of using periodate initiator which avoids the degassing step. The grafted amount of PAAc on PET film and percent polymerization have been examined by varying the UV irradiation time from 30 to 300 minutes. As the UV irradiation time is increased up to 150 minutes, both of grafting density and percent polymerization jump up to the maximum and then, become stable as shown in Figure 2.5. Therefore, it is possible that a certain period time is required for all the steps in polymerization mechanism (i.e. starting from initiation to termination) to take place [25-27].

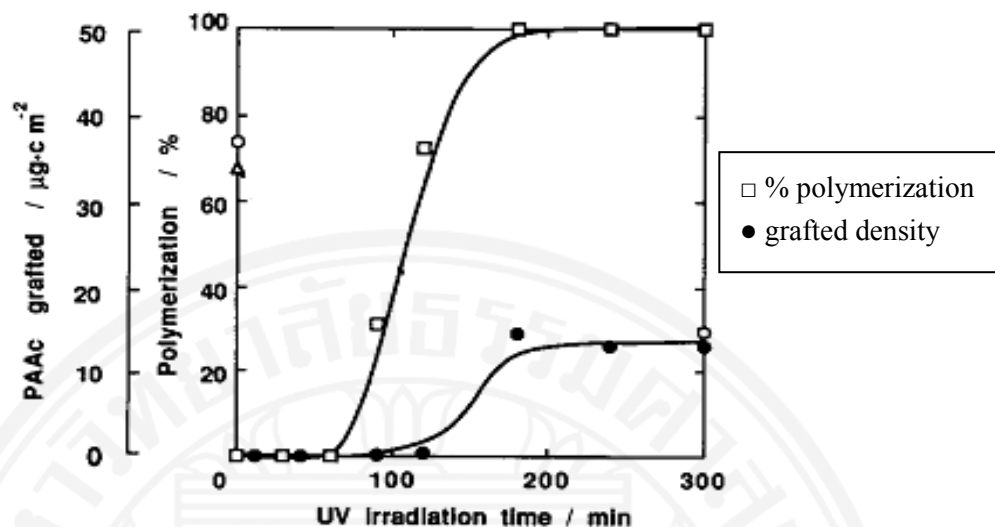


Figure 2.5: Effects of irradiation time on the graft polymerization of PAAc onto the PET film surface <sup>[26]</sup>

## 2.5 Effect of grafting density of PNIAM on cell adhesion/ detachment properties

The amount of grafted PNIAM on TCPS surface has a strong influence on the mobility of grafted PNIAM chain which leads to control the ability of PNIAM behavior that can respond to temperature. As a consequence, it affects the wettability of grafted surface as well as the cell adhesion and detachment process due to its uncontrollable hydrophobic–hydrophilic transition at its LCST. According to the research by Okano and his coworkers, the change in surface wettability and cell adhesion/ detachment properties of PNIAM-grafted surfaces with different graft densities and thicknesses are observed as shown in the following Table 2.2 [1, 14, 15].

Table 2.2 Surface wettability and cell adhesion/ detachment properties of PNIAM with different graft densities

	Graft amount ( $\mu\text{g/cm}^2$ )	Contact angle ( $\theta$ ) <sup>c</sup>		Cell adhesion	Cell detachment
		37°C	20°C	37°C	20°C
PIPAAm-1.4	1.4±0.1	77.9±0.6	65.2±1.2	Yes	Yes
PIPAAm-2.9	2.9±0.1	69.5±1.2	60.0±0.06	No	-
PIPAAm-5.0	1080	49.6 (40°C)	11.5 (10°C)	No	-

From the contact angle results, the change in surface wettability is observed as the graft density of PNIAM changes. The change in contact angle from  $80^\circ$  to  $65^\circ$  occurs on the grafted surface of  $1.4 \mu\text{g}/\text{cm}^2$ , indicating the transition of hydrophobic to hydrophilic property of PNIAM with respect to temperature. The higher the grafted amount of PNIAM, the smaller the contact angles at below and above LCST. They have also reported with an illustration (Figure 2.6) showing the behavior of different chain mobility for different amount of PNIAM grafted layers at human physiological temperature of  $37^\circ\text{C}$  [14, 15].

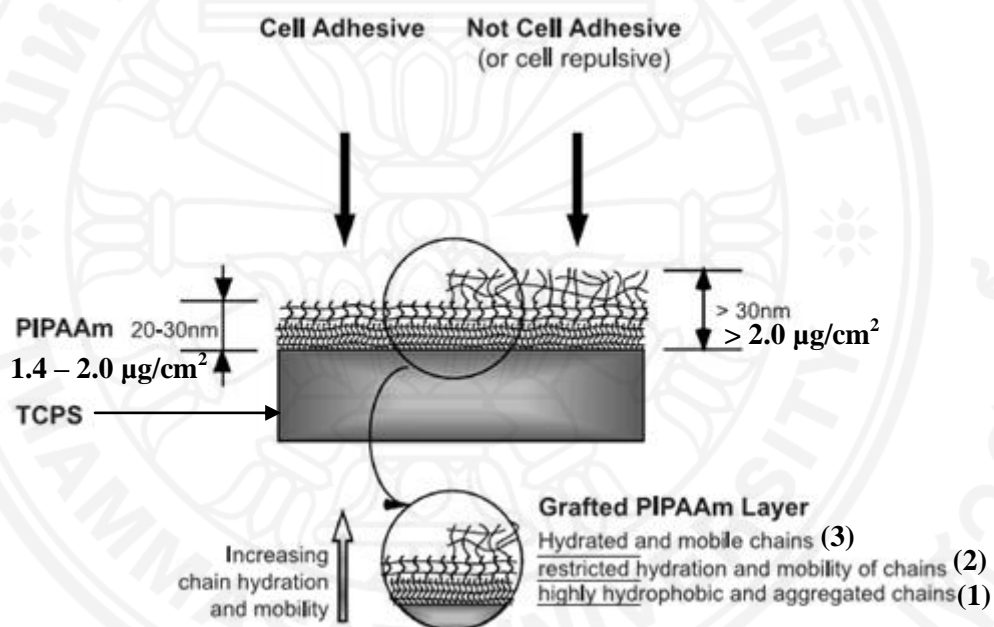


Figure 2.6: Influence of PNIAM-grafted densities on chain mobility and cell-adhesive characteristics [15]

The PNIAM grafted layers are divided into three layers depending on the change in interaction with the neighboring surface molecules in each layer. The first layer is the starting point of PNIAM covalently bonded to the hydrophobic TCPS surface. In this layer, the grafted chains have strong hydrophobic interaction, and resistance to hydration. Therefore, these chains aggregate and compact together on TCPS surfaces at  $37^\circ\text{C}$ . This behavior affects the neighboring surface molecules in the second layer of PNIAM grafted chains. Their chain mobility is also restricted so that they have weak interaction with water molecules at  $37^\circ\text{C}$ . These chains in the second layer possess temperature controlled chain mobility due to the consecutive

bonding between well-restricted chains from the first layer. PNIAM grafted surfaces with the graft density range of 1.4–2.0  $\mu\text{g}/\text{cm}^2$  falls in the second layer with restricted chain mobility. In the third layer with the grafted amount of more than 2  $\mu\text{g}/\text{cm}^2$  or 30 nm, restriction in PNIAM grafted chains is gradually reduced and relatively free to interact with water molecules. Therefore, it is obvious that the higher grafting density of PNIAM causes the great increase in grafted chain mobility leading to increase the hydrophilicity of surface even at 40°C [14, 15].

From the studies on various types of cell, this change in surface wettability of PNIAM grafted surfaces also affects on cell adhesion and detachment properties. In the second layer shown in Figure 2.6, the optimal grafting density for cell adhesion and detachment is observed between 1.4 and 2.0  $\mu\text{g}/\text{cm}^2$ . The grafted chains in this layer possess temperature controlled cell adhesion and detachment properties. This property is associated with the interaction between cell-adhesive protein, fibronectin (FN), and the PNIAM grafted surface. If the grafted density of PNIAM is lower than 1.4  $\mu\text{g}/\text{cm}^2$ , cell can adhere and proliferate on the surface but cell detachment cannot occur on that surface. Similarly, cells cannot adhere to the grafted surfaces with more than 2.0  $\mu\text{g}/\text{cm}^2$ . In the third layer, the interaction between the cell-adhesive proteins and the grafted surface is not strong enough to support cell attachment on the surface due to unlimited hydration and high chain mobility of PNIAM grafted layer at 37°C [15].

## **2.6 Characterization methods**

### **2.6.1 Attenuated Total Reflection Fourier Transform Infrared Spectroscopy (ATR-FTIR) measurement**

Attenuated Total Reflection (ATR) technique in combination with Fourier Transform Infrared Spectroscopy (FTIR) can be applied for both qualitative and quantitative analysis for PNIAM grafted TCPS surface. In this technique, the accessory is equipped with the ATR crystal which has the refractive index significantly greater than that of the sample so that total internal reflection process can occur. Moreover, there is no further preparation required for surface samples in this technique.

PNIAM grafted surface must be well-contact with the ATR crystal so that the evanescent wave coming out with  $0.5 \mu - 5 \mu$  beyond the crystal surface can strike on the sample surface and total internal reflection process can occur. The attenuated energy from each evanescent wave is passed back to the IR beam and followed by passing to the detector in the IR spectrometer as shown in Figure 2.7. This leads to generate an infrared spectrum [28].

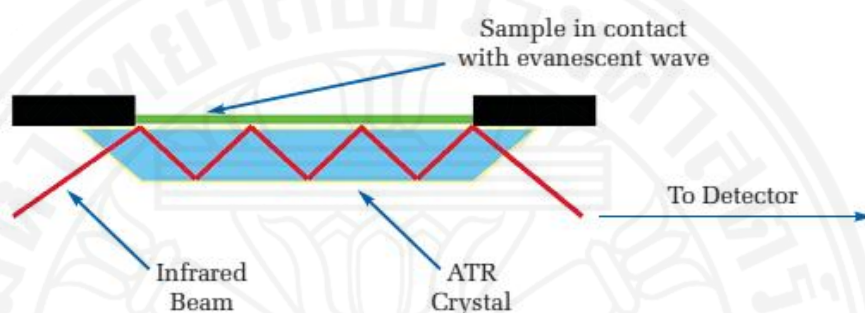


Figure 2.7: A multiple reflection in ATR system [28]

In qualitative analysis of FTIR spectrum, Wong-in et al. group determined the presence of the secondary amide ( $C=O$  stretching) at  $1663.1 \text{ cm}^{-1}$ , and secondary open chain amide at  $1551.2 \text{ cm}^{-1}$  in PNIAM grafted TCPS surface. These peaks are absent in the spectrum of the ungrafted TCPS but they are found in that of linear PNIAM as shown in Figure 2.8 [9].

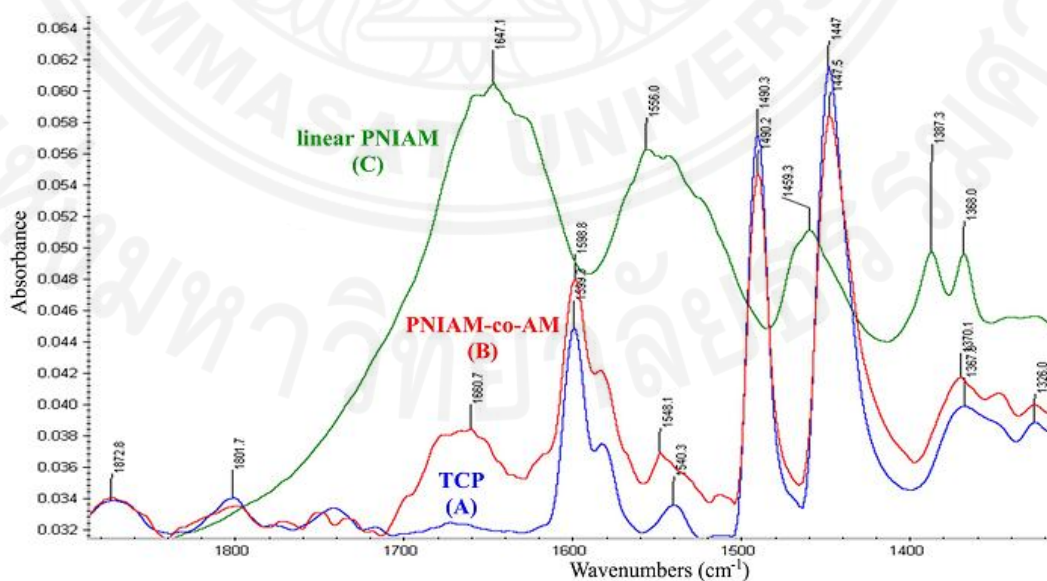


Figure 2.8: FTIR spectra of (A) ungrafted TCPS, (B) PNIAM-co-AM grafted TCP surface and (C) linear PNIAM, for wavenumbers ranging from 1800 to  $1400 \text{ cm}^{-1}$ . (The peak at around  $1660 \text{ cm}^{-1}$  represents the secondary amide in the AM copolymer)

From the studies of quantitative analysis, the reference peak used for polystyrene substrate was the mono-substituted aromatic ring with a strong absorption band at  $1600\text{ cm}^{-1}$ . The amide carbonyl (amide I) peak appeared in the region of  $1650\text{ cm}^{-1}$  was chosen as a characteristic peak of PNIAM. Hence, the relationship between the peak intensity ratio ( $I_{1650}/I_{1600}$ ) and the known amount of PNIAM cast on TCPS dishes ( $\mu\text{g}/\text{cm}^2$ ) was determined by constructing a calibration curve. That relation can be used to determine the unknown amount of PNIAM grafted samples by their respective peak intensity ratios [5, 14, 29].

### **2.6.2 KBr- Fourier Transform Infrared Spectroscopy (KBr-FTIR) measurement**

The KBr technique of FTIR measurement is usually applied for qualitative analysis of powdered form samples. In this technique, preparation step of sample is required before the measurement. The powdered samples must be able to mix with KBr, and can be pressed into a pellet form. As KBr cannot absorb infrared from FTIR, the characteristic peaks are produced by the different modes of vibration of molecules in the samples due to the excitation by energy from infrared.

According to Fundueanu et al. (2009), the IR spectra of linear PNIAM-co-AM and cross-linked microsphere PNIAM-co-AM have been compared to observe the cross-linked region ( $1000\text{--}1100\text{ cm}^{-1}$ ) as shown in Figure 2.9. The main characteristic peaks present in both linear and cross-linked PNIAM-co-AM are also circled in blue: N-H stretching in amide groups at  $3430\text{ cm}^{-1}$ , C=O stretching in secondary amide at  $1650\text{ cm}^{-1}$ , and  $\text{CH}_3$  vibration modes in isopropyl group at  $1387\text{--}1367\text{ cm}^{-1}$  [30].

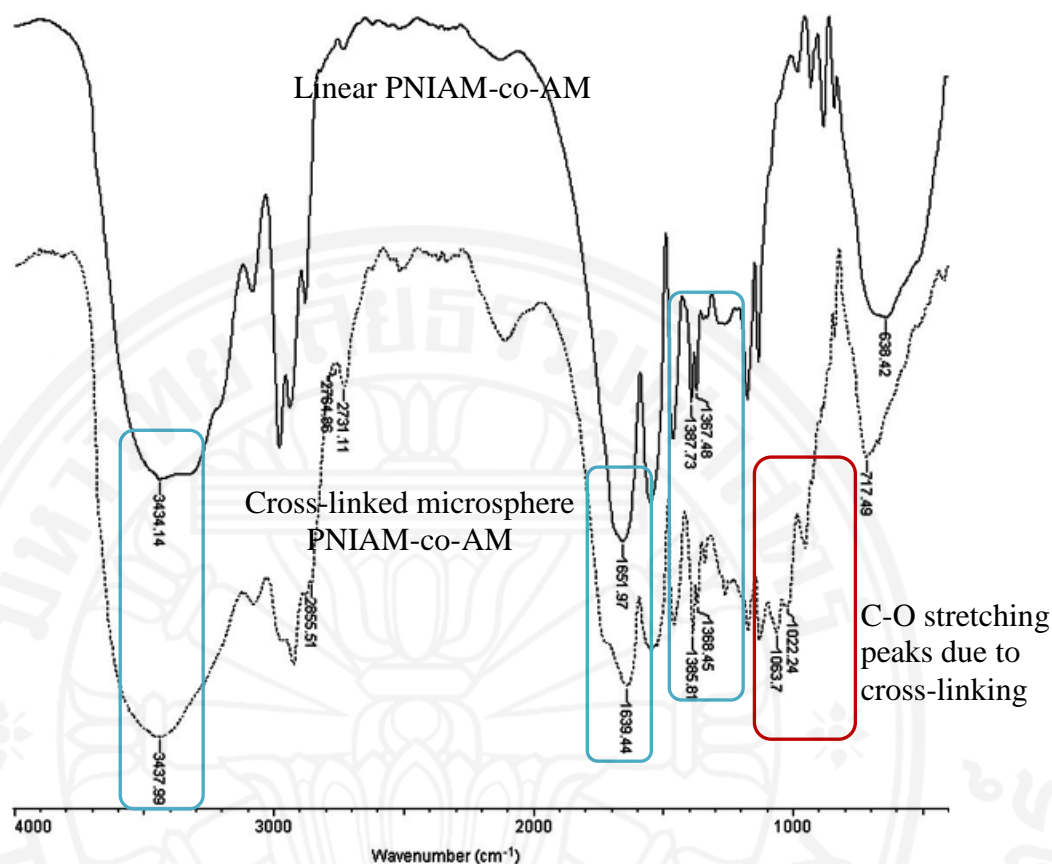


Figure 2.9: IR spectra of linear PNAM-co-AM and cross-linked microspheres<sup>[30]</sup>

### 2.6.3 Contact Angle Measurement

Contact angle measurement is used to characterize for the temperature-responsive behavior of PNAM in terms of the wettability of the surface. The wettability is determined by measuring the contact angle ( $\theta$ ) which is the angle between the tangent line drawn from the water droplet surface and the solid surface as shown in Figure 2.10.

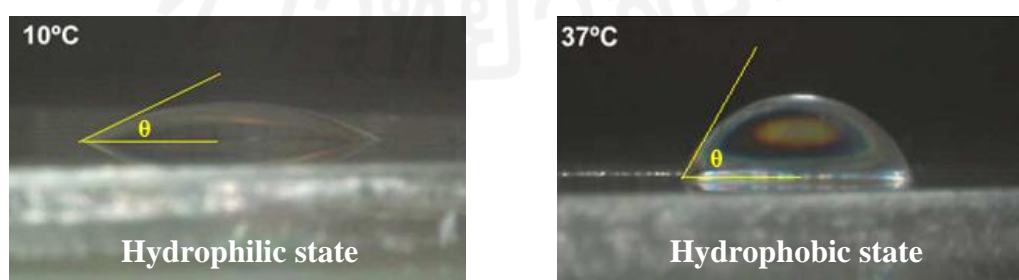


Figure 2.10: Temperature-dependent wettability changes for PNAM grafted surfaces at 10 °C and 37 °C<sup>[15]</sup>



The contact angle can demonstrate the water affinity behavior of PNIAM grafted surface at the temperature before and after phase transition of PNIAM (i.e. from 10°C to 37°C). In hydrophilic state at 10°C, the amide group of PNIAM will interact with water molecules through hydrogen bonding [31]. Thus, the drop of water spreads over the surface and the contact angle decreases. In the hydrophobic state at 37°C, there is only weak interaction between amide group and water molecules. Therefore, the drop of water does not spread and the contact angle increases [21].

In the research by Wong-in et al., the characteristic of PNIAM grafted surface can be observed at the temperature ranging from 20°C to 45°C while the contact angle measurement of ungrafted TCPS surface is taken as a control as shown in Figure 2.11. The contact angles of the ungrafted surface remain stable between 95° and 98° although the temperature is varied. On the other hand, the contact angles of the PNIAM grafted surface increase significantly from 58° to 75° when the temperature is increased from 30° to 35°C, respectively [9, 12]. Therefore, the result from contact angle measurement is useful indication of the temperature-responsive phase transition behavior of PNIAM grafted surface which is the required condition for the cell adhesive and detachment properties.

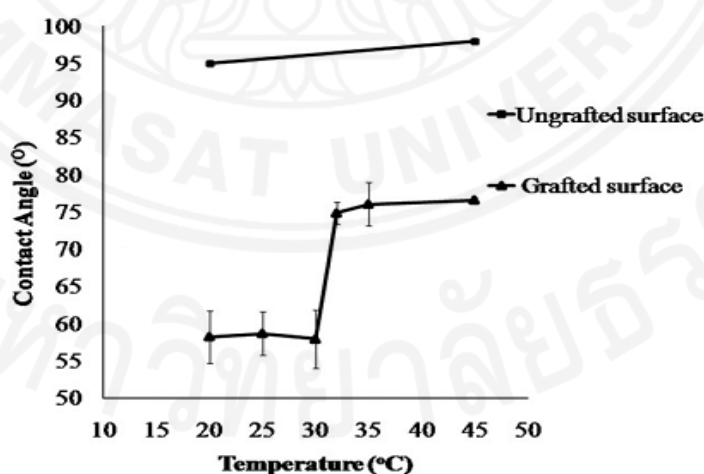


Figure 2.11: Contact angles of the PNIAM-co-AM grafted surface and ungrafted surface at various temperatures <sup>[9, 12]</sup>

## 2.6.4 Intrinsic Viscosity Measurement

Glass capillary viscometers are useful in intrinsic viscosity determination of macromolecules including polymers in the simplest way. The viscosity of solution correlates with the flow time through the glass capillary viscometer. The flow time of pure solvent ( $t_o$ ) and the flow time of polymer solution ( $t$ ) with different concentrations are required to perform the graphical determination of viscosity by constructing Huggins plot and Kraemer plot [32, 33]. A series of dilution can be done to obtain different concentrations of polymer solution.

In order to determine the intrinsic viscosity  $[\eta]$  by using Huggins plot ( $\eta_{sp}/c$  Vs.  $c$ ), the reduced viscosity ( $\eta_{sp}/c$ ) can be determined from the polymer concentration

$$(c) \text{ and the specific viscosity } (\eta_{sp}) \left( \eta_{sp} = \frac{t - t_o}{t_o} = \frac{t}{t_o} - 1 \right).$$

If the specific viscosity is related to the polymer concentration through the intrinsic viscosity by the power series (i.e.  $\eta_{sp} = k_o[\eta]c + k_1[\eta]^2c^2 + \dots$  where,  $k$  is constant and  $k_o = 1$ ), the Huggins equation is obtained dividing by the concentration and truncating to the second term ( $k_1[\eta]^2c$ ), and the y-intercept of Huggins plot ( $\eta_{sp}/c$  Vs.  $c$ ) gives the intrinsic viscosity.

**Huggins equation:**  $\boxed{\frac{\eta_{sp}}{c} = [\eta] + k_H [\eta]^2 c}$ ; where  $k_H$  is the Huggins constant

If Kraemer plot ( $\ln \eta_r/c$  Vs.  $c$ ) is applied, the relative viscosity ( $\eta_r$ ) can be determined by  $\eta_r = \frac{\eta}{\eta_o} \cong \frac{t}{t_o}$  due to the similar densities of solvent ( $\rho_o$ ) and polymer solution ( $\rho$ ) at very dilute concentration. As the relative viscosity ( $\eta_r$ ) correlates with

the specific viscosity ( $\eta_{sp}$ ) by  $\left( \eta_{sp} = \frac{t}{t_o} - 1 = \eta_r - 1 \right)$ , the Kramer equation is obtained

by rearranging the Huggins equation and taking natural logarithm, and the y-intercept of Kraemer plot ( $\ln \eta_r/c$  Vs.  $c$ ) gives the intrinsic viscosity [32, 33].

**Kraemer equation:**  $\boxed{\frac{\ln (\eta_r)}{c} = [\eta] + k_K [\eta]^2 c}$ ; where  $k_K$  is the Kraemer constant

Figure 2.12 shows the example of intrinsic viscosity determination by Huggins plot and Kraemer plot in which the extrapolation of two plots reach the same y-intercept indicating the viscosity of resulting polymer solution.

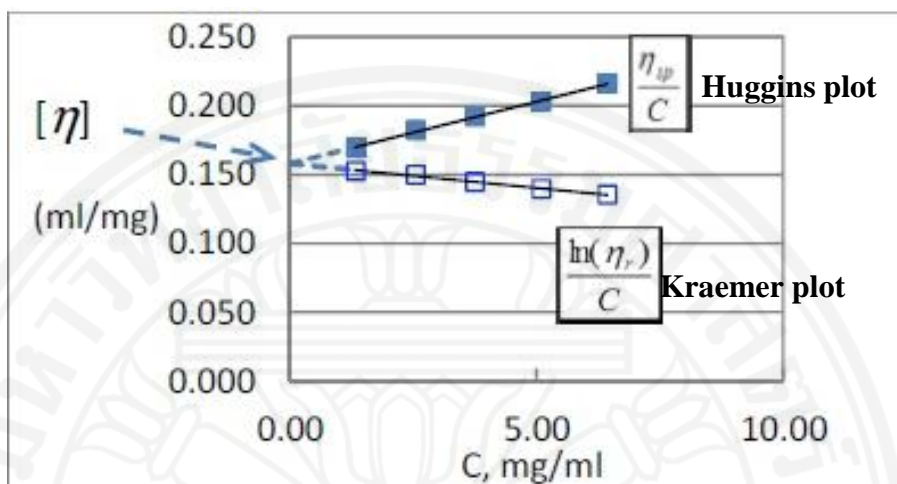


Figure 2.12: Graphical determination of the intrinsic viscosity

From the research by Mumick et al., the intrinsic viscosity determination of PNIAM-co-AM with different monomer ratios has been studied. With the use of intrinsic viscosity as an indication for the volume occupied by a single polymer chain, they have explained the effect of temperature on the behavior of PNIAM-co-AM with the monomer ratio of NIAM/AM = 85 by using intrinsic viscosity [34].

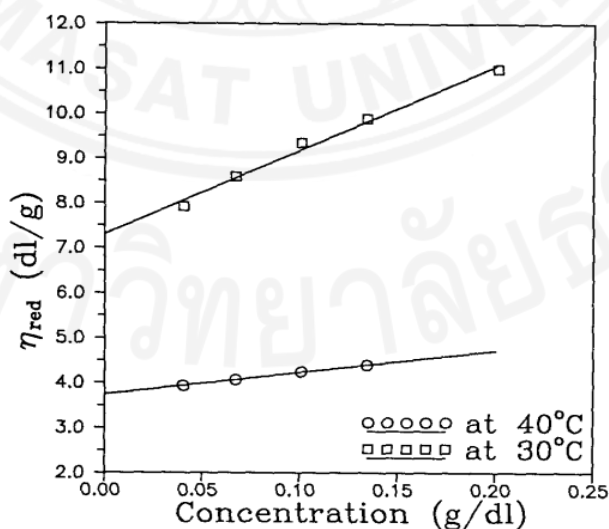


Figure 2.13: Reduced viscosity Vs. concentration of PNIAM-co-AM (NIAM/AM=85) in deionized water at 30°C and 40°C [34]

From Figure 2.13, the intrinsic viscosity of that copolymer solution at 30°C (7.3 dl/g) is higher than its intrinsic viscosity at 40°C (3.7 dl/g). It indicates that the volume occupied by each polymer chain is getting smaller as the temperature increases. Considering the behavior of PNIAM, the hydrophobic property of PNIAM starts to show as closer to its LCST. Thus, at 30°C (nearly LCST), the copolymer chains become compact and have a globule-like conformation. Therefore, the lower intrinsic viscosity at 40°C explains the smaller volume occupied by each chain and more compact globule conformation of the copolymer [34].

## Chapter 3

### Methodology

The methodology is categorized into five parts: (1) Overview of the UV-induced grafting method and required materials; (2) Procedures of grafting PNIAM-co-AM on TCPS surface; (3) Synthesis of linear PNIAM-co-AM; (4) Preparation of measurement for each characterization method; (5) Protocol for cell study analysis.

#### 3.1 Materials required for UV-induced grafting of PNIAM-co-AM on PS surface

- 6-Watt, 254 nm (Model: UVGL-58) Handheld UV Lamp
- 35 mm x 10 mm Tissue Culture Polystyrene (TCPS) dishes

Table 3.1 Chemicals required for UV grafting process

Monomers	Recrystallized <i>N</i> -isopropylacrylamide (NIAM)
	Acrylamide (AM)
Crosslinking agent	<i>N,N'</i> -Methylenebisacrylamide (MBAAm)
Photoinitiator	Potassium periodate (KIO <sub>4</sub> )
Antiseptic solution	90% Ethanol

Note that *N*-isopropylacrylamide (NIAM) was purified by re-crystallization in *n*-hexane at -5°C. Other chemicals were used without further treatment.

#### 3.2 Overview of UV-induced grafting mechanism

The flow chart below shows the overview of steps in UV induced grafting procedure.

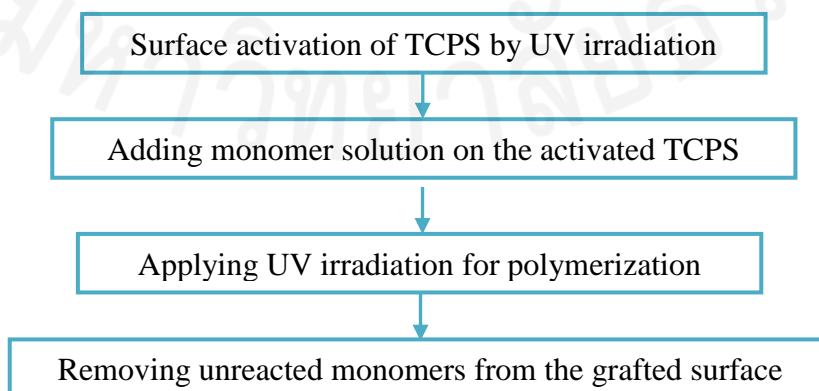


Figure 3.1 Basic steps in UV-induced grafting procedure

The following factors should be considered in the steps of UV-induced polymerization. (The detail mechanism of polymerization process is shown in Appendix C.)

1) Sufficient UV exposure time for surface activation of TCPS surface

According to Curti and Moura (2002), the optimum UV exposure time for activation of PS surface has been determined by drop water contact angle measurements (DWCA). Their results show the decrease in the contact angle as the UV exposure time is increased. The increase in formation of free radicals on the PS surface causes more interaction with the hydrogen ions in water and therefore, the surface hydrophilicity increases which means that the reactive sites on the surface also increase. The optimum UV irradiation time has been chosen at 30 – 40 minutes [21].

2) Require immediate UV exposure to the monomer solution

In the second step, after adding monomer solution onto the activated TCPS surface, there is no radicals formed in the monomers to capture the active sites on the polystyrene. Therefore, after the solution is well spread on the activated surface, UV irradiation must be exposed to initiate the polymerization process.

3) Sufficient UV intensity and exposure time for polymerization

In order to figure out the influence of UV intensity and exposure time on the polymerization process, the UV intensity at different exposure distances was checked by a UV light meter (model: YK-37UVSD), and the UV energy obtained from the (6W, 254 nm) lamp is determined by the equation:

$$\text{UV energy (E)} = \text{UV intensity (I)} \times \text{Exposure time (t)}$$

Figure 3.2 shows the relationship between UV intensity at different exposure distances. UV intensity at zero exposure distance is about 5 times higher than the intensity at 10 cm exposure distance, and the intensity at 10–15 cm exposure distance falls in the minimum range for activation.

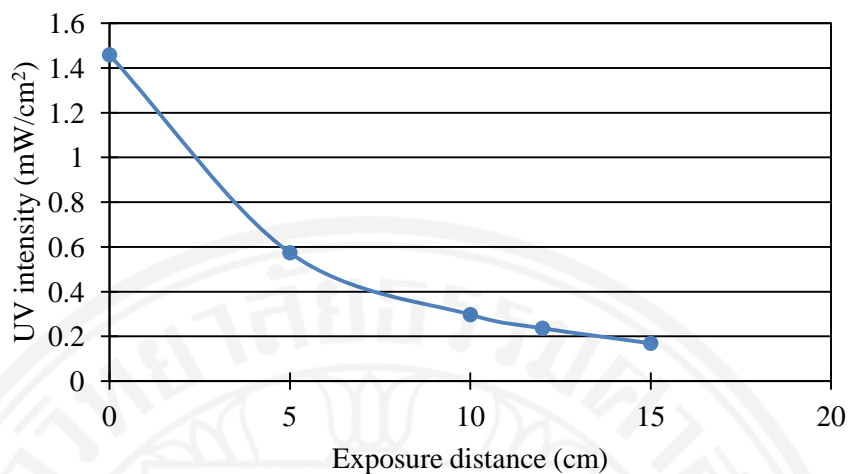


Figure 3.2: Relationship between UV intensity and distance

By using the above equation ( $E = I \times t$ ), the UV energy obtained at 10 cm distance for 1 hour exposure (note that it is a working condition done by Wong-in et al. [9, 12] ) was compared with the energy obtained at 0 cm for 10, 15 and 20 minutes exposure, and the results were compared in Table 3.2.

Table 3.2 Comparison of UV energy at the exposure distance of 0 cm and 10 cm

Distance (cm)	UV intensity (mW/cm <sup>2</sup> )	Time (minutes)	Energy (mJ/cm <sup>2</sup> )
0	1.459	10	875.4
		15	1313.1
		20	1750.8
10	0.297	60	1068.8

### 3.3 Procedures for grafting PNIAM-co-AM on TCPS surface

Two approaches were performed; (1) comparison of intensity and exposure time influence on polymerization, and (2) time study of UV polymerization time after controlling other influencing parameters.

#### 3.3.1 Preparation of PNIAM-co-AM grafted TCPS surface using the protocol in Wong-in et al.

Based on the procedure by Wong-in et al., the influence of intensity and exposure time on the polymerization process was compared. UV polymerization was

carried out at the exposure distance of 10-15 cm for 1 hour and at zero distance exposure for 10,15 and 20 minutes.

1. Apply UV light (6-Watt, 254 nm) to the TCPS dish for 30 minutes to activate the PS surface.
2. Prepare the monomer solution based on 500  $\mu\text{L}$  for one TCPS dish:

Chemicals	C (mol/L)	Weight (g)
NIAM	1	0.0566
AM	1.04	0.0370
MBAAm	0.02	$1.542 \times 10^{-3}$
KIO <sub>4</sub>	0.005	$0.575 \times 10^{-3}$

3. Add 500  $\mu\text{L}$  of solution to each TCPS dish.
4. Cover the dish with Aluminum foil and keep it overnight.
5. Remove 200  $\mu\text{L}$  of solution and then apply UV light for polymerization process.
6. Dry the dish under vacuum condition at room temperature for 24 hours.
7. Wash the dish with 90% ethanol for 3 times.
8. Keep the dish in the vacuum oven for 24 hours to evaporate ethanol.

The resulting grafted surfaces were checked by ATR-FTIR measurement to confirm the existence of PNIAM-co-AM on TCPS surface.

### 3.3.2 Preparation of PNIAM-co-AM grafted TCPS surface with varying UV exposure time

The surface of commercial TCPS dishes were activated by applying UV light for 30 minutes. In the following step, 30  $\mu\text{L}$  of aqueous solution containing monomers NIAM (1 mol/L), AM (1.04 mol/L), crosslinker MBAAm (20 mmol/L) and photoinitiator KIO<sub>4</sub> (5 mmol/L) was added to each TCPS dish and spin-coating machine was used to spread the solution uniformly on the surface by operating at the spinning speed of 1500 rpm for 5 minutes. Then, the dishes were exposed to UV light immediately for polymerization at different exposure times starting from 30 minutes,



1 hour, 1.5 hours, 2 hours, 2.5 hours and 3 hours. The PNIAM-co-AM grafted TCPS dishes were kept at room temperature under vacuum condition for 24 hours. After that, the dishes were washed with ethanol three times to remove unreacted monomers and dried in the vacuum oven for another 24 hours. Figure 3.3 schematically shows the grafting procedure.

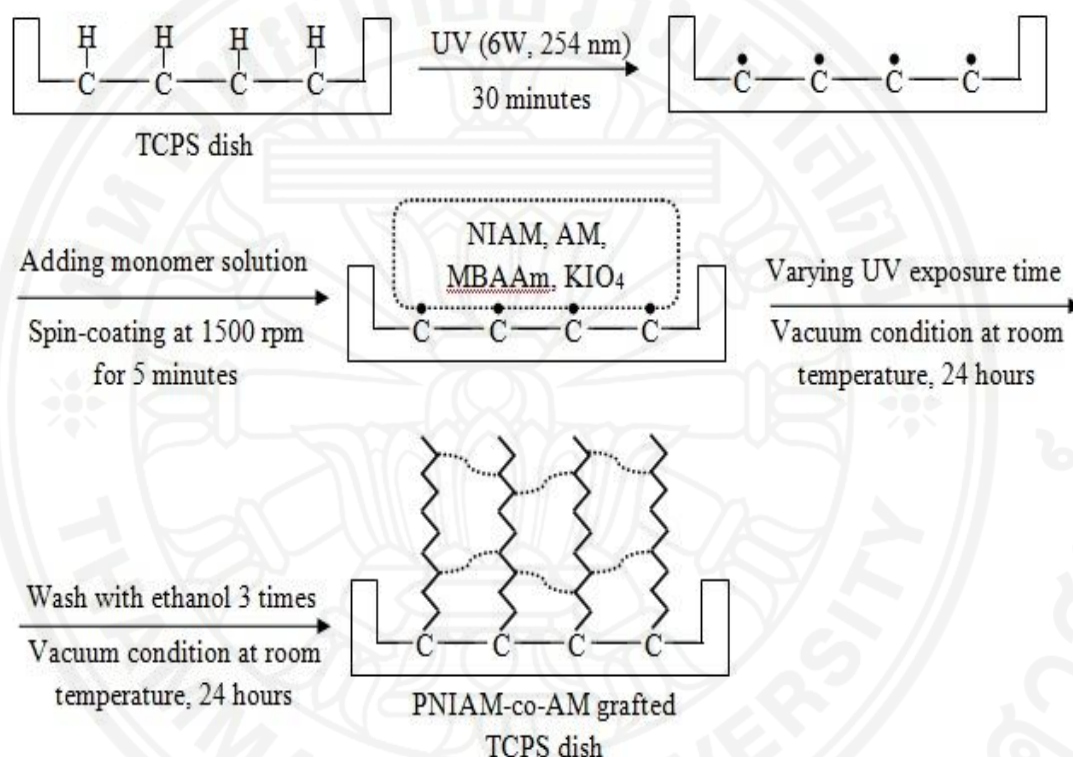


Figure 3.3: The schematic of UV induced grafting polymerization of PNIAM-co-AM on TCPS surface

Note that in this procedure, the spin-coating technique (unpublished report) was applied to control the uniformity of grafted surface.

### 3.4 Synthesis of linear poly(N-isopropylacrylamide-co-acrylamide)

Three types of synthesis of PNIAM-co-AM by free radical polymerization were performed. The materials and compositions used in each synthesis were shown in Table 3.3 and Table 3.4.

### 3.4.1 Materials required for synthesis

Table 3.3: Synthesis of PNIAM-co-AM (1:1 ratio)

Materials	% wt	C (mol/L)	Amount in 100 mL DI water
N-isopropylacrylamide (NIPAAm)	1.3	0.1105	1.3 g
Acrylamide (AAm)	0.8	0.1161	0.8 g
Ammonium persulfate (APS)	0.5	0.022	0.5 g

Table 3.4: Synthesis of PNIAM-co-AM (2:1 ratio)

Materials	% wt	C (mol/L)	Amount in 100 mL DI water
N-isopropylacrylamide (NIPAAm)	2.5	0.2251	2.5 g
Acrylamide (AAm)	0.8	0.1125	0.8 g
Ammonium persulfate (APS)	0.5	0.022	0.5 g

Note that synthesis of 2:1 ratio of PNIAM-co-AM was performed in order to use in the further study of calibration curve construction.

### 3.4.2 Procedure of synthesizing PNIAM-co-AM

De-ionized water was added to a three-necked bottle and nitrogen gas was purged into the water for 1 hour to create an inert atmosphere. After 1 hour, NIAM and AM monomers were added into the de-ionized water. When all monomers were completely dissolved, ammonium persulfate was added as an initiator. Then, degassing process was stopped and the solution was heated up to 55–60°C. The temperature was maintained at 55–60°C for 3 hours under inert atmosphere. The synthesized co-polymer, PNIAM-co-AM, was precipitated in acetone and dried in the oven at room temperature for 24 hours.

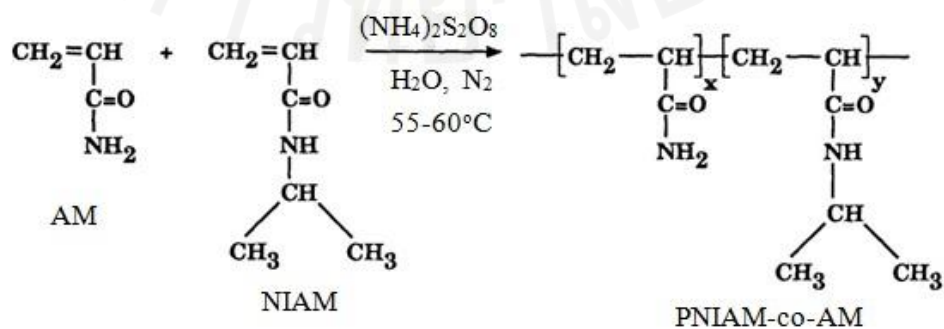


Figure 3.4: Copolymer synthesis of PNIAM-co-AM

Note that the temperature maintained for synthesis of 2:1 ratio of PNIAM-co-AM was 50–55°C, and the re-precipitation in acetone was required after filtration of resulting polymer due to cross-linking.

### **3.5 Characterization methods**

Four characterization methods were performed; (1) KBr-FTIR measurement, and (2) Intrinsic viscosity determination for synthesized PNIAM-co-AM; (3) Quantitative analysis by ATR-FTIR measurement, and (4) Contact angle measurement for PNIAM-co-AM grafted TCPS surfaces.

#### **3.5.1 KBr-FTIR measurement for synthesized PNIAM-co-AM**

In order to perform the characterization of synthesized PNIAM-co-AM, KBr-FTIR technique was used to identify the functional groups in the co-polymer and the mixed monomers of NIAM and AM in the percent weight ratio of 1.3: 0.8. In the KBr-FTIR technique, samples were mixed with KBr powder and pressed to make a pellet. The pellets were examined by Fourier Transform Infrared Spectroscopy (FTIR) Thermo Scientific (Nicolet iS5) (iD1 - Transmission). The spectra were measured in the range of 500-4000  $\text{cm}^{-1}$  with 64 scans and a spectral resolution of 2  $\text{cm}^{-1}$ .

#### **3.5.2 Intrinsic Viscosity Determination**

The intrinsic viscosity measurement was carried out to determine the viscosity of the synthesized linear PNIAM-co-AM samples. The samples were dissolved in de-ionized water and the flow time measurement was taken at 10, 20 and 37°C by using the capillary viscometer of the Cannon-Fenske Routine Viscometer type (75 P573, CANNON). The solution was maintained at a constant temperature within  $\pm 0.1^\circ\text{C}$  for 10-15 minutes during the measurement by using a temperature-controlled water bath as shown in Figure 3.5.



Figure 3.5: A temperature-controlled water bath and a viscometer chamber

The flow time of pure solvent ( $t_0$ ) and the flow of polymer solution ( $t$ ) at different concentrations was recorded three times for each measurement and the average value was taken. The copolymer solutions of lower concentrations were obtained by successive dilution. First, 40 mg of PNAM-co-AM was dissolved in 10 mL of DI water, and the concentration was reduced by adding 5 mL of water in a series of dilution until 6<sup>th</sup> or 7<sup>th</sup> dilution. In order to construct the Huggins plot and the Kraemer plot, the specific viscosity ( $\eta_{sp}$ ) and the relative viscosity ( $\eta_r$ ) were determined as following:

$$\eta_{sp} = \frac{t}{t_0} - 1 ; \eta_r = \frac{t}{t_0}$$

The y-intercept of these two plots can be extrapolated to determine the intrinsic viscosity as shown in the following equations.

$$\text{Huggins equation: } \frac{\eta_{sp}}{c} = [\eta] + k_H [\eta]^2 c$$

$$\text{Kraemer equation: } \frac{\ln(\eta_r)}{c} = [\eta] + k_K [\eta]^2 c$$

### 3.5.3 Quantitative analysis by ATR-FTIR measurement

As for the PNAM-co-AM grafted TCPS surfaces, Attenuated Total Reflection (ATR) in combination with FTIR was also applied to investigate the surfaces. The ATR accessory was equipped with a diamond ATR crystal. The surfaces were placed over the ATR crystal and measured by single bounced ATR-FTIR (iD7) (Nicolet iS5)

(Thermo Scientific). The spectra were measured in the range of 525-4000  $\text{cm}^{-1}$  with 64 scans and a spectral resolution of 2  $\text{cm}^{-1}$ .



Figure 3.6: FTIR with a diamond ATR crystal (Single bounce technique)

### 3.5.3.1 Preparation of known concentration for calibration curve construction

In order to perform the quantitative analysis by ATR-FTIR technique, a calibration curve was required to find out the relationship between the known amount of grafted PNIAM-co-AM and the intensity ratio or area ratio of characteristic peaks. Therefore, known concentrations of linear PNIAM-co-AM was prepared in the mixed solvent 2-propanol and methanol in the ratio of 1:1 and the amount of grafted PNIAM-co-AM on TCPS surface in  $\mu\text{g}/\text{cm}^2$  was determined as shown in Table 3.5.

Table 3.5: Pre-determined concentrations of PNIAM-co-AM based on the expected range of grafting density ( $\mu\text{g}/\text{cm}^2$ )

Amount of PNIAM-co-AM ( $\mu\text{g}/\text{cm}^2$ )	Amount of PNIAM-co-AM on PS dish ( $\mu\text{g}$ )*	C (mg/mL)
5	48.11	0.24
3	28.86	0.144
2	19.24	0.096
1	9.62	0.048
0.5	4.81	0.024

\*Note: Amount of PNIAM-co-AM solution added to cover the whole surface area of PS dish ( $A = \pi(3.5)^2/4 = 9.621 \text{ cm}^2$ ) is 200  $\mu\text{L}$ .

### 3.5.3.2 Procedure for calibration curve construction

The control sample was also prepared by adding 200  $\mu\text{L}$  of mixed solvent into the PS dish. The solution was vaporized for overnight and then, the samples were measured by a single bounced ATR-FTIR. Two characteristic peaks were chosen to determine the peak intensity ratio and peak area ratio for analysis. The first peak was the secondary amide group from PNIAM-co-AM at the wavenumber of  $1654\text{ cm}^{-1}$  due to C=O stretching vibration. The second one was the benzene group from polystyrene at  $1600\text{ cm}^{-1}$  due to C-C stretching vibration in aromatic ring which were taken as a reference peak.

The area of these two peaks was determined for the known amount of PNIAM-co-AM grafted surfaces, and a calibration curve was constructed between the peak area ratio ( $A_{1654}/A_{1600}$ ) and the known grafted amount of PNIAM-co-AM. As the use of single bounced ATR, the measurement was taken at eight different positions to confirm the grafted amount at every point, which are 4 peripheral positions and 4 positions at 1 cm around the center as shown below.

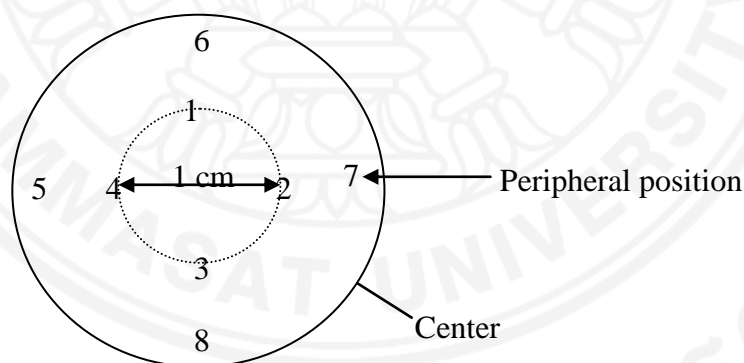


Figure 3.7 Positions on a PNIAM grafted surface selected for ATR measurement

### 3.5.4 Contact angle Measurement

The contact angle measurement was used to investigate the hydrophobic-hydrophilic transition of the PNIAM-co-AM grafted surfaces with response to its LCST. An un-grafted polystyrene surface was used as a control. The sample was kept on a heat-exchanger aluminium plate which was connected to the water bath to control the temperature at  $40^{\circ}\text{C}$  and  $10^{\circ}\text{C}$ . The experiment set up for measurement was shown in Figure 3.8.



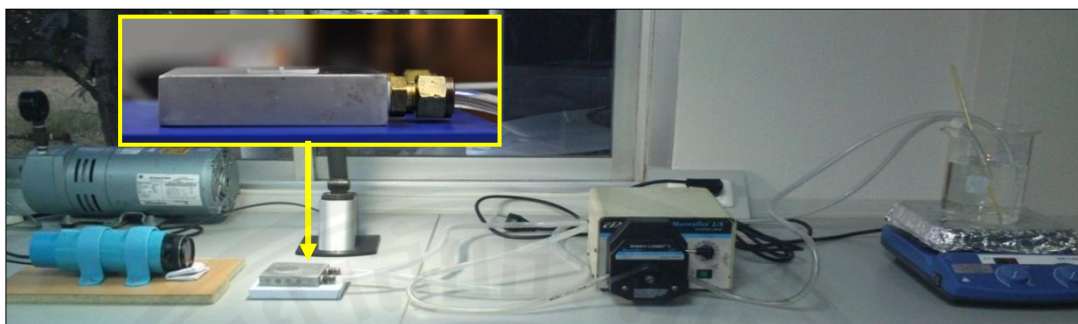


Figure 3.8: Sample placed on a heat-exchanger aluminum plate in the set up for contact angle measurement

The samples were allowed to equilibrate 15 minutes before each measurement. The image of water droplet on each sample was captured at three different positions and the contact angles were measured by using ImageJ program. Then, the average angle of each sample was calculated.

### 3.6 Protocol for cell study analysis

The primary human dermal fibroblast (HDFa) (passage 8-11) were provided by Faculty of Medicine, Chulalong-korn University (Thailand). The cell was maintained in the medium that consisting of DMEM and Ham's F12 medium at a 3:1 ratio, supplemented with 10% FBS and 1% of Antibiotic-Antimycotic, and all cells were cultured at 37 °C with 5% CO<sub>2</sub>. In the pre-construction step, the PNIAM-co-AM grafted culture plates were sterilized by using acidic ethanol (70% EtOH) and were washed twice in sterile phosphate buffered saline (PBS).

For cell harvesting, PNIAM-co-AM grafted TCPS dish with 1-hour and 2-hour UV polymerization time were used. The cell was seeded onto the co-polymer grafted dishes in intensity of  $3.5 \times 10^5$  cell/cm<sup>2</sup>. Then, the dishes were kept in the 37°C incubator for 24 hour or until 100% confluency. In harvesting monolayer cell sheet, the medium was changed to the fresh medium without serum which was warmly kept at 37°C. Then, the culture dishes were kept at the low temperature incubation for two steps; 10°C for 30 minutes, and followed by 20°C for 60 minutes. The sheet was transferred to a new dish by pipette and kept the sheet attach to the surface for 60 minutes.

## Chapter 4

### Result and Discussion

This chapter is divided into four main parts on discussion: (1) Results of FTIR and intrinsic viscosity for synthesized PNIAM-co-AM; (2) Grafting density results of PNIAM-co-AM grafted surfaces with different UV polymerization times; (3) Contact angle results of PNIAM-co-AM grafted surfaces; (4) Cell study analysis results (prepared by Ms. Kanokaon Benchapathanphorn, KMUTT).

#### 4.1 Characterization results of synthesized PNIAM-co-AM

##### 4.1.1 Peak analysis in KBr-FTIR spectra of PNIAM-co-AM

In this section, KBr-FTIR measurement was used to check whether the copolymer obtained from synthesis was linear or cross-linked. Linear PNIAM-co-AM is required to use in calibration curve construction. The functional groups responsible for the occurrence of main characteristic peaks in KBr-FTIR spectra are shown in the structures of linear PNIAM-co-AM and two monomers NIAM and AM (Figure 4.1).

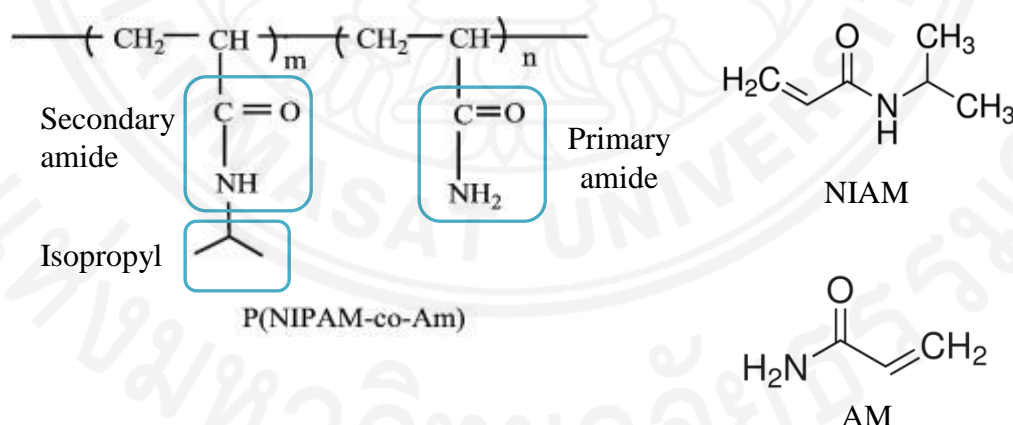


Figure 4.1: Structures of linear PNIAM-co-AM and its monomers

From the characterization by KBr-FTIR technique, the characteristic peaks of linear PNIAM-co-AM which includes primary amide, secondary amide (Amide I, II, III band) and isopropyl groups [30, 35, 36] were observed in the FTIR spectrum of synthesized linear PNIAM-co-AM as shown in Figure 4.2. Those characteristic peaks were also confirmed by the FTIR spectrum of the mixed monomers NIAM and AM



shown in Figure 4.3. Two double bond peaks in the spectrum of mixed monomers at the wavenumber of  $1426\text{ cm}^{-1}$  (due to  $\text{CH}_2=$  vibration) and  $1620.9\text{ cm}^{-1}$  ( $\text{C}=\text{C}$  stretching) [37] were disappeared in the spectrum of linear PNIAM-co-AM. The peak absorptions at the respective wavenumbers together with assignment of each functional group are indicated in Table 4.1.

Table 4.1: Characteristic absorption peaks in FTIR spectrum of synthesized linear PNIAM-co-AM [30, 35, 36]

Absorption peaks at wavenumber ( $\text{cm}^{-1}$ )	Functional group
3430 – 3437	N-H stretching of primary ( $\text{CONH}_2$ ) and secondary amide ( $\text{CONH}$ )
2872 – 2975	Asymmetric and antisymmetric stretching of C-H bond
~ 1650	C=O stretching (Amide I band) of secondary amide
1559 – 1547	N-H bending motion (Amide II band) of secondary amide
1459 – 1368	Asymmetric $\text{CH}_3$ deformation and $\text{CH}_3$ bending of isopropyl – $\text{C}(\text{CH}_3)_2$ group
~ 1172	C-N stretching in secondary amide (Amide III band)
~ 1131	$\text{CH}_3$ rocking vibration in – $\text{NH.C}(\text{CH}_3)_2$
619 – 669	$\text{NH}_2$ deformation vibration in primary amide

In the synthesis of the copolymer in 2:1 ratio, gel formation occurred as the concentration of monomers was increased. In Figure 4.4, the cross-linked peaks were found in 2:1 ratio of PNIAM-co-AM at  $1026$  and  $1079\text{ cm}^{-1}$ . Cross-linking between amide groups in copolymerization process resulted in the C–O bond vibration. This cross-linked region disappeared after removing some cross-linked parts by filtration and re-precipitation as much as possible.

The resulting linear PNIAM-co-AM of 1:1 mole ratio was used to prepare the known concentrations of PNIAM-co-AM for plotting calibration curve in quantitative analysis of ATR-FTIR measurement. The linear 2:1 ratio of PNIAM-co-AM will be used for further study of calibration curve construction when the monomer ratio is increased.

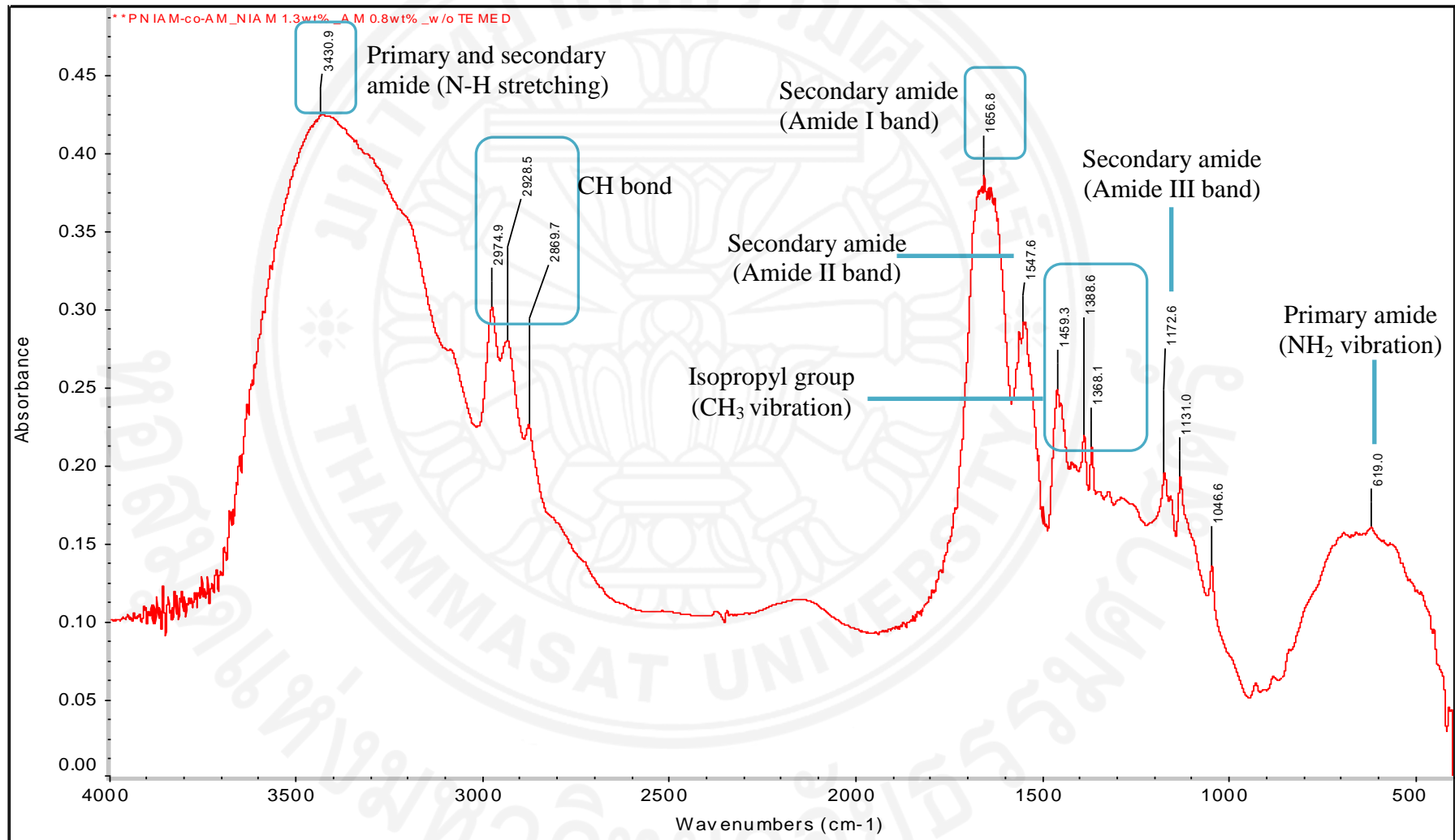


Figure 4.2: KBr-FTIR spectrum of linear PNIAm-co-AM (1:1 ratio)

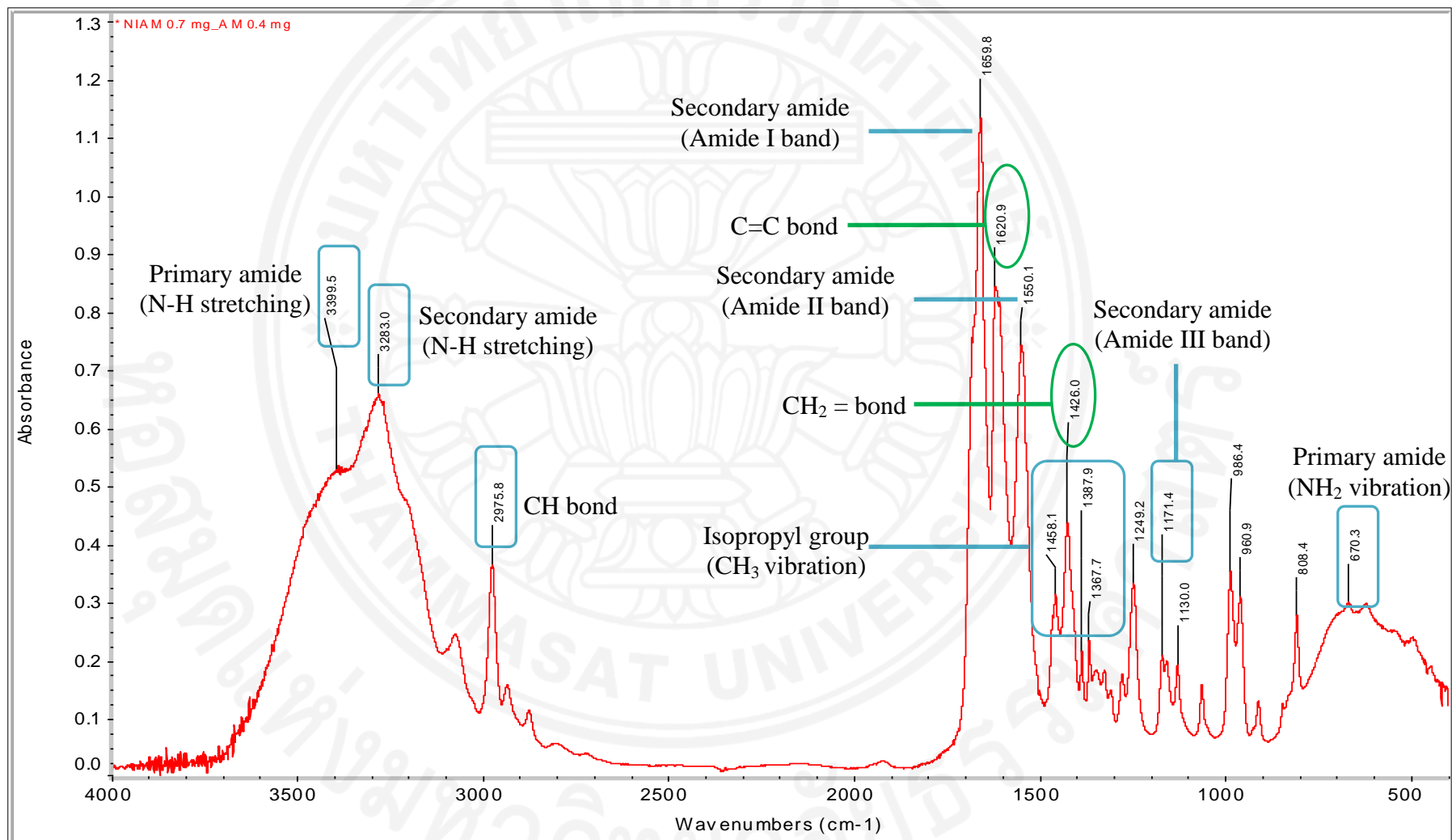


Figure 4.3: KBr-FTIR spectrum of recrystallized NIAM and AM monomers

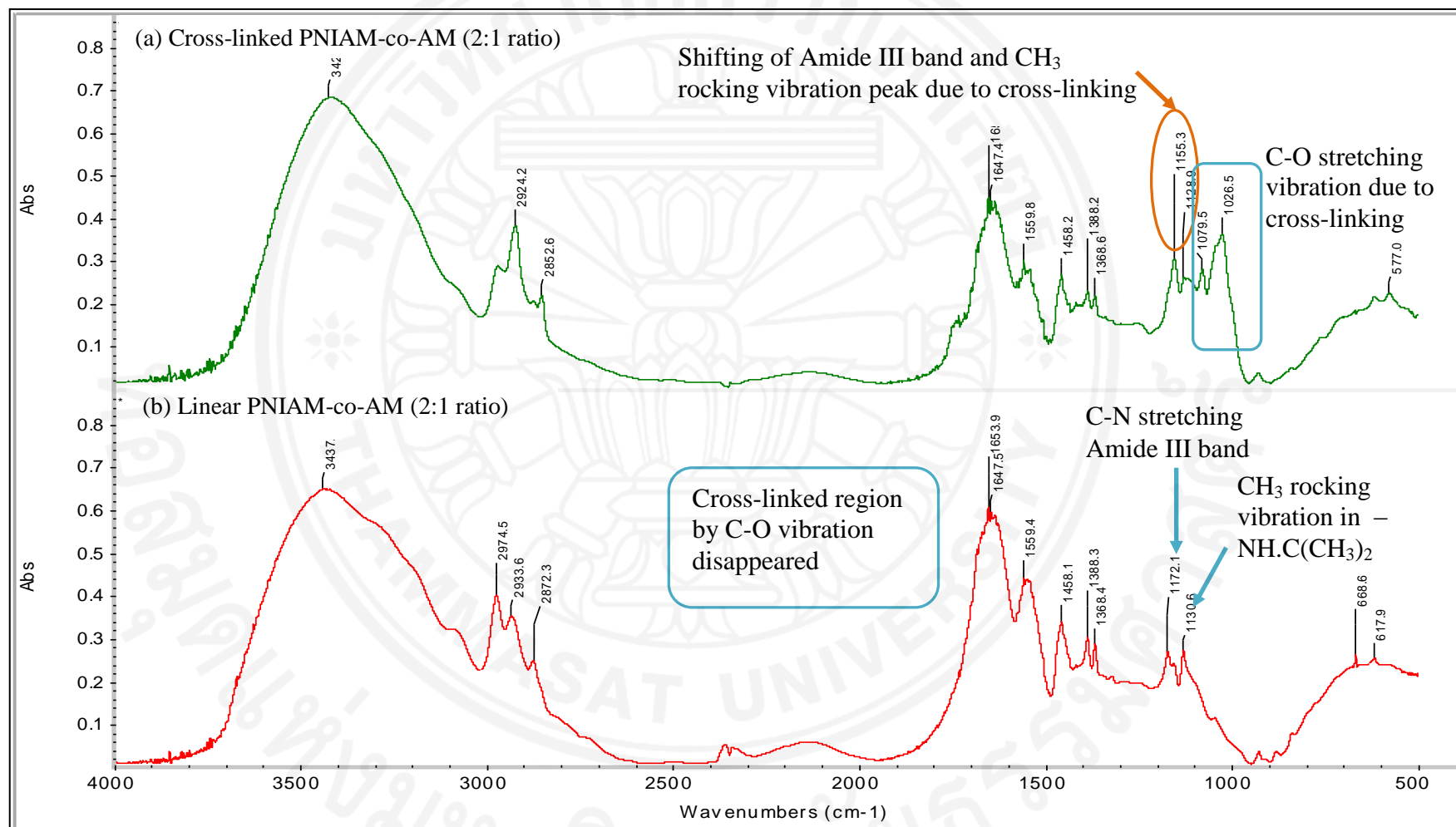


Figure 4.4: Comparison of KBr-FTIR spectra of (a) crosslinked PNIAm-co-AM (2:1 ratio) and (b) linear PNIAm-co-AM (2:1 ratio) after reprecipitation

#### 4.1.2 Results of intrinsic viscosity measurement at different temperatures

As a supplementary analysis for the linear PNIAM-co-AM (1:1 ratio and 2:1 ratio) obtained from synthesis, intrinsic viscosity measurement of that copolymer was carried out at 10, 20 and 37°C in aqueous solution. The average flow time (t) decreased as the concentration was lowered after each dilution.

The parameters such as the reduced viscosity ( $\eta_{sp}/c$ ) and relative viscosity ( $\eta_r$ ) at different polymer concentrations (c) were determined in order to construct the Huggins plot ( $\eta_{sp}/c$  vs. c) and the Kraemer plot ( $\ln \eta_r/c$  vs. c). The results of each parameter at different temperatures were shown in Table 4.2, 4.3 and 4.4. Then, the intrinsic viscosity determined from the y-intercept of Huggins and Kraemer plot at different temperatures were compared in order to observe the change in the conformation of PNIAM-co-AM from hydrophilic to hydrophobic property in response to temperature.

(Note: All data points for Huggins and Kraemer plots are shown in Appendix C.)

Table 4.2: Average flow time and reduced viscosity of 1:1 ratio PNIAM-co-AM at 10°C and 37°C

c (mg/mL)	at 10°C			at 37°C		
	t (s)	$\eta_{sp}/c$	$\ln \eta_r/c$	t (s)	$\eta_{sp}/c$	$\ln \eta_r/c$
4.00	297.2	0.143	0.113	142.4	0.104	0.087
2.33	258.5	0.159	0.135	128.6	0.120	0.105
1.36	226.8	0.148	0.135	116.6	0.117	0.109
0.79	210.7	0.147	0.139	110.1	0.120	0.114
0.46	200.5	0.135	0.131	105.8	0.112	0.110
0.27	196.0	0.141	0.138	103.4	0.103	0.102
0.16	193.0	0.139	0.138	102.1	0.093	0.093
0.09	191.6	0.163	0.162	101.4	0.092	0.092

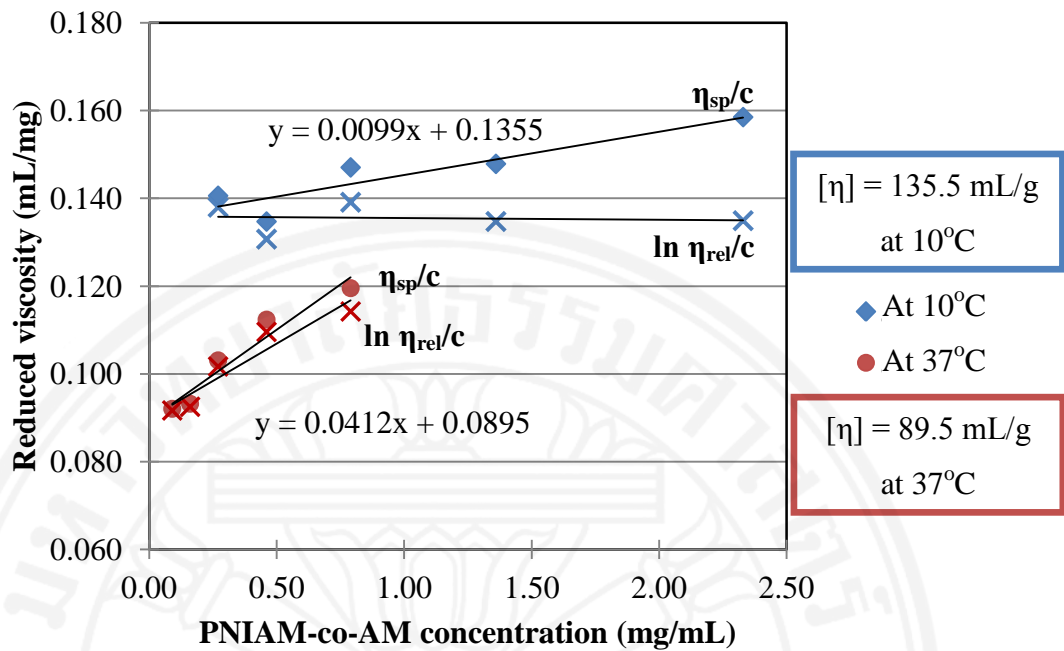


Figure 4.5: Intrinsic viscosity of 1:1 ratio of PNIAM-co-AM at 10 and 37°C

As the intrinsic viscosity implies the volume occupied by a single polymer chain, a drop of viscosity observed in Figure 4.5 from 135.5 mL/g at 10°C to 89.5 mL/g at 37°C indicated the decrease in occupied volume of polymer. It means the change in conformation of polymer in solution. As PNIAM has a temperature-responsive property of coil-globule transition at its LCST, the results indicate that flexible extended conformation at 10°C (below LCST) collapse to form coil globular conformation at 37°C (below LCST), which is compact and occupy less volume than extended chain.

A drop of viscosity was also observed in 2:1 ratio of PNIAM-co-AM solution from 171.5 mL/g at 10°C to 85 mL/g at 37°C as shown in Figure 4.6. The result is also consistent with the change in conformation of PNIAM from flexible extended conformation at 10°C to coil globular conformation at 37°C.

Table 4.3: Average flow time and reduced viscosity of 2:1 ratio PNIAM-co-AM at 10°C and 37°C

c (mg/mL)	at 10°C			at 37°C		
	t (s)	$\eta_{sp}/c$	$\ln \eta_{rel}/c$	t (s)	$\eta_{sp}/c$	$\ln \eta_{rel}/c$
4.00	322.0	0.176	0.133	145.5	0.112	0.092
2.33	274.0	0.194	0.160	130.3	0.127	0.111
1.36	236.4	0.186	0.165	117.1	0.121	0.112
0.79	215.8	0.181	0.169	110.1	0.120	0.115
0.46	204.1	0.176	0.169	105.8	0.113	0.110
0.27	197.6	0.173	0.169	103.2	0.096	0.095
0.16	193.9	0.170	0.168	102.1	0.091	0.090

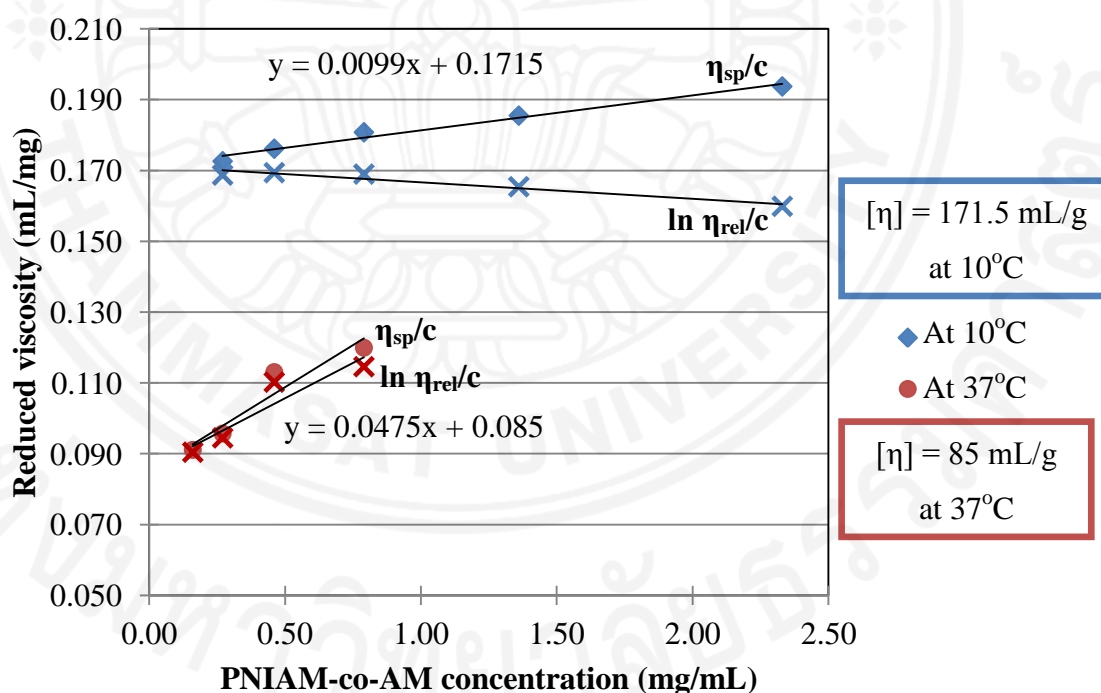


Figure 4.6: Intrinsic viscosity of 2:1 ratio of PNIAM-co-AM at 10 and 37°C

However, the intrinsic viscosity at 20°C for both 1:1 and 2:1 ratio of PNIAM-co-AM was even lower than 37°C; 77.7 mL/g and 4.4 mL/g respectively as shown in Figure 4.7. Therefore, this significant decrease in the intrinsic viscosity at 20°C may



be caused by the molecular characteristics of copolymer that interrupt the occupied volume which leads to the unreliable result of intrinsic viscosity. It is also possible that the collapsed globule-like polymer chain is not permeable enough to the solvent so that the extended chain cannot occur even at below LCST, and causes a drop in occupied volume.

Table 4.4: Average flow time and reduced viscosity of 1:1 ratio and 2:1 ratio of PNIAM-co-AM at 20°C

c (mg/mL)	PNIAM-co-AM (1:1 ratio) at 20°C			PNIAM-co-AM (2:1 ratio) at 20°C		
	t (s)	$\eta_{sp}/c$	$\ln \eta_{rel}/c$	t (s)	$\eta_{sp}/c$	$\ln \eta_{rel}/c$
4.00	220.5	0.126	0.102	233.4	0.147	0.116
2.33	194.0	0.138	0.120	201.7	0.161	0.136
1.36	173.4	0.133	0.122	177.2	0.152	0.138
0.79	161.6	0.128	0.122	163.2	0.141	0.134
0.46	155.5	0.129	0.125	156.4	0.142	0.138
0.27	151.4	0.116	0.114	150.6	0.095	0.094
0.16	149.1	0.098	0.097	147.9	0.048	0.048
0.09	147.9	0.083	0.083			

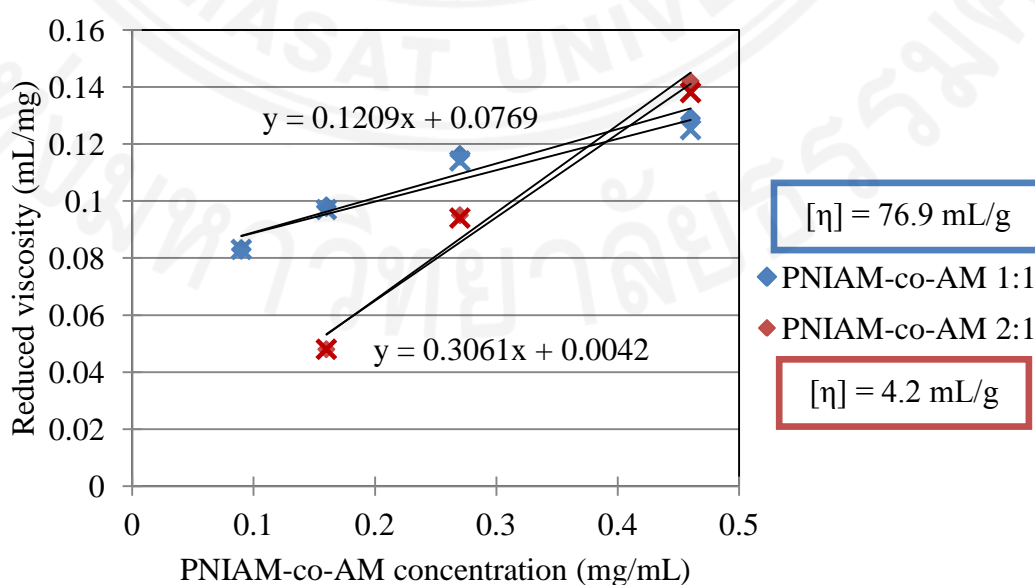


Figure 4.7: Intrinsic viscosity of 1:1 and 2:1 ratio of PNIAM-co-AM at 20°C



There are many factors to consider such as radius of gyration ( $R_g$ ), hydrodynamic radius ( $R_h$ ), molecular weight ( $M_w$ ), and solvent quality. The temperature-dependent ratio of  $R_g$  to  $R_h$  is related to the solvent permeability or the polymer chain distribution, and besides, a power law relationship between ( $R_g$ ,  $R_h$ ) and the molecular weight also indicates the solvent quality at a certain temperature. Shouei Fujishige and his coworkers have investigated these molecular parameters of PNIAM aqueous solution and intrinsic viscosity at 20°C. They have reported that phase transition of PNIAM is independent on the molecular weight in the high  $M_w$  range of  $5 \times 10^4 - 8.4 \times 10^6$ , and the aqueous solution medium is fairly good solvent system at 20°C and, also hydrated polymer chain was observed. Moreover, the ratio of  $R_g$  to  $R_h$  also shows a limit for the permeability of PNIAM chain in the solvent, for instance, the ratio ( $R_g/R_h = 0.926$ ) indicates that the collapsed chain is fully permeable to the solvent [38-40]. Therefore, two cases that concerned with the reliability of intrinsic viscosity results in the synthesized copolymer are the valid range of  $M_w$  and the ratio of  $R_g$  to  $R_h$ .

#### **4.2 Result comparison of the influence of UV intensity and exposure time on polymerization process**

ATR-FTIR measurement was taken for the PNIAM-co-AM grafted surfaces with 1 hour UV exposure time and with 15 minute exposure at high UV intensity (as mentioned in section 3.3.1). This ATR-FTIR technique was equipped with ZnSe (60°C) ART crystal. The spectra were measured in the range of 680-4000  $\text{cm}^{-1}$  with a resolution of 2  $\text{cm}^{-1}$ . From Figure 4.20, the secondary amide peak at 1654  $\text{cm}^{-1}$  was observed only in the PNIAM-co-AM grafted surface with 1 hour UV exposure time. Considering the UV energy, the energy that obtained from 15 minute exposure time is 1313  $\text{mJ}/\text{cm}^2$  and that obtained 1 hour exposure time is 1068  $\text{mJ}/\text{cm}^2$ . With the equivalent amount of energy, using higher intensity does not speed up the polymerization process to take place. Therefore, the results clearly show that the UV exposure time is more important than increasing the UV intensity, and it is important to find out the time required for the whole mechanism in polymerization starting from initiation to termination to occur. Thus, effective UV exposure time that can control the grafted amount of PNIAM-co-AM on TCPS surface is studied in this research.

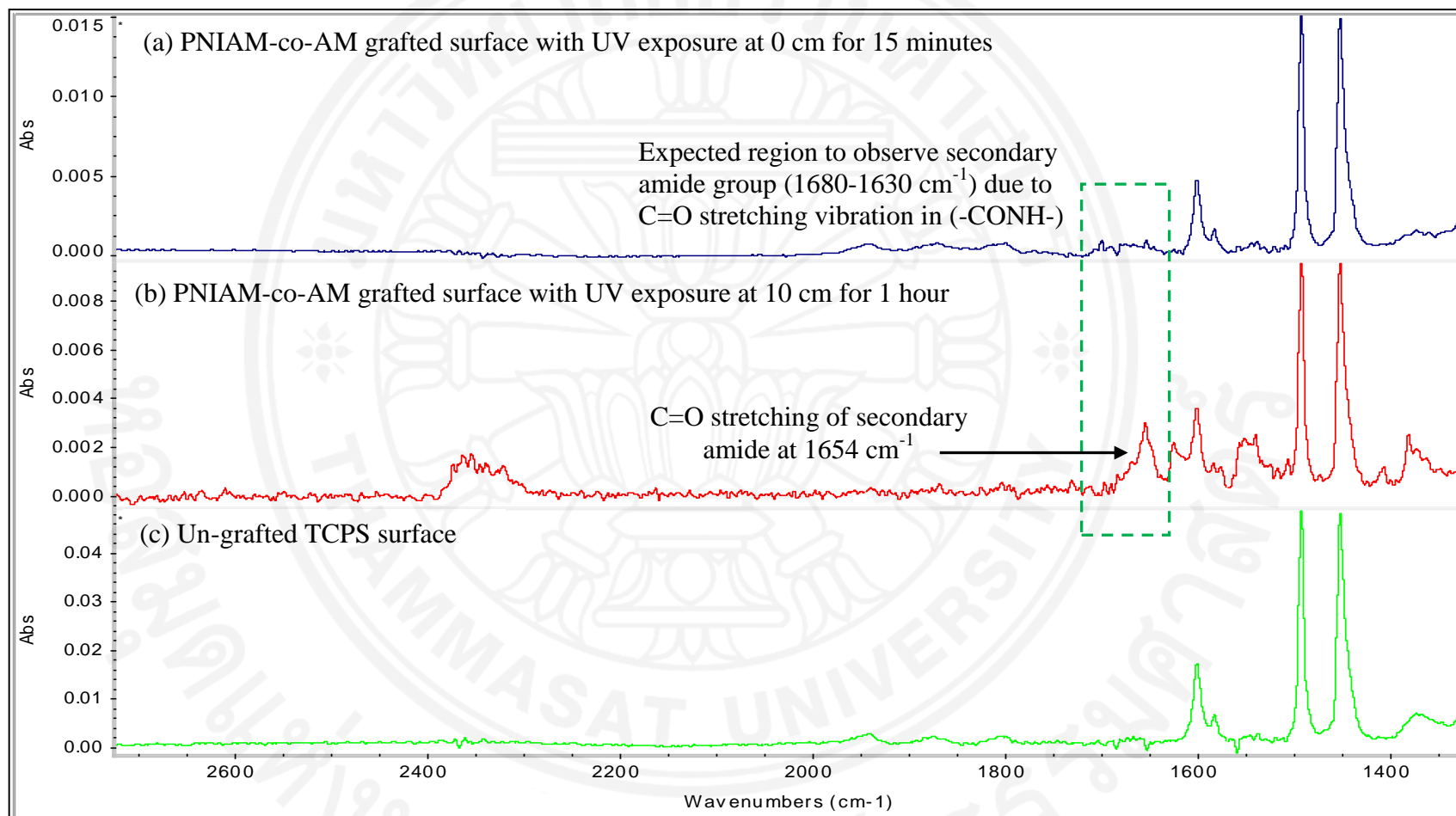


Figure 4.8: ATR-FTIR spectra of PNIAM-co-AM grafted surfaces with different conditions of UV exposure and un-grafted TCPS surface

### 4.3 Quantitative analysis results of PNIAM-co-AM grafted TCPS surfaces

In this section, quantitative analysis was performed by using a calibration curve which relates the peak area ratio and the grafted amount of PNIAM-co-AM on TCPS surface in ATR-FTIR measurement. The two characteristic peaks used in the analysis are at the wavenumber of  $1654\text{ cm}^{-1}$  and  $1600\text{ cm}^{-1}$  as shown in Figure 4.9. For confirmation of the relation obtained from calibration curve, Upcell<sup>TM</sup> PNIAM commercial grafted surface was measured and its graft density results were compared with the reference data by Okano research group [1, 14, 15]. The PNIAM-co-AM grafted surfaces with different UV exposure time were analyzed by using the calibration curve equation obtained from analysis.

(Note: All analysis data are shown in Appendix A.)

#### 4.3.1 Calibration curve construction by using peak area ratio

The peak area of the known grafted amount of PNIAM-co-AM was analyzed at eight different positions (peripheral 4 positions and 4 positions around 1 cm of center) on the surface, and the ratio of two characteristic peaks were determined ( $A_{1654}/A_{1600}$ ) as shown in Table 4.5. The peak area ratio of un-grafted PS surface ( $0.187 \pm 0.028$ ) was used to subtract from the resulting peak area ratio. The y-intercept obtained from calibration curve equation must be approach to zero because there is no grafted amount at zero concentration of polymer.

Table 4.5 Average peak area ratios from eight different positions of known grafted amount of PNIAM-co-AM surfaces

Amount of PNIAM-co-AM ( $\mu\text{g}/\text{cm}^2$ )	Average of peak area ratio ( $A_{1654}/A_{1600}$ )	Subtracted peak area ratio ( $A_{1654}/A_{1600}$ )	SD
0.5	0.258	0.071	0.008
1	0.316	0.129	0.025
2	0.428	0.241	0.037
3	0.490	0.304	0.024
5	0.736	0.550	0.093

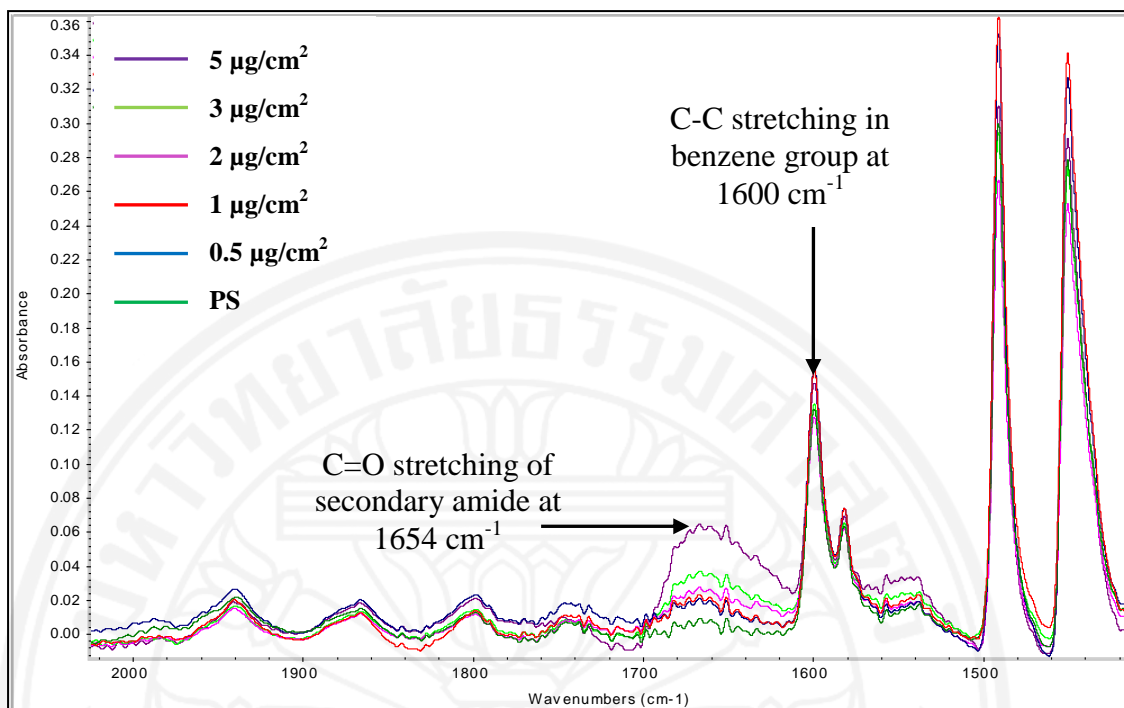


Figure 4.9: ATR-FTIR spectra of known grafted amounts of PNIAM-co-AM on TCPS surfaces

Calibration curve for determining the grafted amount of PNIAM-co-AM on TCPS surface

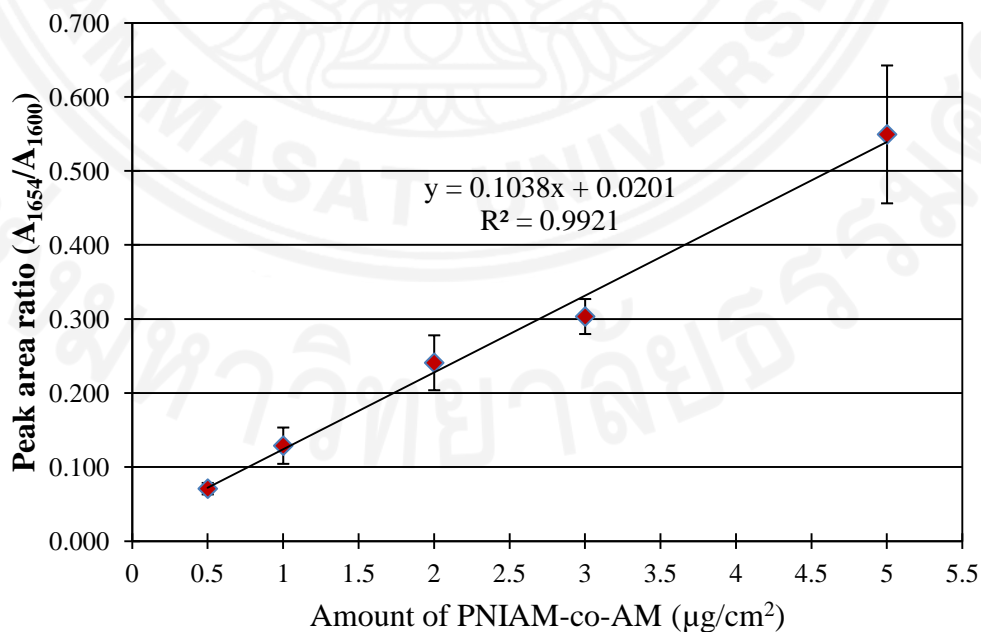


Figure 4.10: Relationship between the peak area ratio and the grafted amount of PNIAM-co-AM

*ATR-FTIR measurement for Commercial Upcell™ PNIAM grafted TCPS surface*

The commercial Upcell™ PNIAM grafted TCPS surface was used to confirm the validity of the calibration curve. The result of peak area ratio from eight different position and the subtracted peak area ratio were shown in Table 4.6.

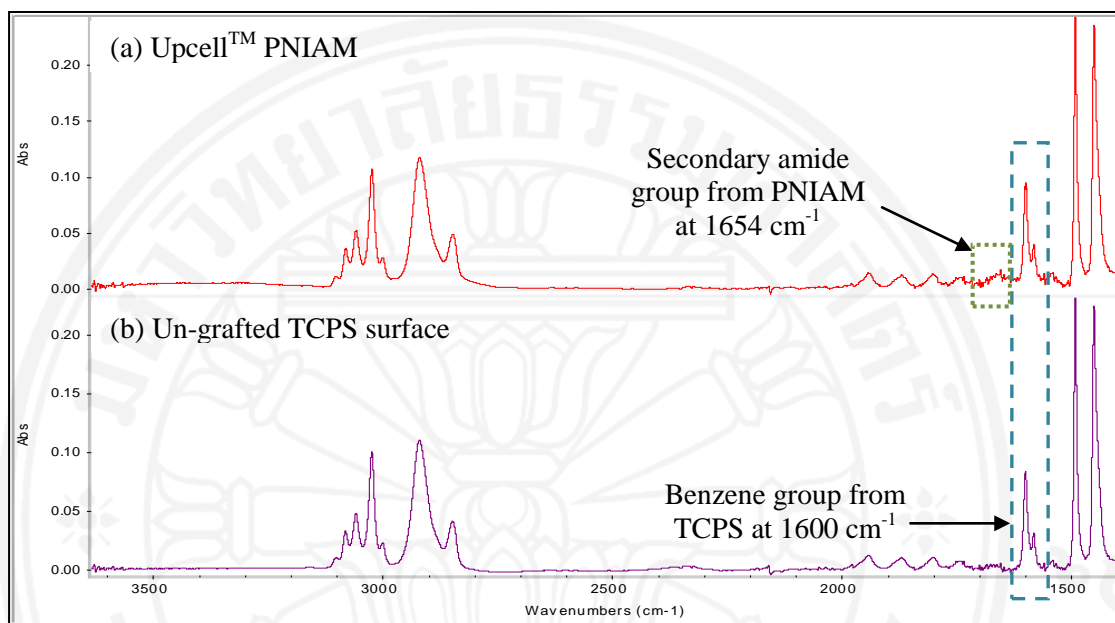


Figure 4.11: ATR-FTIR spectra of (a) commercial Upcell™ PNIAM grafted TCPS surface; (b) Un-grafted TCPS surface

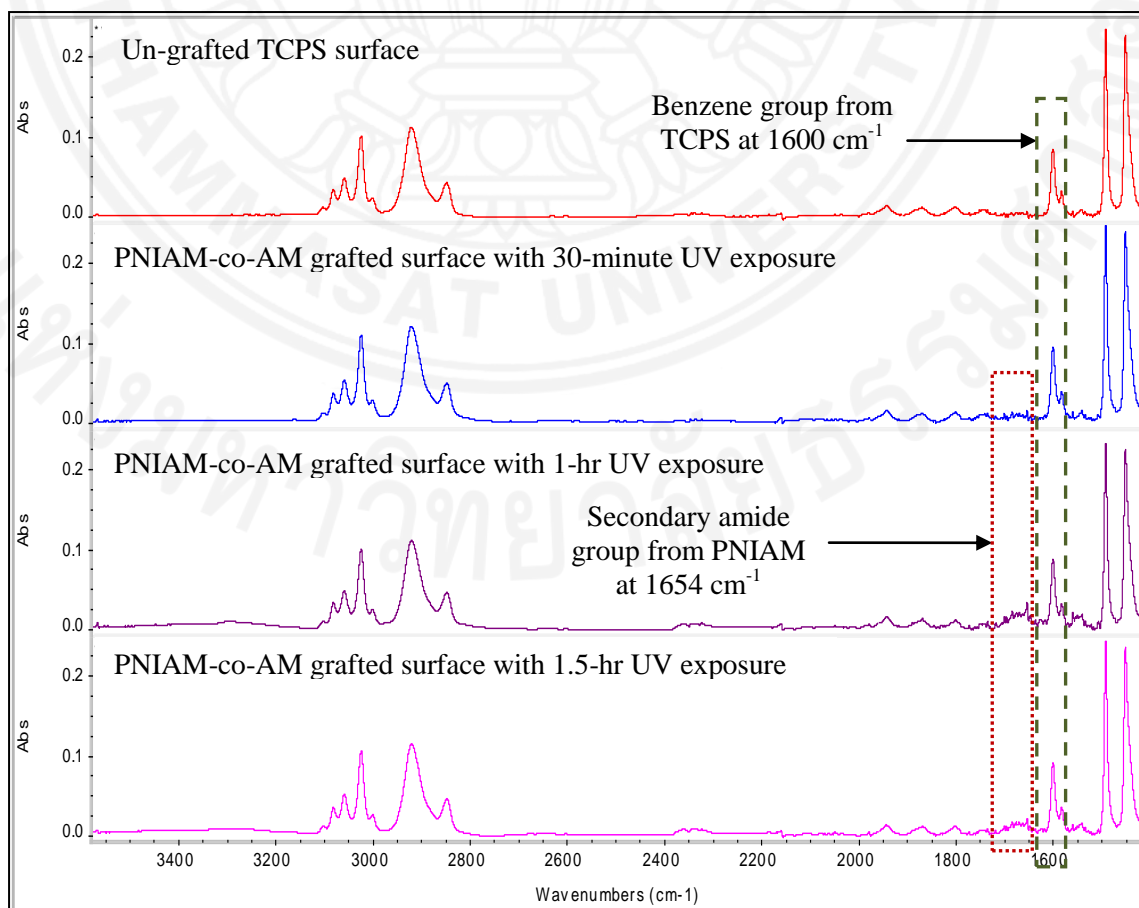
Table 4.6: Peak area ratio at eight different positions of commercial Upcell™ surface

Position	A <sub>1654</sub>	A <sub>1600</sub>	A <sub>1654</sub> /A <sub>1600</sub>
1	0.3324	0.8154	0.4077
2	0.3650	0.8263	0.4417
3	0.3730	0.8029	0.4646
4	0.3426	0.8335	0.4110
5	0.2692	0.7683	0.3504
6	0.2900	0.7520	0.3856
7	0.2767	0.7522	0.3679
8	0.2940	0.7594	0.3871
		Average	0.4020
		Subtracted peak area	0.2150
		SD	0.0377

By substituting the peak area ratio ( $A_{1654}/A_{1600} = 0.215 \pm 0.038$ ) in the calibration curve equation ( $y = 0.1038x + 0.0201$ ), the resulting grafting density is  $1.88 \pm 0.04 \mu\text{g}/\text{cm}^2$ . According to Okano research group, the valid range of grafting density is  $1.4\text{--}2 \mu\text{g}/\text{cm}^2$ , and the commercial Upcell surface has the grafting density of  $1.9\text{--}2 \mu\text{g}/\text{cm}^2$  [5, 8, 15]. Therefore, the grafting density result obtained by calibration curve equation falls in the acceptable range, and the application this equation is reliable for determining the grafted amount of copolymer on TCPS surfaces.

#### 4.3.2 Graft density results of PNIAM-co-AM grafted TCPS surfaces with different UV exposure times

The quantitative ATR analysis were performed for the PNIAM-co-AM grafted TCPS surfaces with varying UV exposure time from 30 minutes, 1 hour, 1.5 hours, 2 hours, 2.5 hours to 3 hours. Comparison of ATR-FTIR spectra between PNIAM-co-AM grafted TCPS surface with different UV exposure times and un-grafted TCPS surface are shown in Figure 4.12.



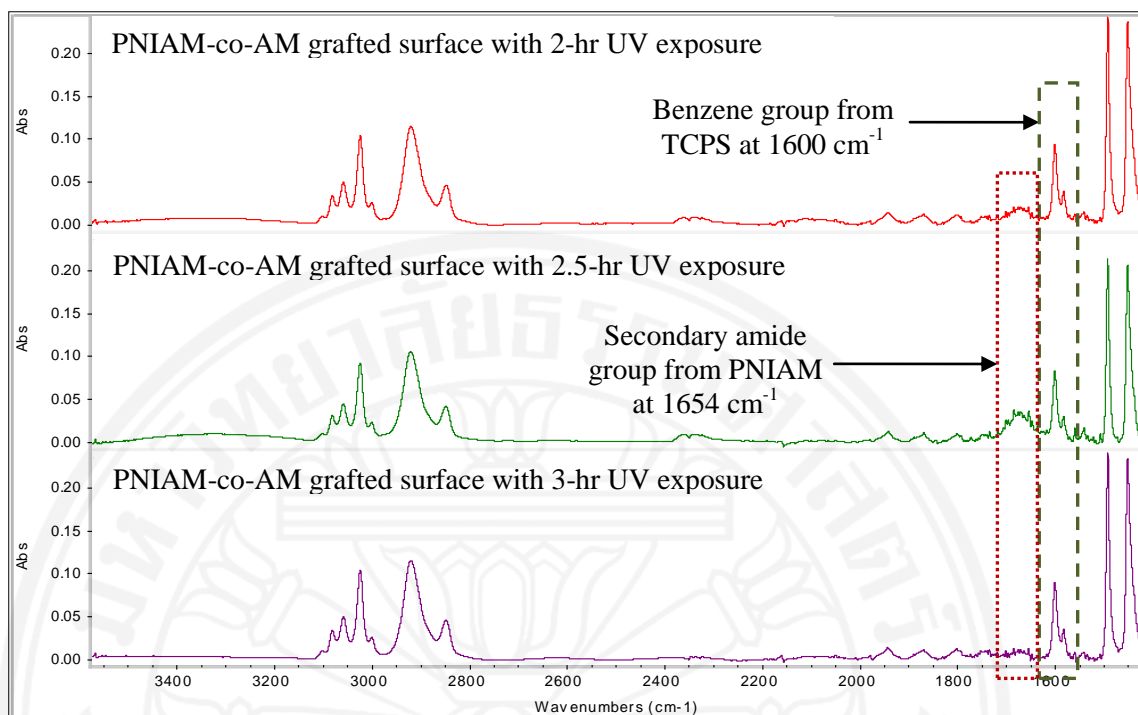


Figure 4.12: ATR-FTIR spectra of un-grafted TCPS surface and PNIAM-co-AM grafted TCPS surfaces with different UV exposure times

The peak area ratio ( $A_{1654}/A_{1600}$ ) at eight different positions were determined for each grafted surface. Hence, the grafting density was determined by using the calibration curve equation obtained from the previous section ( $y = 0.1038x + 0.0201$ ), and the results were shown in Table 4.7.

Table 4.7: Results of peak area ratios and grafting densities of PNIAM-co-AM grafted samples with varying UV exposure time

PNIAM-co-AM grafted sample	$y = A_{1654}/A_{1600}^*$	$x = \text{Grafting density } (\mu\text{g}/\text{cm}^2)^*$
30-minute UV exposure	$0.090 \pm 0.05$	$0.68 \pm 0.05$
1-hour UV exposure	$0.194 \pm 0.06$	$1.68 \pm 0.06$
1.5-hour UV exposure	$0.213 \pm 0.06$	$1.86 \pm 0.06$
2-hour UV exposure	$0.231 \pm 0.09$	$2.03 \pm 0.09$
2.5-hour UV exposure	$0.270 \pm 0.06$	$2.41 \pm 0.06$
3-hour UV exposure	$0.118 \pm 0.04$	$0.94 \pm 0.04$

(\*Data expressed in Average  $\pm$  SD; n = 8 positions)



From the results, the increase in the amount of grafted PNIAM-co-AM on TCPS surfaces was observed as the UV polymerization time increased until 2.5-hour UV exposure time and then, a significant drop in grafting density was observed after 3-hour UV exposure as shown in Figure 4.13.

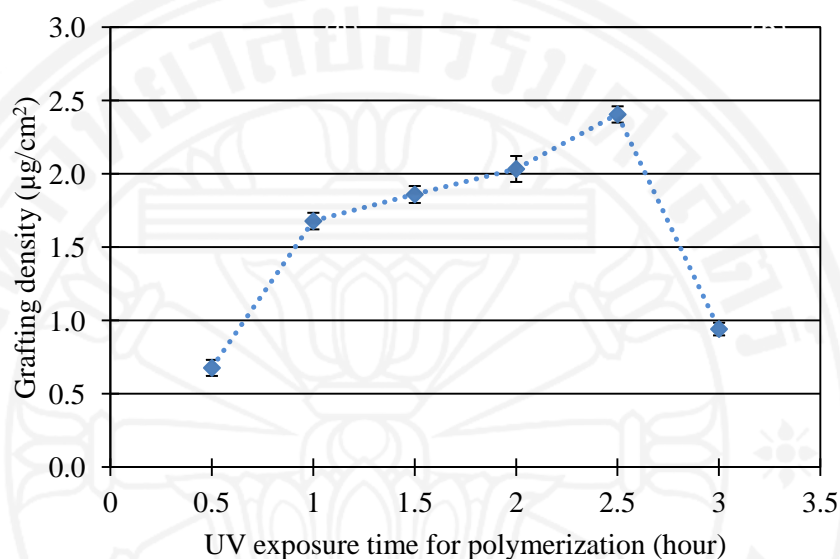


Figure 4.13: Amount of grafted PNIAM-co-AM on TCPS surfaces at different UV exposure times

From Figure 4.13, it can be seen that 30 minutes UV exposure time might be insufficient for polymerization mechanism to occur, showing the lowest yield of grafted layer. The grafted surfaces with UV polymerization time of between 1 and 2 hours obtained grafting density of between 1.68 and 2.03  $\mu\text{g}/\text{cm}^2$  which falls in the valid range of grafting density from 1.4 to 2  $\mu\text{g}/\text{cm}^2$  for cell adhesion and detachment. The grafting density was increased up to 2.41  $\mu\text{g}/\text{cm}^2$  for 2.5-hour UV polymerization time. As the grafted amount increased, the mobility of grafted PNIAM-co-AM chain was also expected to be increased due to the formation of longer cross-linked copolymer chain. The grafted surface with 3-hour UV exposure time showed a decrease in grafting density of about 1  $\mu\text{g}/\text{cm}^2$  due to the chain scission of the grafted copolymer on the surface, which was induced by excited free radicals from long time exposed to UV and those un-grafted polymers were removed after washing with ethanol.



#### 4.4 Contact angle results of PNIAM-co-AM grafted TCPS surfaces with different UV exposure times

The contact angle results of the PNIAM-co-AM grafted samples and the control un-grafted polystyrene surface at 40°C and 10°C were shown in Table 4.8. The change in surface wettability is observed as the temperature changes except the un-grafted polystyrene surface.

(Note: All images of contact angles are shown in Appendix B.)

Table 4.8: Contact angle measurement of un-grafted polystyrene surface and PNIAM-co-AM grafted TCPS surfaces at 40°C and 10°C

Samples	At 40°C	At 10°C
Un-grafted PS	77.34 ± 0.79°	76.62 ± 1.27°
30-minute UV exposure	62.70 ± 1.62°	57.29 ± 0.84°
1-hour UV exposure	64.34 ± 1.41°	42.64 ± 1.11°
1.5-hour UV exposure	65.64 ± 2.37°	41.88 ± 2.98°
2-hour UV exposure	67.42 ± 1.24°	43.98 ± 3.29°
2.5-hour UV exposure	48.65 ± 0.67°	36.55 ± 2.20°
3-hour UV exposure	57.01 ± 0.87°	52.47 ± 3.25°

(\*Data expressed in Average ± SD; n = 3 positions)

Figure 4.14 showed that all PNIAM-co-AM grafted TCPS surfaces displayed the change in their surface behavior from hydrophilic to hydrophobic property by the transition of contact angles from 10°C (below LCST) to 40°C (above LCST). Among the grafted surfaces, the surfaces with the UV exposure time of between 1 and 2 hours showed the obvious transition of contact angles in which the drop in angle was occurred from 64° – 67° at 40°C to 41° – 43° at 10°C. This is because within the range of grafting density 1.68 – 2.03  $\mu\text{g}/\text{cm}^2$ , the mobility of PNIAM-co-AM chain was well restricted so that relevant hydrophobic-hydrophilic behavior was observed at its phase transition temperature.

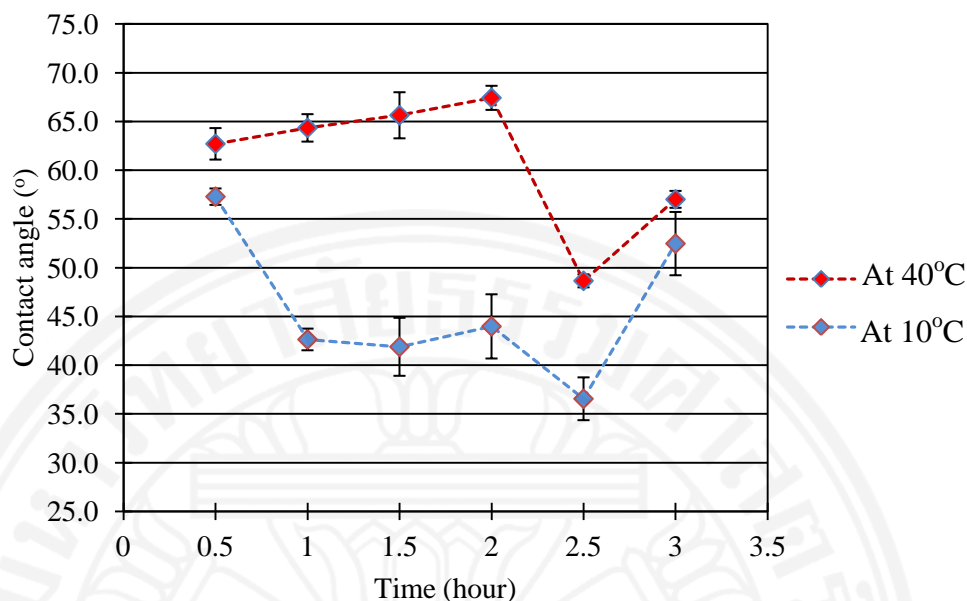


Figure 4.14: Contact angles of PNIAM-co-AM grafted surfaces with varying UV exposure time

However, an obvious decrease in contact angles was observed for the grafted surface with 2.5-hour UV exposure which have the grafting density of  $2.4 \mu\text{g}/\text{cm}^2$  at both temperatures  $40^\circ\text{C}$  and  $10^\circ\text{C}$ . This is because copolymer chain formed was longer with the thicker layer so that extended chain exposed more interaction of amide group ( $-\text{NH}_2$ ) with water on the surface. As a result, hydrophilicity of the surface increased. It had been reported that the PNIAM chain mobility and its ability for hydration was high in the grafted layer above  $2 \mu\text{g}/\text{cm}^2$  causing the grafted surface to be more hydrophilic [15]. As for the grafted surface with 30-minute and 3-hour UV exposure time, it showed only a small gap of transition of contact angles and an increase in hydrophobicity at  $10^\circ\text{C}$  which implied that low grafting yield did not provide the sufficient chain extension.

#### 4.5 Estimation of PNIAM content in the grafted copolymer

As PNIAM is the main polymer responsible for cell adhesion/detachment property with respect to temperature, it is necessary to figure out the composition of PNIAM in the grafted copolymer. The quantitative determination of PNIAM content was done by using the result of KBr-FTIR spectrum (in **section 4.1.1**) and  $^1\text{H}$  NMR

spectrum of synthesized PNIAM-co-AM (1:1 ratio). As  $^1\text{H}$  NMR spectroscopy can also examine the chemical structures of synthesized copolymer, the analysis from NMR spectrum can be applied as a comparison of the FTIR spectrum analysis.

#### 4.5.1 Analysis by FTIR

From KBr-FTIR spectrum of 1:1 PNIAM-co-AM (Figure 4.2), the N-H stretching from the primary and secondary amide peak from the copolymer was observed in the region between the wavenumber 3070 and 3440  $\text{cm}^{-1}$ . According to the nature of amide peak, the N-H stretching of primary amide shows two bands at 3350  $\text{cm}^{-1}$  and 3200  $\text{cm}^{-1}$  while that of secondary amide shows a strong band at 3460–3300  $\text{cm}^{-1}$  and a weak band at 3100–3070  $\text{cm}^{-1}$  [41, 42]. Table 4.9 shows the peak fitting results obtained in the region between the wavenumber 3800 and 2760  $\text{cm}^{-1}$ .

Table 4.9: Peak results of synthesized PNIAM-co-AM (1:1 ratio)

Peak Type	Center X	Height	FWHM	Area
Gaussian	3073.799	0.3439	110.123	40.3147
Gaussian	3188.928	0.4873	129.865	67.3589
Gaussian	3309.112	0.5648	147.909	88.919
Gaussian	3440.64	0.6523	158.731	110.2155
Gaussian	3574.151	0.4725	162.499	81.7309

From the peak fitting results, two strong bands of N-H stretching of primary amide were observed at 3188  $\text{cm}^{-1}$  and 3309  $\text{cm}^{-1}$ . The peaks that described secondary amide group appeared at 3440–3300  $\text{cm}^{-1}$  and a weak band at 3073  $\text{cm}^{-1}$ . As there were overlapped regions among the peaks (3440–3070  $\text{cm}^{-1}$ ), the overlapped area was subtracted from the total area before converting to the composition of each polymer in PNIAM-co-AM. Table 4.10 shows the results from peak area calculation and percent composition of primary and secondary amide in PNIAM-co-AM.

$$\% \text{ Composition} = (A_{\text{N-H band}}/A_{3070 - 3440}) \times 100\%$$

Table 4.10: Composition of PNIAM and AM in 1:1 ratio of PNIAM-co-AM

Peak	Total area	Subtracted area	% Composition
$A_{3070-3440}$	306.8081	236.9581	-
Primary amide ( $A_{3180}, A_{3309}$ )	156.2779	86.4279	36.4
Secondary amide ( $A_{3073}, A_{3300-3460}$ )	239.4492	180.7492	76.3

(Areas of overlapped region are shown in Appendix C.)

Hence, from the results, the composition of secondary amide is 76.3% which represents the PNIAM content while that of primary amide is 36.4% which represents the acrylamide content in the 1:1 ratio of synthesized PNIAM-co-AM.

#### 4.5.2 Analysis by NMR

From the  $^1\text{H}$  NMR spectrum of synthesized PNIAM-co-AM as shown in Figure 4.15, the chemical shift at 0.942 ppm indicated the methyl ( $\text{CH}_3$ ) protons from isopropyl group in PNIAM [43] with the integration value of 6.251 and the chemical shift at 3.699 ppm showed the ( $\text{CH}_2$ ) protons from the backbone PNIAM [43] with the integration value of 1. These integration values were normalized as shown below in order to determine the percent content of PNIAM in the copolymer.

$$\text{Integration for PNIAM, } I_{PNIAM} = 6.251 \Rightarrow \frac{6.251}{3 \text{ protons}} = 2.08$$

$$\text{Integration for } \text{CH}_2 \text{ in backbone polymer (BP), } I_{BP} = 1 \Rightarrow \frac{1}{2 \text{ protons}} = 0.5$$

$$\% \text{ Content of PNIAM} = \frac{2.08}{(2.08 + 0.5)} \times 100 \% = 80.6 \%$$

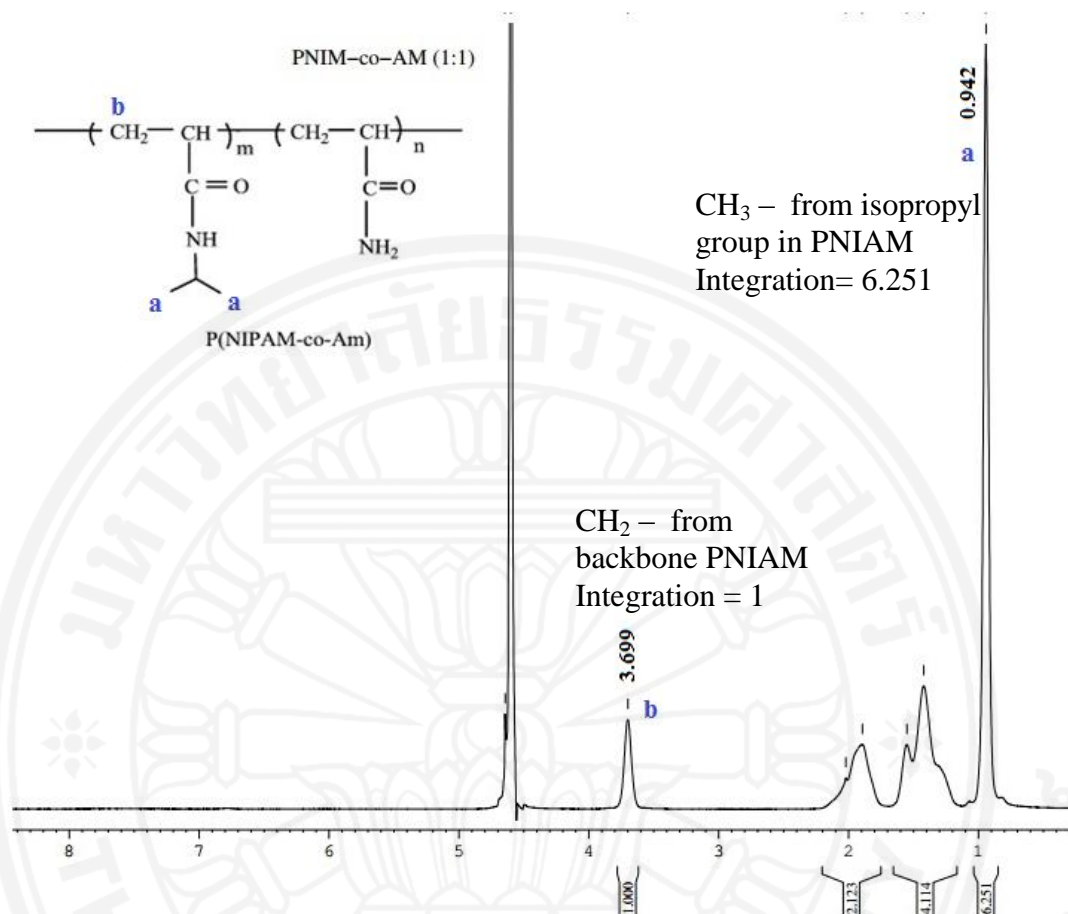


Figure 4.15: <sup>1</sup>H NMR spectrum of 1:1 ratio of synthesized PNIAM-co-AM

Therefore, from two characterization methods, PNIAM content obtained was **76.3%** by **FTIR** analysis and **80.6%** by **NMR** analysis. From FTIR analysis, as there were overlapped areas among the peaks ( $3073 - 3440 \text{ cm}^{-1}$ ), estimation of these areas included in the calculation gave the rough estimation of PNIAM composition in the copolymer. However, the advantage was the ability to estimate the acrylamide polymer composition as well. In NMR analysis, the determination by using methyl protons from isopropyl group gave a distinct indication of PNIAM but, it was unable to determine the acrylamide content because the amide proton (NH-) was too weak to detect for both primary and secondary amides.

### 4.5.3 Determination of grafted PNIAM on TCPS surfaces

From the calibration curve construction (section 3.5.3), the amount of PNIAM in the grafted the copolymer was determined by using the result of PNIAM content from both FTIR and NMR analysis. Table 4.11 shows the estimated grafted amount of PNIAM ( $\mu\text{g}/\text{cm}^2$ ) on the TCPS surface, and a corrected calibration curve is shown in Figure 4.16.

Table 4.11: Estimated grafted amount of PNIAM in copolymer grafted surfaces

C (mg/mL) of PNIAM-co-AM	FTIR (76.3% PNIAM)		NMR (80.6% PNIAM)	
	C (mg/mL) of PNIAM	Amount of PNIAM ( $\mu\text{g}/\text{cm}^2$ )	C (mg/mL) of PNIAM	Amount of PNIAM ( $\mu\text{g}/\text{cm}^2$ )
0.024	0.018	0.381	0.019	0.402
0.048	0.037	0.761	0.039	0.804
0.096	0.073	1.523	0.096	1.608
0.144	0.110	2.284	0.116	2.413
0.24	0.183	3.807	0.193	4.021

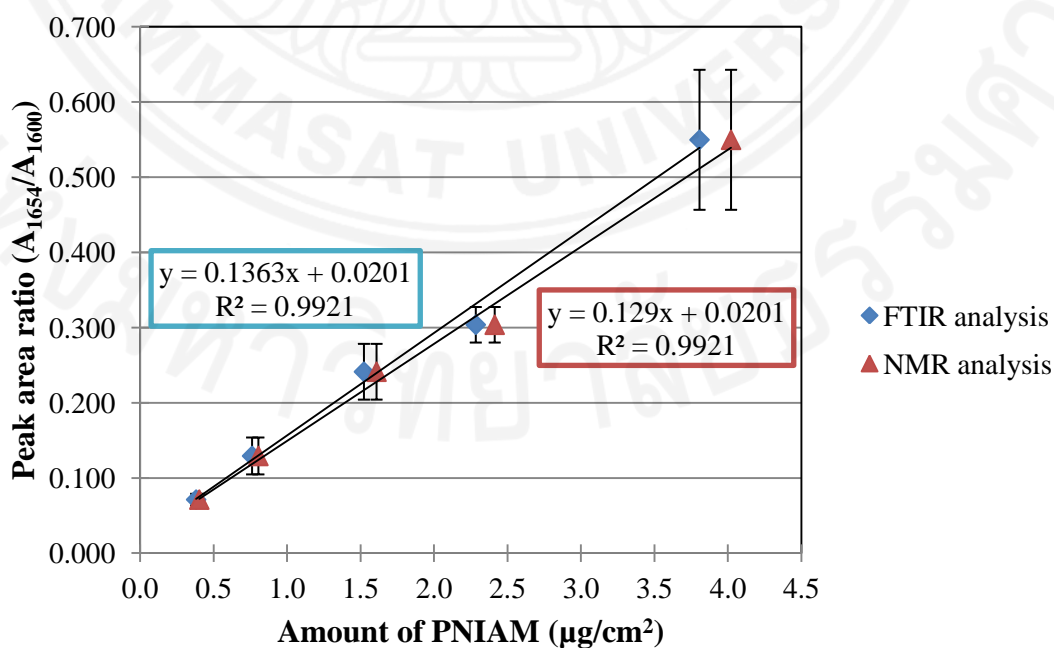


Figure 4.16: Relationship between peak area ratio and amount of grafted PNIAM

Confirmation of calibration curve equation with Upcell™

By substituting the peak area ratio of Upcell™ ( $A_{1654}/A_{1600} = 0.215 \pm 0.038$ ) in the calibration curve equations obtained from both analysis,

	<b>Estimated amount of PNIAM (<math>\mu\text{g}/\text{cm}^2</math>)</b>	<b>Reference amount (<math>\mu\text{g}/\text{cm}^2</math>)</b>
FTIR analysis	$1.43 \pm 0.04$	1.9 – 2
NMR analysis	$1.51 \pm 0.04$	

Estimated PNIAM grafted amount at different UV exposure times

Reanalyzing the peak area ratio results of the copolymer grafted amount on TCPS surfaces from section 4.3.2 by using the corrected calibration curve equations, the grafted amount PNIAM at different UV exposure times is obtained as shown in Figure 4.17. The comparison of estimated amount of PNIAM on the grafted surfaces with 1 – 2.5-hour UV exposure time is summarized in Table 4.12.

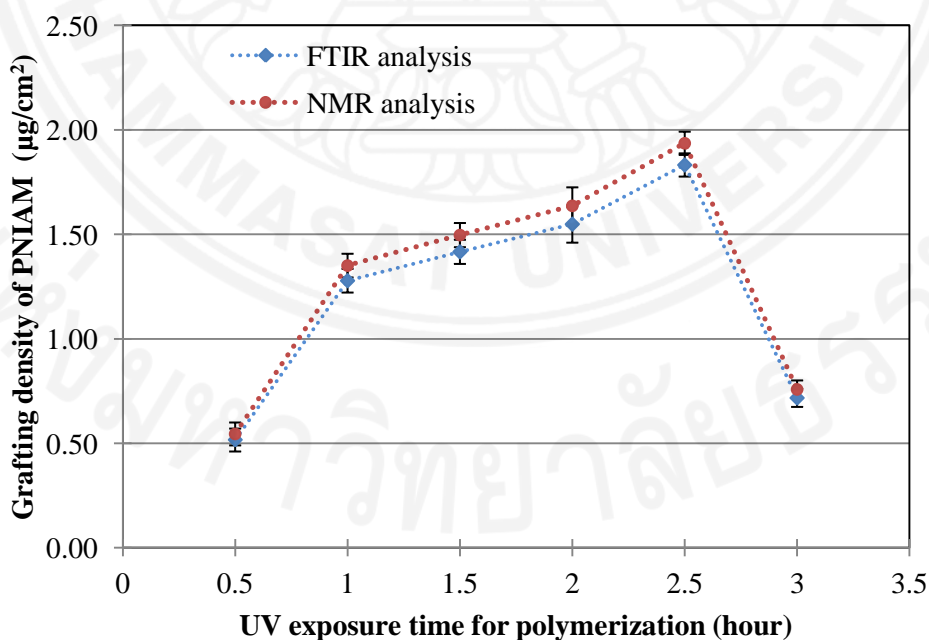


Figure 4.17: Estimated grafted amount of PNIAM on TCPS surfaces at different UV exposure times

Table 4.12: Summary of grafted PNIAM amount on the surfaces with 1 – 2.5-hour UV exposure time

UV exposure time (hrs)	Estimated amount of PNIAM ( $\mu\text{g}/\text{cm}^2$ )		Reference amount ( $\mu\text{g}/\text{cm}^2$ )
	FTIR	NMR	
1	$1.28 \pm 0.06$	$1.35 \pm 0.06$	Optimal range between $1.4 \pm 0.1$ and $2.0 \pm 0.1$
1.5	$1.42 \pm 0.06$	$1.50 \pm 0.06$	
2	$1.55 \pm 0.09$	$1.64 \pm 0.09$	
2.5	$1.83 \pm 0.06$	$1.94 \pm 0.06$	

From the reanalysis, the grafted amount of PNIAM from 1- to 2.5-hour UV exposure surfaces falls in the optimal range of grafting density. Although the grafted amount of PNIAM is lower than  $2 \mu\text{g}/\text{cm}^2$  in the 2.5-hour UV exposure sample, the highest hydrophilicity of the grafted surface was observed from the contact angle measurement (section 4.6) which might be the cause of copolymerization with acrylamide. It is possible that thicker grafted layer favors the exposure of hydrophilic ( $-\text{NH}_2$ ) from primary amide group on the grafted surface. Therefore, the optimal grafted amount of PNIAM in the copolymer PNIAM-co-AM grafted surfaces is estimated to be between  $1.3$  and  $1.7 \mu\text{g}/\text{cm}^2$ .

#### 4.6 Results from cell study analysis

Figure 4.18 shows the behavior of human fibroblast monolayer cell sheet as response to changing the temperature which was observed under an inverted microscope. A clear gap between the cell sheet and the rim of well plate was observed after second incubation which indicated the detachment of human fibroblast monolayer cell sheet from PNIAM-co-AM grafted surfaces. After harvesting, the detached cell sheets showed some breakage at the rim of sheet, but there was no hole at the centre of sheet which proved the cell detachment without any severe damage for PNIAM-co-AM grafted surfaces with 1- and 2-hour UV exposure time.



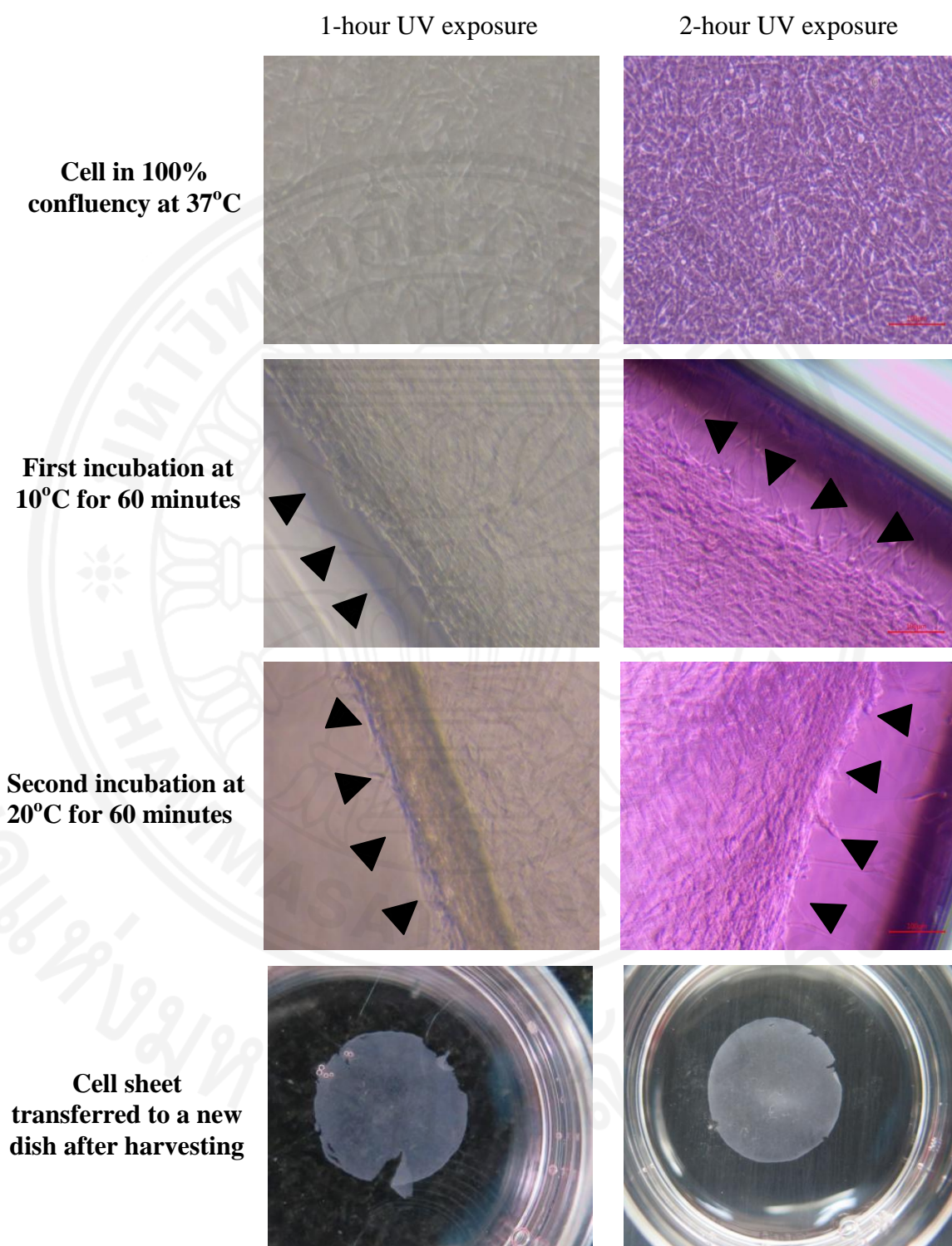


Figure 4.18: Detachment of human dermal fibroblast monolayer cell sheet from PNIAM-co-AM grafted surfaces

## Chapter 5

### Conclusions and Recommendations

This research investigated the effective UV exposure time for grafting PNIAM-co-AM onto the TCPS surface that can provide an optimum grafting density for cell adhesion and detachment process. Along with this research, synthesis of linear PNIAM-co-AM was performed in order to obtain the calibration curve equation for determining the grafting density of PNIAM-co-AM grafted surfaces with different UV exposure times. Hence, it leads to achieve the main objective of the UV time study effect on the grafting density of PNIAM-co-AM grafted surfaces. Moreover, the nature of synthesized PNIAM-co-AM with response to the temperature by intrinsic viscosity determination also comes in as a supplementary study, and provides supporting information. In the following sections, the important points in each finding are summarized and the possible ways to improve are also discussed in the recommendation.

#### 5.1 Summary of findings

##### 5.1.1 Summary of synthesized PNIAM-co-AM

In the synthesis of PNIAM-co-AM, the concentration of monomers has been found as an interference in polymerization of linear copolymer. The suitable concentration to obtain the linear copolymer is found out to be 1.3 wt% of NIAM and 0.8 wt% of AM for copolymerization in the mole ratio of 1:1. Gel formation is occurred as the concentration of monomers increase two times. In the copolymerization of 2:1 mole ratio, when the NIAM concentration is jumped up to 2.5 wt%, some cross-linked parts are observed in the resulting copolymer. From FTIR and NMR analysis, the estimated composition of PNIAM in the synthesized copolymer was obtained as 76.3% and 80.6%.

From the intrinsic viscosity measurement of linear PNIAM-co-AM (1:1 and 2:1 ratio) at 10°C, 20°C and 37°C, a drop in the viscosity from 10°C to 37°C displays the nature of PNIAM-co-AM in aqueous solution which changes its conformation from extended chain to coiled globule. However, unusual nature was observed at 20°C

for both 1:1 and 2:1 ratio of PNIAM-co-AM by displaying a significant drop in viscosity. It may be the cause of impermeable coil-globule copolymer from the solvent even at below LCST so that the extended chain cannot come out to occupy the right space in the aqueous solution. Therefore, in the case of PNIAM-co-AM obtained from synthesis with unknown molecular weight, radius of gyration, and hydrodynamic radius, the result from intrinsic viscosity measurement cannot be completely reliable.

### **5.1.2 Summary of UV exposure time study for PNIAM-co-AM grafted surfaces**

From the study, the minimum UV exposure time required to occur polymerization process is found out to be 1 hour. Due to the use of a small amount of periodate initiator, polymerization mechanism is well-controlled but, it takes time for initiation process of both monomers. A significant jump in graft density of PNIAM-co-AM can be observed during the first one hour of UV exposure time. The grafted PNIAM-co-AM amount increases with the increasing UV polymerization time until 2.5-hour exposure. The effective UV polymerization time for PNIAM-co-AM grafted surfaces is found out between 1 and 2 hours which provide the grafting density of 1.68–2.03  $\mu\text{g}/\text{cm}^2$ . From the corrected calibration curve obtained by estimated PNIAM content in the copolymer grafted layer by FTIR and NMR analysis, the grafted amount of PNIAM in 1–2-hour UV exposure surfaces is obtained between 1.3 and 1.7  $\mu\text{g}/\text{cm}^2$  which is close to the optimum range of 1.4–2  $\mu\text{g}/\text{cm}^2$ . The results of cell study analysis also show that a successful detachment of a Human Dermal Fibroblast (HDFa) monolayer cell sheet is observed in both PNIAM-co-AM grafted surfaces with 1- and 2-hour UV exposure time.

From the contact angle measurement, the chain mobility and surface wettability of the grafted surfaces with 30 minutes to 3 hours of UV exposure time are also consistent with the findings by Okano research group [14, 15]. The contact angle results of the grafted surface with 1–2-hour UV exposure time shows the appropriate hydrophobic-hydrophilic alteration when lowering the temperature because the chain mobility is well-restricted in the grafted layer of 1.4–2  $\mu\text{g}/\text{cm}^2$ . The increase in

surface hydrophilicity is observed even above LCST for the 2.5-hour UV exposure sample with total grafted copolymer of  $2.4 \mu\text{g}/\text{cm}^2$  due to the less restriction of chain mobility in the thicker layer. Similarly, the surface hydrophobicity is high in the grafted surfaces with lower than  $1.4 \mu\text{g}/\text{cm}^2$  even below LCST because of the limited chain mobility of the aggregated chain in that layer.

## 5.2 Recommendation for further study

For the synthesis of linear PNIAM-co-AM, it is recommended to use the concentration of monomers to be 1.3 wt% of NIAM and 0.4 wt% of AM in the further synthesis of 2:1 mole ratio of PNIAM-co-AM in order to avoid from cross-linking. Moreover, the use of AIBN initiator (Azobisisobutyronitrile) can help to create a good inert atmosphere during free radical polymerization process because decomposition of AIBN initiator produces nitrogen gas. This inert atmosphere can prevent from the unwanted termination by combining with oxygen and cross-linking process. In the work by Gheorghe Fundueanu and his coworkers, they have used AIBN initiator in 1,4-dioxane solvent to synthesize linear PNIAM-co-AM by free radical polymerization [30]. In the UV time study for PNIAM-co-AM grafted surfaces, although 1-hour UV exposure time is effective enough for polymerization process and cell sheet detachment, the amount of grafted PNIAM is at the minimum limit of the optimum range ( $\sim 1.3 \mu\text{g}/\text{cm}^2$ ). Therefore, it is recommended to apply the UV exposure time of 1.5 hours for polymerization because the grafting density of PNIAM itself is obtained as  $1.4 - 1.5 \mu\text{g}/\text{cm}^2$  which completely falls in the optimum range.

## References

1. Matsuda, N., et al. (2007). Tissue Engineering Based on Cell Sheet Technology. *Advanced Materials*, Vol. 19, 3089-3099.
2. Yamato, M., et al. (2007). Temperature-responsive cell culture surfaces for regenerative medicine with cell sheet engineering. *Progress in Polymer Science*, Vol. 32, 1123-1133.
3. Yamato, M. and T. Okano. (2004). Cell sheet engineering. *Materials Today*, Vol. 7, 42-47.
4. Yang, J., et al. (2005). Cell sheet engineering: Recreating tissues without biodegradable scaffolds. *Biomaterials*, Vol. 26, 6415-6422.
5. Tsuda, Y., et al. (2004). Control of cell adhesion and detachment using-temperature and thermoresponsive copolymer grafted culture surfaces. *Journal of Biomedical Materials Research - Part A*, Vol. 69, 70-78.
6. Teruo, O., et al. (1993). A novel recovery system for cultured cells using plasma-treated polystyrene dishes grafted with poly(N-isopropylacrylamide). *Journal of Biomedical Materials Research*, Vol. 27, 1243-1251.
7. Noriko, Y., et al. (1990). Thermo-responsive polymeric surfaces; control of attachment and detachment of cultured cells. *Die Makromolekulare Chemie, Rapid Communications*, Vol. 11, 571-576.
8. Nandkumar, M.A., et al. (2002). Two-dimensional cell sheet manipulation of heterotypically co-cultured lung cells utilizing temperature-responsive culture dishes results in long-term maintenance of differentiated epithelial cell functions. *Biomaterials*, Vol. 23, 1121-1130.
9. Wong-In, S., et al. (2013). Multilayered mouse preosteoblast MC3T3-E1 sheets harvested from temperature-responsive poly(N-isopropylacrylamide-co-acrylamide) grafted culture surface for cell sheet engineering. *Journal of Applied Polymer Science*, Vol. 129, 3061-3069.
10. Cheng, X., et al. (2005). Surface Chemical and Mechanical Properties of Plasma-Polymerized N-Isopropylacrylamide. *Langmuir*, Vol. 21, 7833-7841.

11. Pan, Y.V., et al. (2001). Plasma Polymerized N-Isopropylacrylamide: Synthesis and Characterization of a Smart Thermally Responsive Coating. *Biomacromolecules*, Vol. 2, 32-36.
12. Wong-in, S., et al. (2011). The Temperature Responsive Poly (N-isopropylacrylamide-co-acrylamide) grafted culture surface for Cell Sheet Engineering. *World Academy of Science, Engineering and Technology*, Vol. 5, 928-932.
13. Wu, G., et al. (2006). Novel thermo-sensitive membranes prepared by rapid bulk photo-grafting polymerization of N,N-diethylacrylamide onto the microfiltration membranes Nylon. *Journal of Membrane Science*, Vol. 283, 13-20.
14. Akiyama, Y., et al. (2004). Ultrathin Poly(N-isopropylacrylamide) Grafted Layer on Polystyrene Surfaces for Cell Adhesion/Detachment Control. *Langmuir*, Vol. 20, 5506-5511.
15. Kikuchi, A. and T. Okano. (2005). Nanostructured designs of biomedical materials: applications of cell sheet engineering to functional regenerative tissues and organs. *Journal of Controlled Release*, Vol. 101, 69-84.
16. Isenberg, B.C., et al. (2008). A thermoresponsive, microtextured substrate for cell sheet engineering with defined structural organization. *Biomaterials*, Vol. 29, 2565-2572.
17. Klouda, L. and A.G. Mikos. (2008). Thermoresponsive hydrogels in biomedical applications. *European Journal of Pharmaceutics and Biopharmaceutics*, Vol. 68, 34-45.
18. Deng, K., et al. (2009). Synthesis and characterization of a novel temperature-pH responsive copolymer of 2-hydroxypropyl acrylate and aminoethyl methacrylate hydrochloric salt. *Express Polym Lett*, Vol. 3, 97-104.
19. Iwata, T., et al. (2014). *Cell Sheet Engineering for Periodontal Regeneration*.
20. Canavan, H.E., et al. (2005). Cell sheet detachment affects the extracellular matrix: A surface science study comparing thermal liftoff, enzymatic, and mechanical methods. *Journal of Biomedical Materials Research Part A*, Vol. 75A, 1-13.

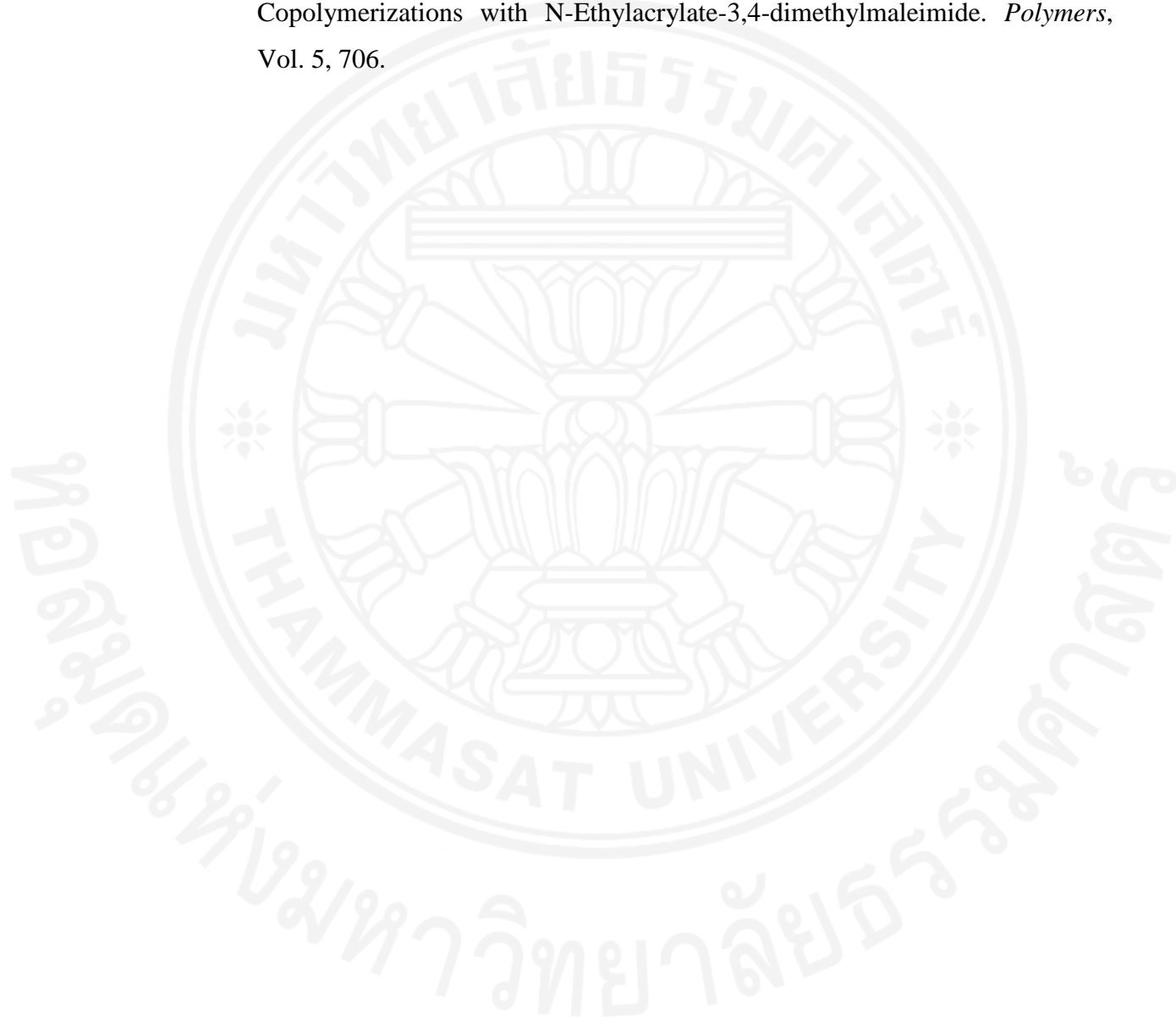
21. Curti, P.S., et al. (2002). Surface modification of polystyrene and poly(ethylene terephthalate) by grafting poly(N-isopropylacrylamide). *Journal of Materials Science: Materials in Medicine*, Vol. 13, 1175-1180.
22. Curti, P.S., et al. (2005). Characterization of PNIPAAm photografted on PET and PS surfaces. *Applied Surface Science*, Vol. 245, 223-233.
23. Weiss, P. (1967). *Photo-induced polymerization*, in *Pure and Applied Chemistry*.(587).
24. Ferreira, P., et al. (2011). Photocrosslinkable Polymers for Biomedical Applications.
25. Uchida, E., Y. Uyama, and Y. Ikada. (1990). A novel method for graft polymerization onto poly(ethylene terephthalate) film surface by UV irradiation without degassing. *Journal of Applied Polymer Science*, Vol. 41, 677-687.
26. Uchida, E., Y. Uyama, and Y. Ikada. (1993). Surface graft polymerization of ionic monomers onto poly(ethylene terephthalate) by UV-irradiation without degassing. *Journal of Applied Polymer Science*, Vol. 47, 417-424.
27. Uchida, E., H. Iwata, and Y. Ikada. (2000). Surface structure of poly(ethylene terephthalate) film grafted with poly(methacrylic acid). *Polymer*, Vol. 41, 3609-3614.
28. PerlinElmerLife and AnalyticalSciences. (2005). *FT-IR Spectroscopy - Attenuated Total Reflectance (ATR)*. Shelton, CT 06484-4794 USA).
29. Fukumori, K., et al. (2009). Temperature-responsive glass coverslips with an ultrathin poly(N-isopropylacrylamide) layer. *Acta Biomaterialia*, Vol. 5, 470-476.
30. Fundueanu, G., M. Constantin, and P. Ascenzi. (2009). Poly(N-isopropylacrylamide-co-acrylamide) cross-linked thermoresponsive microspheres obtained from preformed polymers: Influence of the physico-chemical characteristics of drugs on their release profiles. *Acta Biomaterialia*, Vol. 5, 363-373.
31. Hirose M, et al. (2000). Temperature-Responsive surface for novel co-culture systems of hepatocytes with endothelial cells: 2-D patterned and double layered co-cultures. *Yonsei Med J*, Vol. 41, 14.



32. Pamies, R., et al. (2008). Determination of intrinsic viscosities of macromolecules and nanoparticles. Comparison of single-point and dilution procedures. *Colloid and Polymer Science*, Vol. 286, 1223-1231.
33. Panda, S., et al. Evaluation Of Huggins' Constant, Kraemer's Constant And Viscosity Concentration Co-Efficient Of Polymer PVA (Mw= 1, 25,000) In Distilled Water, 1N NaOH And 1N KOH.
34. Mumick, P.S. and C.L. McCormick. (1994). Water soluble copolymers. 54: N-isopropylacrylamide-co-acrylamide copolymers in drag reduction: Synthesis, characterization, and dilute solution behavior. *Polymer Engineering & Science*, Vol. 34, 1419-1428.
35. Kurecic, M., M. Sfiligoj-Smole, and K. Srana-Kleinschek. (2012). UV polymerization of poly (N-isopropylacrylamide) hydrogel. *Materiali in tehnologije*, Vol. 46, 87-91.
36. Katsumoto, Y., et al. (2002). Conformational Change of Poly(N-isopropylacrylamide) during the Coil-Globule Transition Investigated by Attenuated Total Reflection/Infrared Spectroscopy and Density Functional Theory Calculation†. *The Journal of Physical Chemistry A*, Vol. 106, 3429-3435.
37. Kim, S.Y., et al. (2000). Thermo- and pH-responsive behaviors of graft copolymer and blend based on chitosan and N-isopropylacrylamide. *Journal of Applied Polymer Science*, Vol. 78, 1381-1391.
38. Kubota, K., S. Fujishige, and I. Ando. (1990). Solution Properties of Poly(N-isopropylacrylamide) in Water. *Polym J*, Vol. 22, 15-20.
39. Kubota, K., S. Fujishige, and I. Ando. (1990). Single-chain transition of poly(N-isopropylacrylamide) in water. *The Journal of Physical Chemistry*, Vol. 94, 5154-5158.
40. Kubota, K., et al. (1990). Characterization of Poly(N-isopropylmethacrylamide) in Water. *Polym J*, Vol. 22, 1051-1057.
41. Socrates, G. (1994). *Infrared Characteristic Group Frequencies*. John Wiley & Sons Ltd.



42. Long, D.A. (2004). Infrared and Raman characteristic group frequencies. Tables and charts George Socrates John Wiley and Sons, Ltd, Chichester, Third Edition, 2001. . *Journal of Raman Spectroscopy*, Vol. 35, 905-905.
43. Förster, N., et al. (2013). Photocrosslinkable Star Polymers via RAFT-Copolymerizations with N-Ethylacrylate-3,4-dimethylmaleimide. *Polymers*, Vol. 5, 706.



The image features a large, faint watermark of the Thammasat University logo in the background. The logo is circular and contains the Thai text 'มหาวิทยาลัยธรรมศาสตร์' at the top and 'THAMMASAT UNIVERSITY' at the bottom. In the center of the logo is a multi-armed figure holding a book, with a lotus flower at the base. The word 'Appendices' is centered over the logo.

**Appendices**

## Appendix A

### ATR-FTIR Spectra and Analysis Data

Quantitative ATR results for PNIAM-co-AM grafted surfaces with varying UV exposure time by using the analysis of both peak intensity ratio and peak area ratio are shown in the following tables.

Peak area ratio results of PNIAM-co-AM grafted surface with 30-minute UV exposure

Position	A <sub>1654</sub>	A <sub>1600</sub>	A <sub>1654</sub> /A <sub>1600</sub>
1	0.2271	0.833	0.2726
2	0.2613	0.8194	0.3189
3	0.2817	0.8153	0.3455
4	0.17	0.8235	0.2064
5	0.1986	0.8047	0.2468
6	0.2213	0.8097	0.2733
7	0.2771	0.8065	0.3436
8	0.1728	0.8154	0.2119
		Avg	0.2774
		Subtracted Avg Area	0.0904
		SD	0.0548

Note: Peak area ratio A<sub>1654</sub>/A<sub>1600</sub> of ungrafted PS = 0.187 ± 0.028

*Peak area ratio results of PNIAM-co-AM grafted surface with 1 hour UV exposure*

Position	A <sub>1654</sub>	A <sub>1600</sub>	A <sub>1654</sub> /A <sub>1600</sub>
1	0.3101	0.928	0.3342
2	0.3384	0.8792	0.3849
3	0.3106	0.894	0.3474
4	0.2709	0.8823	0.3070
5	0.3502	0.8508	0.4116
6	0.349	0.8085	0.4317
7	0.4029	0.8423	0.4783
8	0.3143	0.8843	0.3554
		Avg	0.3813
		Subtracted Avg Area	0.1944
		SD	0.0566

*Peak area ratio results of PNIAM-co-AM grafted surface with 1.5-hour UV exposure*

Position	A <sub>1654</sub>	A <sub>1600</sub>	A <sub>1654</sub> /A <sub>1600</sub>
1	0.3039	0.8769	0.3466
2	0.3335	0.8489	0.3929
3	0.3713	0.9347	0.3972
4	0.2801	0.9389	0.2983
5	0.4085	0.8984	0.4547
6	0.4188	0.8706	0.4810
7	0.3813	0.9007	0.4233
8	0.3516	0.8636	0.4071
		Avg	0.4002
		Subtracted Avg Area	0.2132
		SD	0.0578

Peak area ratio results of PNIAM-co-AM grafted surface with 2-hour UV exposure

Position	A <sub>1654</sub>	A <sub>1600</sub>	A <sub>1654</sub> /A <sub>1600</sub>
1	0.3101	0.895	0.3465
2	0.2827	0.6271	0.4508
3	0.3302	0.8891	0.3714
4	0.2665	0.7464	0.3570
5	0.4034	0.8256	0.4886
6	0.4933	0.8272	0.5963
7	0.3572	0.919	0.3887
8	0.2922	0.8437	0.3463
		Avg	0.4182
		Subtracted Avg Area	0.2312
		SD	0.0885

Peak area ratio results of PNIAM-co-AM grafted surface with 2.5-hour UV exposure

Position	A <sub>1654</sub>	A <sub>1600</sub>	A <sub>1654</sub> /A <sub>1600</sub>
1	0.3275	0.8705	0.3762
2	0.3714	0.901	0.4122
3	0.3862	0.9203	0.4196
4	0.3856	0.8738	0.4413
5	0.4438	0.8868	0.5005
6	0.4518	0.8447	0.5349
7	0.3942	0.8691	0.4536
8	0.4459	0.8636	0.5163
		Avg	0.4568
		Subtracted Avg Area	0.2698
		SD	0.0556

*Peak area ratio results of PNIAM-co-AM grafted surface with 3-hour UV exposure*

Position	A <sub>1654</sub>	A <sub>1600</sub>	A <sub>1654</sub> /A <sub>1600</sub>
1	0.3027	0.8817	0.3433
2	0.1657	0.6929	0.2391
3	0.2628	0.7869	0.3340
4	0.2789	0.8499	0.3282
5	0.2323	0.7789	0.2982
6	0.2747	0.7704	0.3566
7	0.2165	0.7523	0.2878
8	0.2067	0.821	0.2518
		Avg	0.3049
		Subtracted Avg Area	0.118
		SD	0.0431

*Calibration curve construction by using peak intensity ratio*

The peak intensity of the known grafted amount of PNIAM-co-AM was analyzed at five different positions on the surface, and the ratio of two characteristic peaks were determined ( $I_{1654}/I_{1600}$ ) as shown in Table A.1.

Table A.1: Peak intensity ratio obtained from five different positions on the PNIAM-co-AM grafted surface

Amount of PNIAM-co-AM ( $\mu\text{g}/\text{cm}^2$ )	Peak intensity ratio ( $I_{1654}/I_{1600}$ ) at five different positions on the grafted surface				
	Center	1	2	3	4
0	0.076	0.072	0.100	0.107	0.089
0.5	0.145	0.124	0.138	0.118	0.149
1	0.213	0.127	0.163	0.166	0.141
2	0.282	0.192	0.235	0.295	0.247
3	0.229	0.305	0.285	0.327	0.285
5	0.784	0.420	0.249	0.547	0.454
10	1.032	0.801	0.881	0.439	0.964

Note that center position shows the highest intensity compared to other 4 positions which can increase the standard deviations (error bars) in the calibration curve.

The average value of the peak intensity ratio was taken for each position and the calibration curve was constructed.

Table A.2: Average peak intensity ratios from five different positions of known grafted amount of PNIAM-co-AM surfaces

Amount of PNIAM-co-AM ( $\mu\text{g}/\text{cm}^2$ )	Average of peak intensity ratio ( $I_{1654}/I_{1600}$ )	SD
0	0.089	0.015
0.5	0.135	0.013
1	0.162	0.033
2	0.250	0.041
3	0.286	0.037
5	0.491	0.196
10	0.823	0.232

Calibration curve for determining the grafted amount of PNIAM-co-AM on TCPS surface

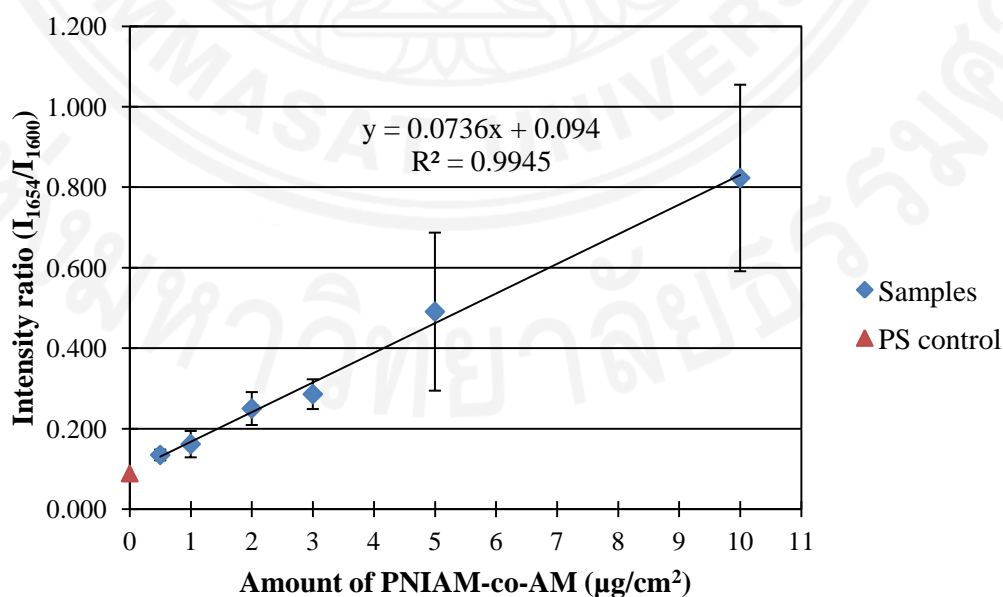


Figure A.1: Relationship between the peak intensity ratio and the grafted amount of PNIAM-co-AM

ATR-FTIR measurement for Commercial Upcell™ PNIAM grafted TCPS surface

Table A.3: Peak intensity ratio of commercial Upcell™ surface

Position on sample	I <sub>1600</sub>	I <sub>1654</sub>	I <sub>1654</sub> /I <sub>1600</sub>
Center	0.0845	0.0177	0.209
1	0.0851	0.0159	0.187
2	0.0835	0.0178	0.213
3	0.0819	0.0159	0.194
4	0.082	0.0166	0.202
		Avg	0.201
		SD	0.011

By using the relation from calibration curve ( $y = 0.0736x + 0.094$ ), the grafting density (x) of the commercial sample obtained  $1.45 \pm 0.01 \mu\text{g}/\text{cm}^2$ . The result falls in the acceptable range of grafting density ( $1.4 - 2 \mu\text{g}/\text{cm}^2$ ).

Graft density results by using peak intensity ratio

The results of ATR-FTIR analysis from PNIAM-co-AM grafted TCPS surfaces with varying UV exposure time of 1 hour, 1.5 hours, 2 hours, 2.5 hour and 3 hours were analyzed by using the peak intensity ratio ( $I_{1654}/I_{1600}$ ). The grafting density was determined by using the relation from calibration curve ( $y = 0.0736x + 0.094$ ) and the results were shown in Table A.4.

Table A.4 Results of intensity ratios and grafting densities of PNIAM-co-AM grafted samples with varying UV exposure time

PNIAM-co-AM grafted sample	$y = I_{1654}/I_{1600} *$	$x = \text{Grafting density } (\mu\text{g}/\text{cm}^2)*$
1 hour UV exposure	$0.195 \pm 0.025$	$1.37 \pm 0.03$
1.5 hour UV exposure	$0.217 \pm 0.183$	$1.67 \pm 0.18$
2 hour UV exposure	$0.243 \pm 0.070$	$2.02 \pm 0.07$
2.5 hour UV exposure	$0.336 \pm 0.096$	$3.29 \pm 0.10$
3 hour UV exposure	$0.408 \pm 0.414$	$4.26 \pm 0.41$

(\*Data expressed in Average  $\pm$  SD where n = 5 times)



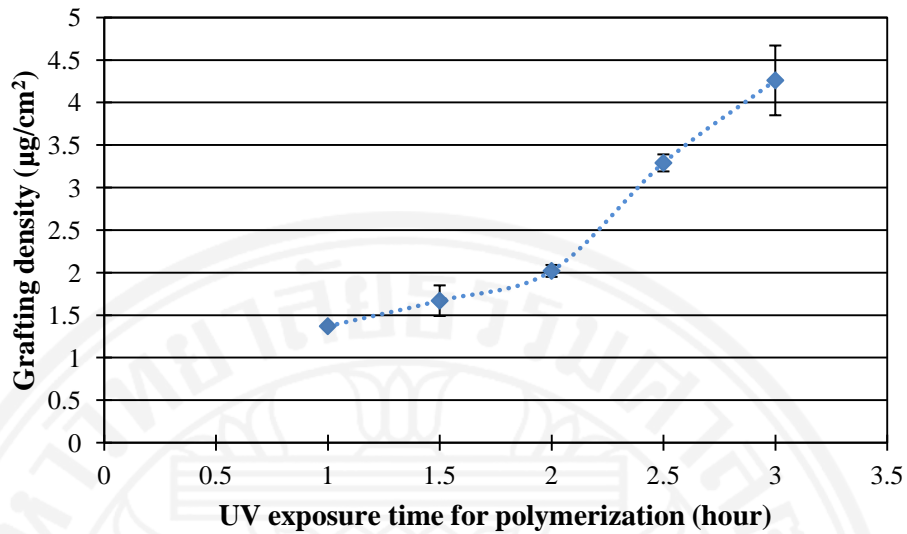


Figure A.2: Amount of grafted PNIAM-co-AM on TCPS surfaces at different UV exposure time

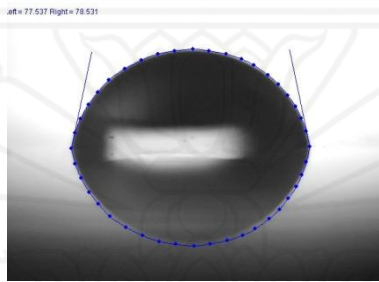
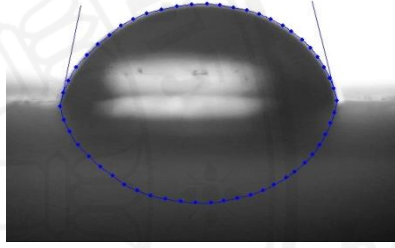
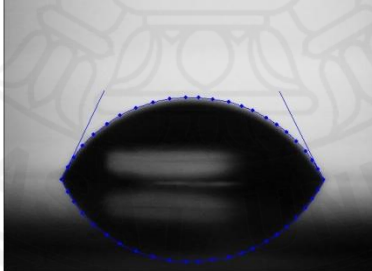
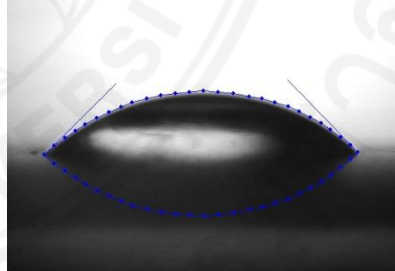
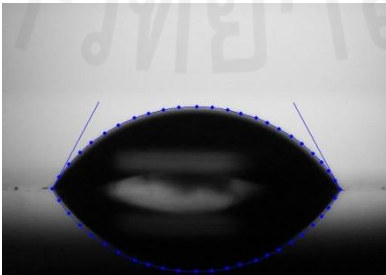
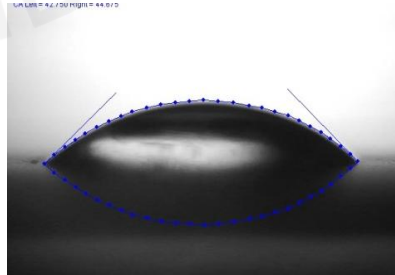
From the results, the increase in the amount of grafted PNIAM-co-AM on TCPS surfaces was observed as the UV polymerization time increased. Figure A.2 shows the amount of grafted PNIAM-co-AM on TCPS surfaces at different UV exposure time starting from 1 hour to 3 hours. The expected range of grafting density from about 1.4 to 2  $\mu\text{g}/\text{cm}^2$  obtained between 1 hour and 2 hour UV exposure time for polymerization.

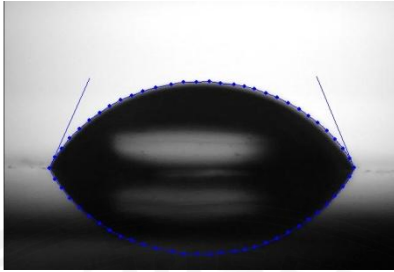
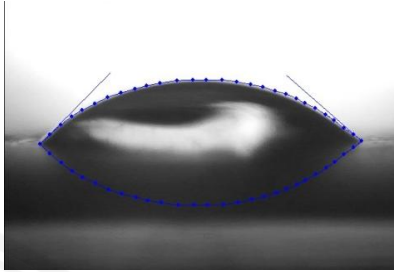
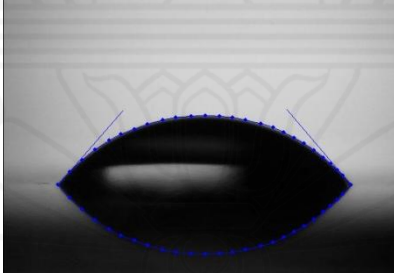
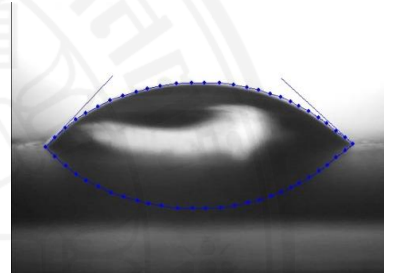
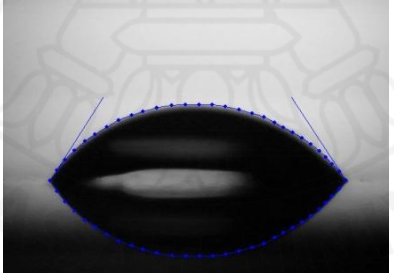
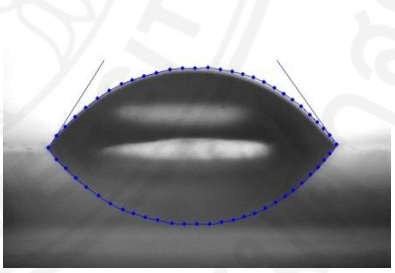
However, the use of peak intensity ratio analysis may not be precise due to the high intensity at the center of grafted surface and unsubtracted peak intensity ratio of PS. It leads to the uncertainty of calibration curve equation.

## Appendix B

### Contact Angle Measurement Data

Contact angle measurement of ungrafted PS surface and PNIAM-co-AM grafted surfaces by varying UV polymerization

	At 40 °C	At 10 °C
	Average ± SD	Average ± SD
Un-grafted PS	 $77.34 \pm 0.79^\circ$	 $76.62 \pm 1.27^\circ$
PNIAM-co-AM grafted surface with 1 hour UV exposure	 $64.34 \pm 1.41^\circ$	 $42.64 \pm 1.11^\circ$
PNIAM-co-AM grafted surface with 1.30 hour UV exposure	 $65.64 \pm 2.37^\circ$	 $41.88 \pm 2.98^\circ$

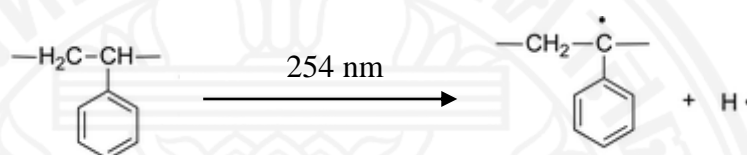
<p>PNIAM-co-AM grafted surface with 2 hour UV exposure</p>	 <p><math>67.42 \pm 1.24^\circ</math></p>	 <p><math>43.98 \pm 3.29^\circ</math></p>
<p>PNIAM-co-AM grafted surface with 2.30 hour UV exposure</p>	 <p><math>48.65 \pm 0.67^\circ</math></p>	 <p><math>36.55 \pm 2.20^\circ</math></p>
<p>PNIAM-co-AM grafted surface with 3 hour UV exposure</p>	 <p><math>57.01 \pm 0.87^\circ</math></p>	 <p><math>52.47 \pm 3.25^\circ</math></p>

## Appendix C

### Supplementary Information

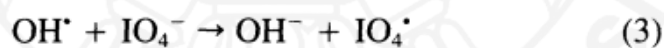
The following steps show the hypothesized mechanism of grafting PNIAM-co-AM on PS surface by UV irradiation (254 nm).

#### Step 1: Formation of radical on TCPS surface



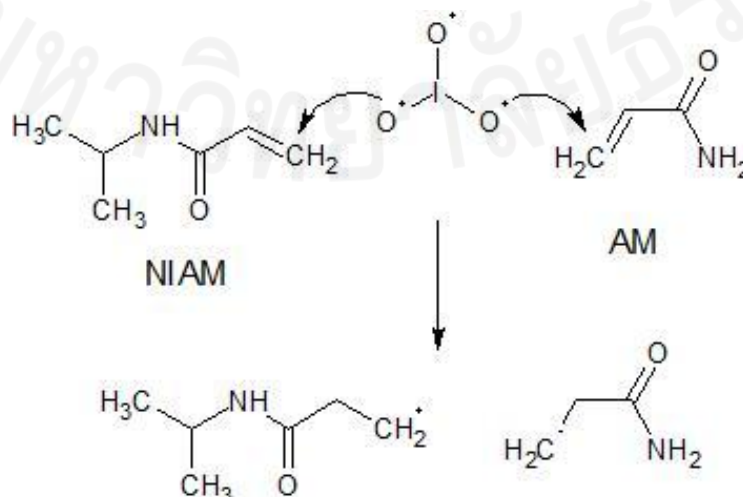
#### Step 2: Photolysis of KIO<sub>4</sub>

According to Wagner and Strehlow (1982), the mechanism of photolysis of periodate ion has been described as follows:



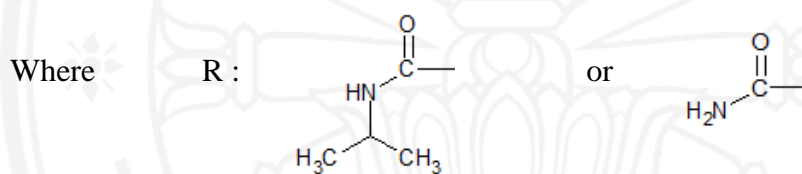
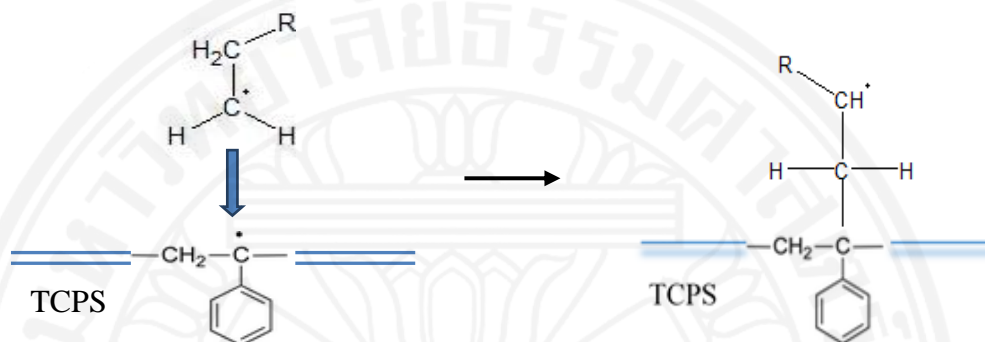
#### Step 3: Formation of free radicals on monomers and crosslinker

The radicals coming out from photolysis of KIO<sub>4</sub> induce to break the double bond in monomers (NIAM and AM) and create the radicals on the first carbon.



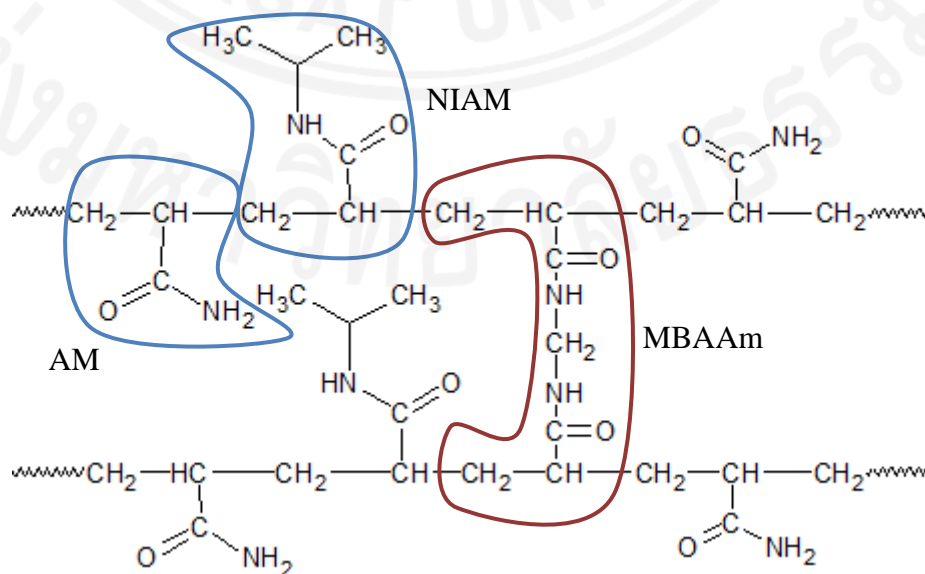
There are three roles of the active radicals on these resulting monomers: (1) reacting with the active sites on the TCPS surface (2) breaking the double bond in the cross-linker and (3) joining two monomers to form the copolymer.

**Step 4: Reacting radicals on the monomers with the active sites on TCPS surface**  
**→ grafting process**



**Step 5: Polymerization of NIAM and AM by crosslinking with MBAAm**

The radicals on NIAM and AM join to form the polymer chain as well as induce to break the double bonds in MBAAm, and then, the growing chain of PNIAM-co-AM take place. The resulting polymer chain will successively grow on the active sites of TCPS surface.



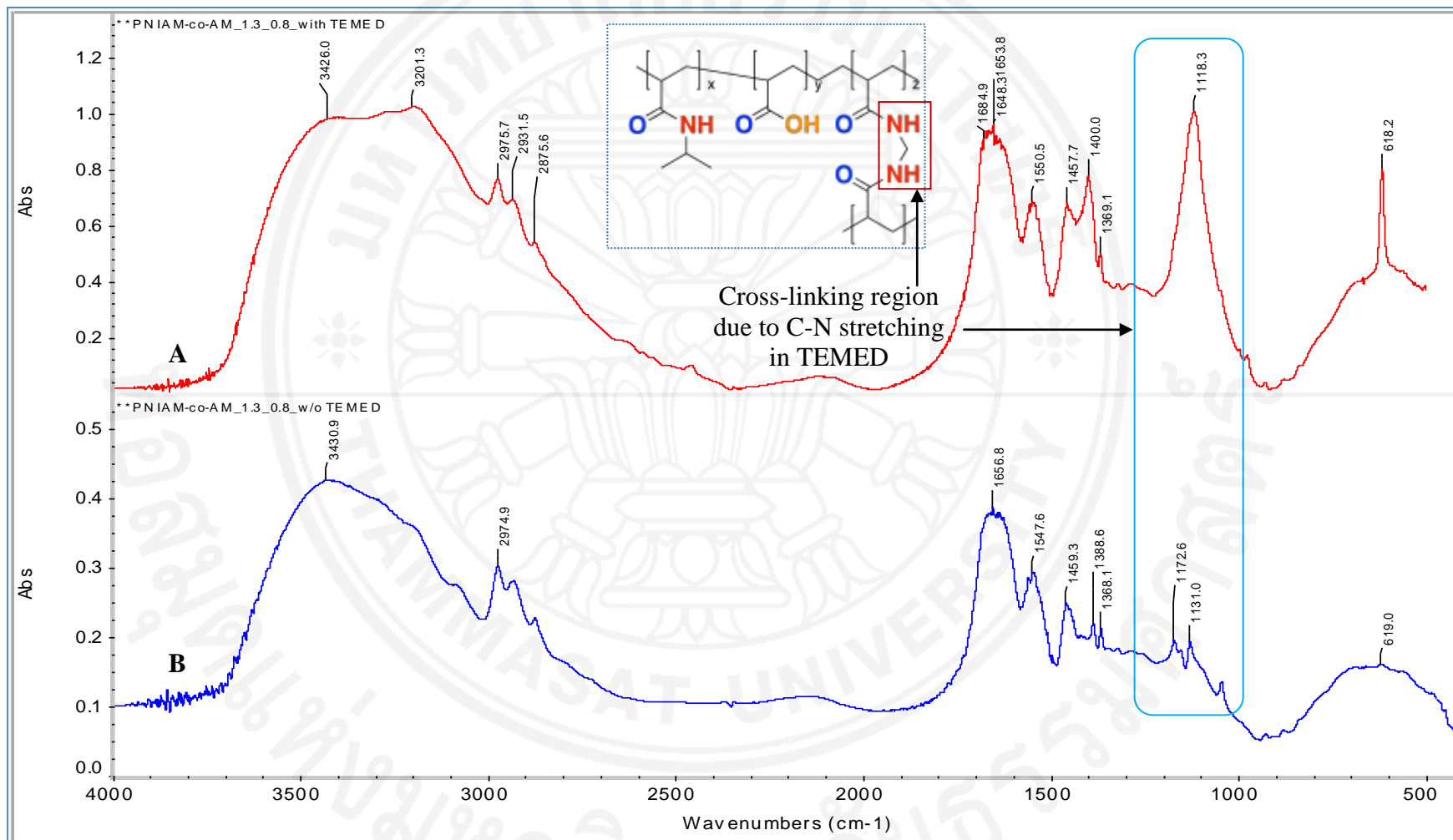


Figure C.1: FTIR spectra of linear PNIAm-co-AM (1:1 ratio) synthesized with TEMED (A) and crosslinked PNIAm-co-AM (1:1 ratio) synthesized without TEMED (B)



Table C.1 : Synthesis of PNIAM-co-AM with TEMED

Materials	% wt	C (mol/L)	Amount in 200 mL DI water
N-isopropylacrylamide (NIPAAm)	1.3	0.1105	2.5 g
Acrylamide (AAm)	0.8	0.1161	1.65 g
Ammonium persulfate (APS)	0.25	0.011	0.5 g
<b>6.67 M</b> Tetramethylethylenediamine (TEMED)	0.14	0.012	360 $\mu$ L

From Figure C.1, the characteristic peaks in FTIR spectrum of synthesized PNIAM-co-AM with TEMED showed similar to that of linear PNIAM-co-AM except in the region between 1000 and 1500  $\text{cm}^{-1}$ . A strong peak at the wavenumber of 1118  $\text{cm}^{-1}$  was observed in the copolymer synthesized with TEMED. This peak overwhelmed Amide III band at 1172  $\text{cm}^{-1}$  which is one of the characteristic peak in linear PNIAM-co-AM. This could result from using TEMED during the reaction in which it not only helped to form more radicals in ammonium persulfate initiator but also cross-linked itself between the resulting polymer chains.

Intrinsic viscosity determination of 1:1 ratio PNIAM-co-AM at 10°C

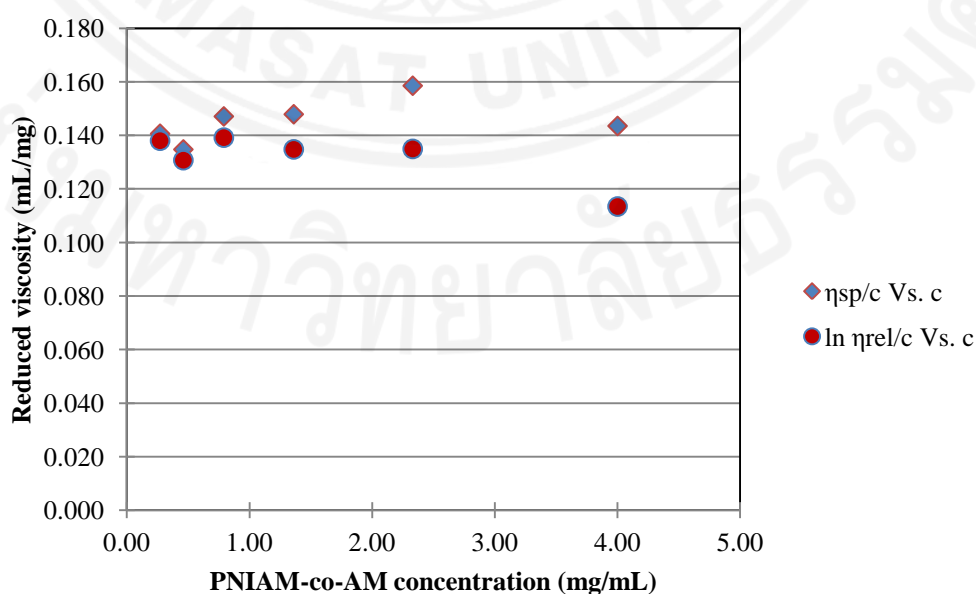


Figure C.2: Huggins plot and Kraemer plot of PNIAM-co-AM (1:1 ratio) at 10°C

Intrinsic viscosity determination of 1:1 ratio PNIAM-co-AM at 20°C

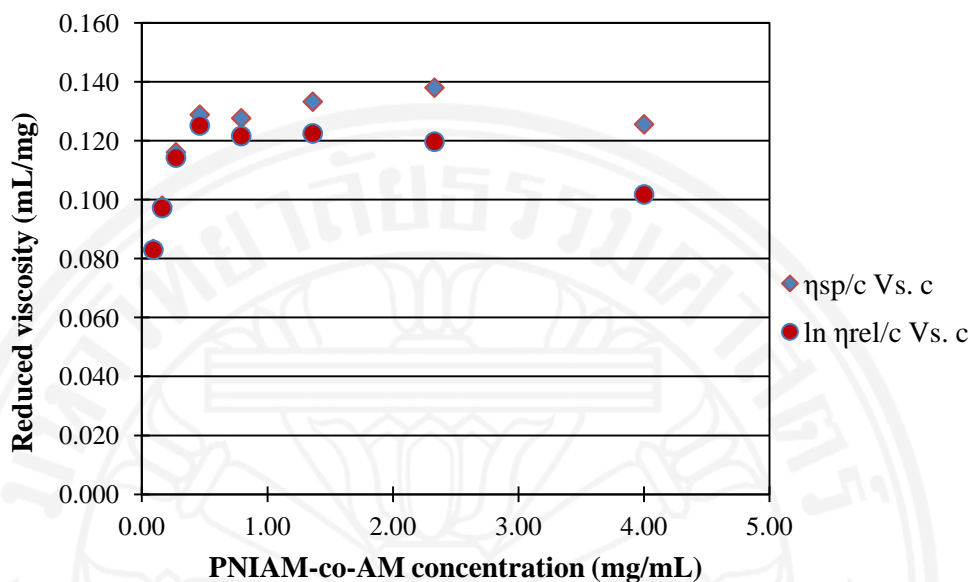


Figure C.3: Huggins plot and Kraemer plot of PNIAM-co-AM (1:1 ratio) at 20°C

Intrinsic viscosity determination of 1:1 ratio PNIAM-co-AM at 37°C

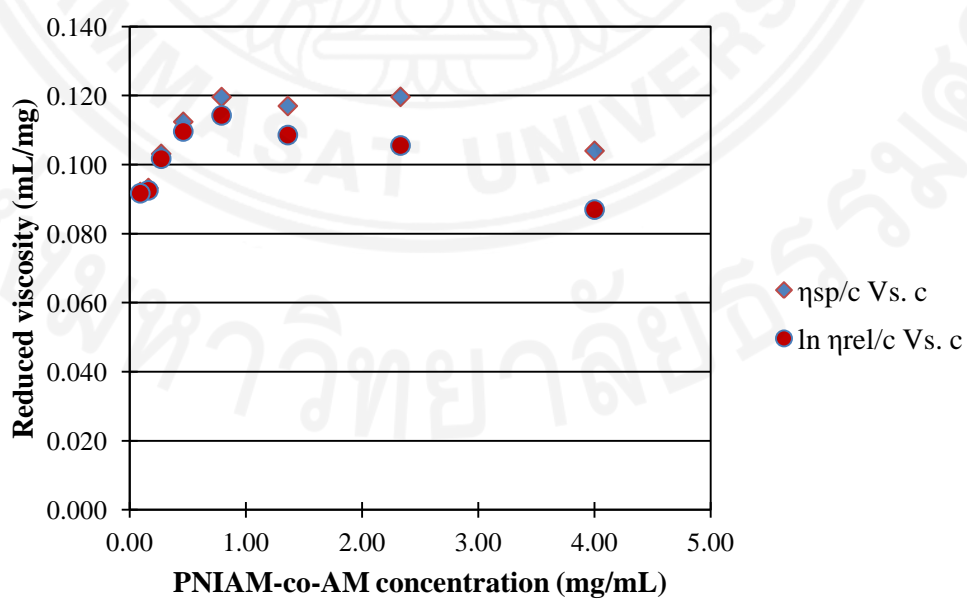


Figure C.4: Huggins plot and Kraemer plot of PNIAM-co-AM (1:1 ratio) at 37°C



Intrinsic viscosity determination of 2:1 ratio PNIAM-co-AM at 10°C

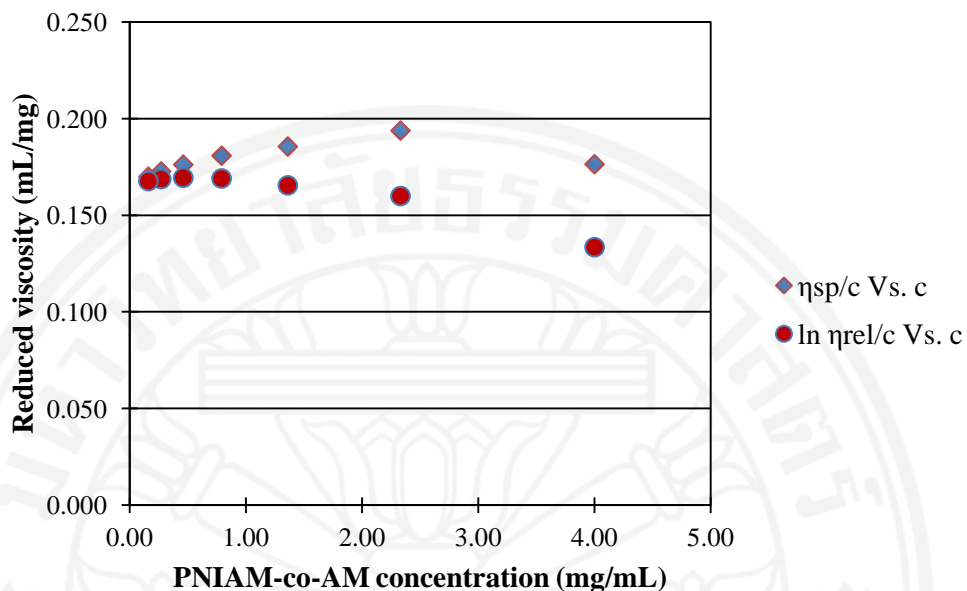


Figure C.5: Huggins plot and Kraemer plot of PNIAM-co-AM (2:1 ratio) at 10°C

Intrinsic viscosity determination of 2:1 ratio PNIAM-co-AM at 20°C

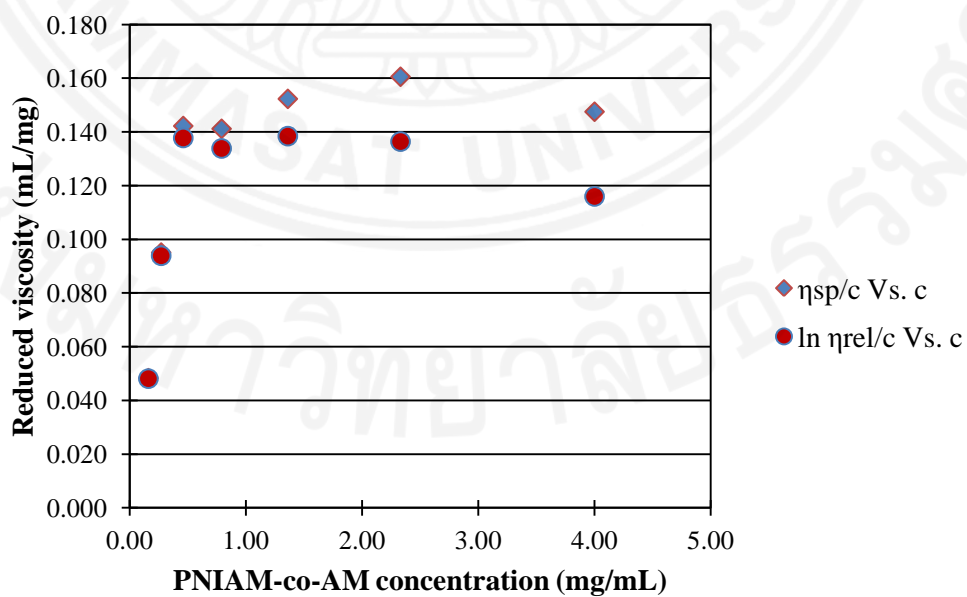


Figure C.6: Huggins plot and Kraemer plot of PNIAM-co-AM (2:1 ratio) at 20°C

Intrinsic viscosity determination of 2:1 ratio PNIAM-co-AM at 37°C

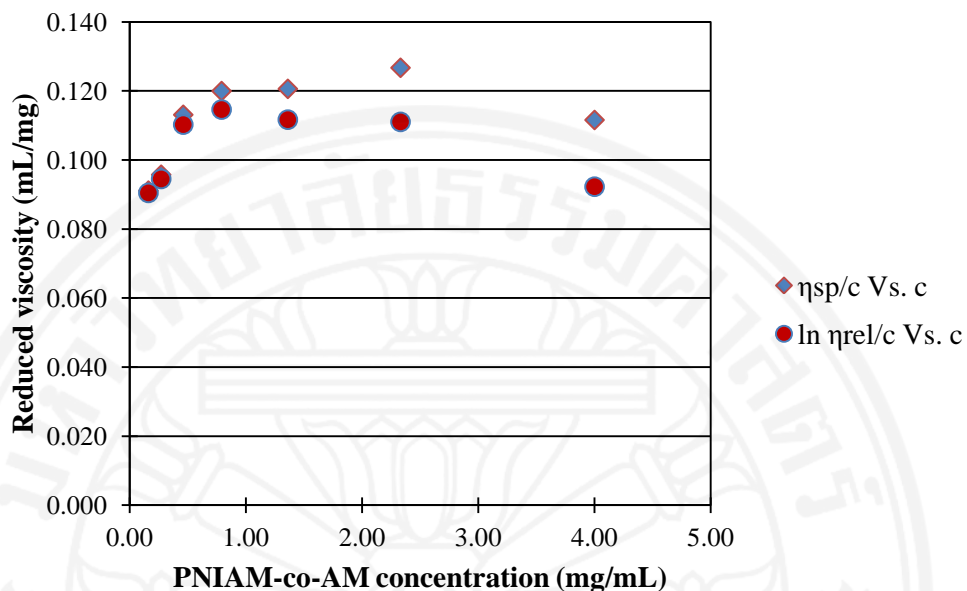


Figure C.7: Huggins plot and Kraemer plot of PNIAM-co-AM (2:1 ratio) at 37°C

Overlapped area calculation in KBR-FTIR spectrum of synthesized PNIAM-co-AM (1:1 ratio)

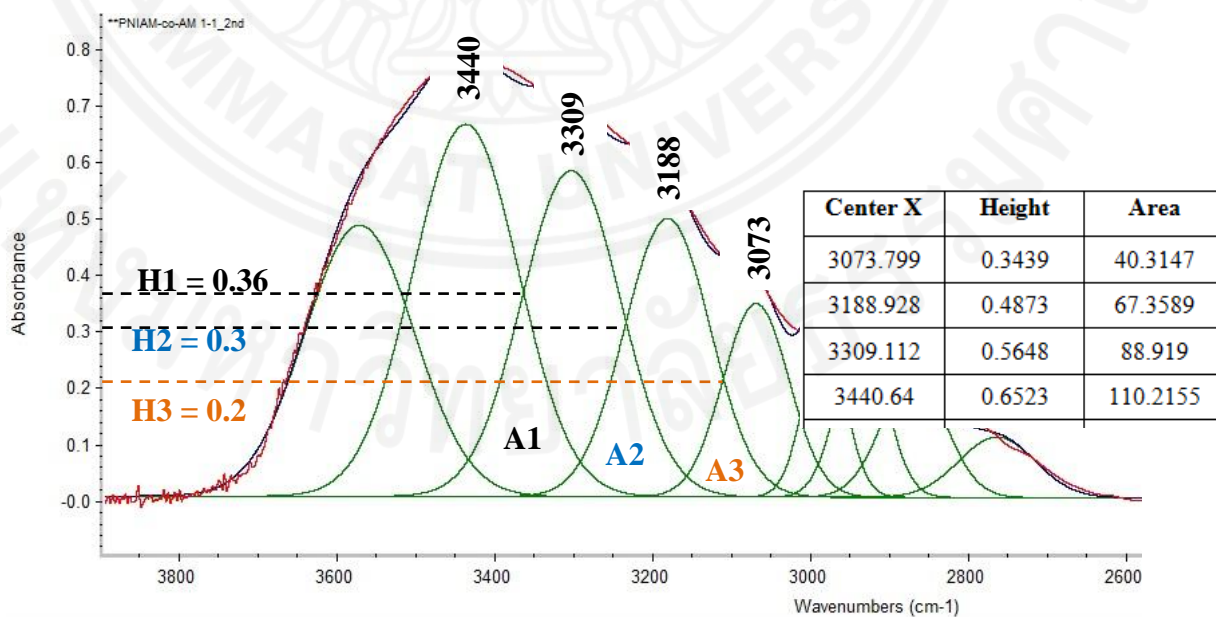


Figure C.8: KBr-FTIR spectrum of 1:1 ratio of PNIAM-co-AM illustrating the N-H stretching of amide peaks from 3440 to 3073  $\text{cm}^{-1}$

Table C.2: Results of overlapped peak areas

	<b>Reference peak</b>	<b>H/ H<sub>ref</sub></b>	<b>A = (H/H<sub>ref</sub>) x A<sub>ref</sub></b>	<b>Avg. Area</b>
A1	3440	0.554	60.7	58.7
	3309	0.643	56.7	
A2	3309	0.536	47.2	44.4
	3188	0.612	41.5	
A3	3188	0.408	27.6	25.5
	3073	0.588	23.4	